CANADIAN THESES ON MICROFICHE

I.S.B.N.

THESES CANADIENNES SUR MICROFICHE

National Library of Canada
Collections Development Branch

Canadian Theses on
Microfiche Service

Ottawa, Canada
K1A 0N4

Bibliothèque nationale du Canada
Direction du développement des collections

Service des thèses canadiennes
sur microfiche

NOTICE

The quality of this microfiche is heavily dependent upon the quality of the original thesis submitted for microfilming. Every effort has been made to ensure the highest quality of reproduction possible.

If pages are missing, contact the university which granted the degree.

Some pages may have indistinct print especially if the original pages were typed with a poor typewriter ribbon or if the university sent us a poor photocopy.

Previously copyrighted materials (journal articles, published tests, etc.) are not filmed.

Reproduction in full or in part of this film is governed by the Canadian Copyright Act, R.S.C. 1970, c. C-30. Please read the authorization forms which accompany this thesis.

THIS DISSERTATION
HAS BEEN MICROFILMED
EXACTLY AS RECEIVED

AVIS

La qualité de cette microfiche dépend grandement de la qualité de la thèse soumise au microfilmage. Nous avons tout fait pour assurer une qualité supérieure de reproduction.

S'il manque des pages, veuillez communiquer avec l'université qui a conféré le grade.

La qualité d'impression de certaines pages peut laisser à désirer, surtout si les pages originales ont été dactylographiées à l'aide d'un ruban usé ou si l'université nous a fait parvenir une photocopie de mauvaise qualité.

Les documents qui font déjà l'objet d'un droit d'auteur (articles de revue, examens publiés, etc.) ne sont pas microfilmés.

La reproduction, même partielle, de ce microfilm est soumise à la Loi canadienne sur le droit d'auteur, SRC 1970, c. C-30. Veuillez prendre connaissance des formules d'autorisation qui accompagnent cette thèse.

LA THÈSE A ÉTÉ
MICROFILMÉE TELLE QUE
NOUS L'AVONS REÇUE

NL-339 (r. 82/08)

Canada

TO

MY MOTHERLAND

ACKNOWLEDGEMENTS

This research was conducted under the direction of Professor M.H. Back, whose constant help with enlightenment on Chemical Kinetics is most gratefully appreciated. With deep gratitude the author wishes to thank Professor K.J. Laidler for his valuable discussions. Thanks are due as well to Drs. R.A. Back, F.P. Lossing, J.L. Holmes and H. Teitelbaum for helpful and constructive suggestions and to my colleague Y. Hsuanyu for helpful discussion and encouragement.

The author also wishes specially to thank the government of the People's Republic of China and the Natural Science and Engineering Research Council of Canada for financial support during the course of these studies.

Finally, the author wishes to express his special deep gratitude to his wife for her incessant help and encouragement during these years.

LIST OF TABLES

LIST OF FIGURES

ABSTRACT

The kinetics of the reaction of hydrogen with thin films of carbon has been studied over the temperature range 870-1150 K and at pressures of hydrogen from 50-300 Torr. Thin films of carbon of average thickness about 20 nm were deposited on the surface of a quartz reactor by the pyrolysis of methane at 1100 K and the kinetics of the reaction with hydrogen were studied in a static system. The products of the reaction were methane, ethane and ethylene, formed in successive hydrogenation steps, which in the low temperature region occurred largely on the surface of the carbon. In this region the activation energy of the rate of formation of methane was about 6 kcal/mol. At temperatures above about 1050 K the thermal dissociation of hydrogen provided a source of radicals which caused a rapid increase in the rate of hydrogenation, both heterogeneous and homogeneous, giving an activation energy for the rate of formation of methane of 51 kcal/mol. A self-inhibition was observed, probably caused by a heterogeneous polymerization reaction leading to the formation of higher molecular weight products which remained adsorbed on the surface.

The effect of the presence of chemi-sorbed oxygen on the reactivity of the carbon films has been studied. A small amount of oxygen, 100-1300 ppm, in the reactant

hydrogen increased significantly the rate of formation of CH_4 and C_2H_4 at 1111 K and at a total pressure of 177 Torr. From the results an activation energy of 80 kcal/mol for desorption of the surface oxide was estimated. The results are interpreted to show that the rate of the reaction is significantly enhanced by the presence of the surface oxide.

A system for the measurement of the rate constant for the elementary reaction

$$C_2H_5 + H_2 \rightarrow C_2H_6 + H$$

in the temperature range 1111-1200 K is described and is based on the thermal production of an equilibrium concentration of hydrogen atoms. In a mixture of hydrogen with about 10 ppm ethylene this reaction is the rate-controlling step in the hydrogenation of ethylene. The rate constant obtained for this reaction is represented by the following expression

$$\log k_3(\text{L mol}^{-1}\text{s}^{-1}) = 10.6 - 23000/2.3RT$$

The kinetics of the rate of conversion of ethane to ethylene in the presence of a large excess of H_2 has been studied over the temperature range 876-1016 K. The results show that the rate-controlling step is

$$H + C_2H_6 \rightarrow H_2 + C_2H_5$$

and the value obtained for the rate constant is

$$\log k_{-3}(L\ mol^{-1}s^{-1}) = 11.72 \pm 0.05 - \frac{12800 \pm 200}{2.3RT}$$

This value is compared with values obtained from other methods over the temperature range 300-1400 K. By comparison of k_3 and k_{-3}, two sets of independent measurements, a value of 28 kcal/mol for the heat formation of C_2H_5 is suggested.

The rate constant for dissociation of ethane

$$C_2H_6 \rightarrow 2CH_3$$

has been measured over the temperature range 940-1040 K at pressures where k/k^{∞} ranged from 0.8 - 0.2, under conditions of nearly infinite dilution with hydrogen and with mixtures of hydrogen and xenon. Both gases were weak colliders and the efficiencies relative to ethane showed a decline with increasing temperature. The average energy transferred per deactivating collision, $\langle \Delta E \rangle$, also declined from 1.7 to 1.3 kcal/mol and was the most important factor in the change in collisional efficiency over the temperature range of the measurements.

PART ONE

KINETICS OF THE REACTION OF HYDROGEN WITH THIN FILMS OF CARBON

CHAPTER 1

INTRODUCTION

The gasification of carbon by hydrogen has been of interest to chemists for many years. Because of the simplicity of the reacting species this reaction should present an ideal system in which heterogeneous reaction kinetics could be examined. The first definitive kinetic work on the carbon-hydrogen system was performed by Barrer in 1935 on both amorphous carbon[1][2] and graphite.[3] The early literature on the carbon-hydrogen reaction has been reviewed by Burns[4] and by Walker, Rusinko and Austin.[5] The carbon-hydrogen reaction has received more attention in recent years because it has assumed an important role in several energy-production technologies, in particular, production of substitute natural gas by coal gasification and graphite corrosion in the high-temperature gas-cooled reactor. More recent work has been reviewed by Lewis[6] and by Krakowski and Olander.[7]

Many studies have been made with coal and coal char[9][8] and many have focused on the reaction catalyzed by metal.[10][11] Even studies involving pure graphite have used a diversity of reactor systems, analytical techniques, and environmental conditions. The different forms of carbon and the history of their formation have a great

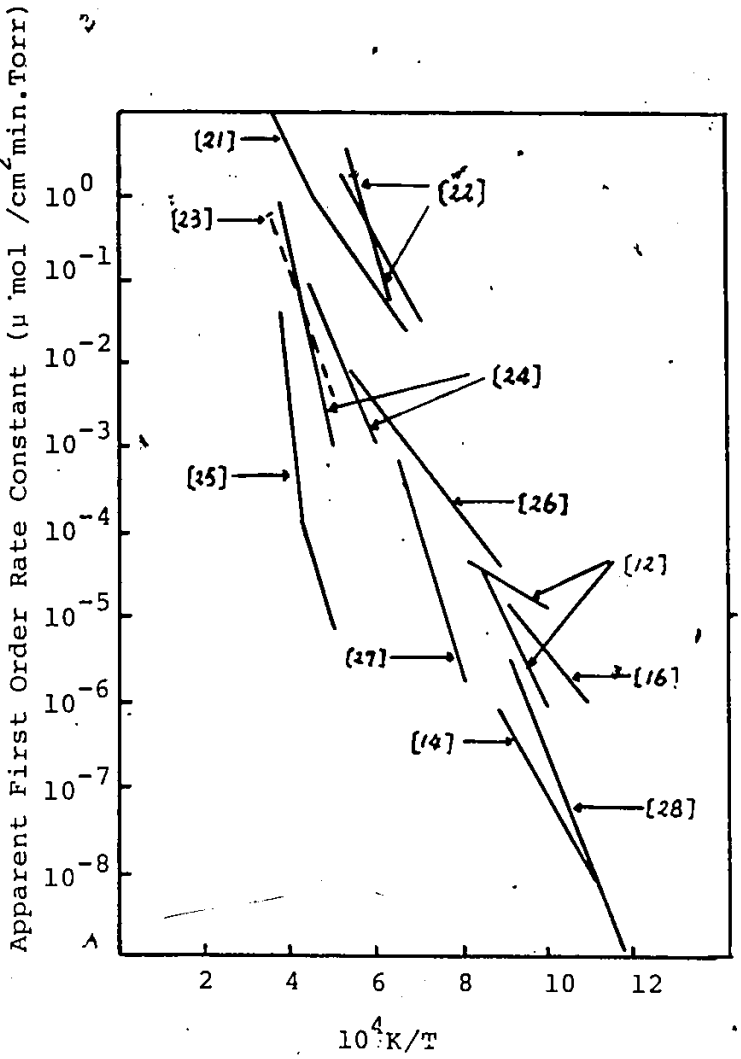

Figure 1. Kinetic Data on the Carbon-Hydrogen Reaction

Table 1

Reference	System	Order with respect to H^2	Activation Energy kcal/mol	Carbon used
Blackwood [14]	Flow System High Pressure 923-1143 K	1	30.0	Coconut Char
			42.9	Graphite
Hedder [27]	Flow System High Pressure 1273-1473 K	1	85.4	Graphite
Gulbransen, et al. [22]	Flow System Low Pressure 1473-1873 K	0	71.9	Graphite
Rogers and Sesonske [30]	Flow System High Pressure 1473 K	0	37.7 to 77.9 according to sample	Various purities Graphie
Breisacher and Marx [29]	Flow System High Pressure 853-1073 K	0.6	69.9 at high temp. 12.0 at low temp.	Graphite
Corney and Thomas [28]	Flow System Low Pressure (800 Torr) 723-1073 K	-	65.1 above 873 K	Graphite
Imai, et al. [15]	Flow System Atmospheric Pressure 1298 K	1.5	22.0	Graphite of various purities
A. de Koranyi [16]	Flow System Low Pressure 1010-1473 K	1.2	35.4	Graphite

influence on the reactivity. There appears to be no general agreement concerning the order of the rate with respect to hydrogen, and probably as a consequence, no agreement on the activation energy. This is partly due to the variation in reactivity of the carbon used as reactant and partly due to the wide range of conditions, such as temperature and pressure, used in studies of the reaction. The purity of hydrogen is also an important factor as will be shown in the present work. This wide variation in kinetic parameters of the reaction has been the main difficulty in formulating a mechanism and it is not surprising that attempts to derive a rate equation for the reaction have had limited success. Previous measurements of the rate of the reaction are summarized as an Arrhenius plot in Figure 1 and other details of the measurements are summarized in Table 1.

In most studies, methane is the main, and usually the only, product reported.

$$2H_2 + C \rightarrow CH_4$$

In spite of this simple stoichiometry the details of the mechanism by which the hydrogenation occurs are not well understood.

Among the first suggestions concerning the mechanism was that of Zielke and Gorin.[12] They passed hydrogen through a packed bed of 65-100 mesh Disco char that was

charred at low temperature and carried out their investigation over a pressure range of 10 to 20 atm and over a temperature range of 1088 to 1200 K. The measured rate was based on carbon disappearance and a gasified carbon was assumed to be converted to methane. The mechanism proposed by Zielke and Gorin involved successive hydrogenation of neighbouring edge carbon atoms to give $=\overset{H}{C}-$, $-\overset{H}{\overset{|}{C}}-$, $-\overset{H}{\overset{|}{\underset{H}{|}}}-H$ and finally methane. This basic mechanism has been modified but not effectively changed by most of the subsequent work.[8][15][16]

Blackwood[17] and Blackwood and McTaggart[18] studied the reaction at temperatures near to 1000 K and found methane was the only product. They suggested that the function of the activated sites was to dissociate the hydrogen molecule. Following dissociative adsorption, Blackwood supposed that one atom was chemisorbed while the other atom was free to migrate to other adsorption positions or to be adsorbed at the original active site. The mechanism for the adsorption process was proposed as follows:

$$C + H_2 \underset{k_{-1}}{\overset{k_1}{\rightleftharpoons}} (C\text{-}H)(H) \underset{k_{-2}}{\overset{k_2}{\rightleftharpoons}} (CH_2)$$

$$C + H_2 \underset{k_{-3}}{\overset{k_3}{\rightleftharpoons}} (CH_2)$$

The subsequent steps whereby methane is formed were somewhat uncertain. The hydrogenation of $-CH_2-CH_2-$ and subsequent bond rupture was considered by Zielke and Gorin as the rate determining step in the methane formation. Blackwood and co-workers, however, considered it unlikely that the CH_3 group is formed in significant amounts. Instead, the final methane formation step was taken to be:

$$(CH_2) + H_2 \underset{k_{-4}}{\overset{k_4}{\rightleftharpoons}} CH_4$$

Recently an extensive analysis of data by Shaw[31] has shown that the kinetics of the formation and decomposition of methane in the presence of char and hydrogen may be described by a two-step hydrogenation process on the carbon surface in which CH_2 leads directly to methane.

At high temperatures (2000-3500 K), some investigators believe that the hydrogen-carbon reaction mechanism involves atomic hydrogen. Clark and Fox[23] have investigated the kinetics of the gasification of carbon by hydrogen using a graphite filament (0.2 and 0.5 mm dia.) heated to temperatures in the range 2000 K to 3500 K with pressures of H_2 from 0.01 to 1 atm. Below 3000 K only methane and ethane were formed, whereas acetylene, and propane in some cases, were found above 3000 K. Clark and Fox assumed the rate of hydrocarbon formation to be given by

$$R = k_{SR} K_D^{1/2} P_{H_2}$$

where k_{SR} is the rate constant for the surface reaction leading to gaseous hydrocarbon product and K_D represents the equilibrium dissociation constant for hydrogen gas $H_2 \rightleftharpoons 2H$. The constant k_{SR} was calculated to be 80 ± 20 μ mole sec^{-1} $torr^{-3/2}$ for the pressure range 0.01 to 1.0 atm and was independent of temperature over the range 2000 K to 2800 K. Hence, the conclusion was made that most of the activation energy associated with carbon gasification is associated with hydrogen dissociation. This hypothesis was further substantiated by the value of 51 kcal mol^{-1} ($\frac{1}{2}$ ΔH_D) obtained from the Arrhenius plot of the rate for hydrogen pressures of 0.01, 0.50 and 0.92 atm. According to the mechanism proposed by Clark and Fox, the CH_3 radical may be formed by attack of H atom on CH_2, the carbon-hydrogen complex followed by escape from the surface. Reaction in the gas phase gives CH_4 by combination with a hydrogen atom or ethane by combination with another methyl radical.

Lowrie[25] attempted to elucidate the mechanism for acetylene formation in the temperature range of 2073 to 2773 K by utilizing mixtures of deuterium and hydrogen. If acetylene is formed through a process that involves a single molecule of hydrogen, only C_2H_2 and C_2D_2 would be

formed. Equal amounts of hydrogen and deuterium were used and the analysis of the products showed the ratio C_2H_2/C_2HD to be 1/2, indicating the reaction mechanism involves atomic hydrogen.

Some results from studies of the reaction of carbon with H atoms generated independently have been helpful in understanding the carbon hydrogenation process. King and Wise[36] reported an activation energy for the H atom-carbon reaction of 9.2 to 7.1 kcal mol^{-1} in the range 365-500 K and 5.15 kcal mol^{-1} in the range 450-715 K. Snelson[37] found an activation energy in the range 0.9-4.5 kcal mol^{-1} depending on the temperature region. Recently, Balooch and Olander[38] investigated the reaction of an atomic hydrogen beam with pyrolytic graphite at temperatures from 500 to 2000 K. The hydrogen atom sticking probability on graphite was measured as 0.02 and 0.006 for the prison and basal plane orientation respectively. The activation energy for the H atom-carbon reaction was estimated in the range 0.9 to 3.3 kcal mol^{-1}.

At temperatures above 2000 K the previous work suggested that the gasification of carbon by hydrogen most probably involves atomic hydrogen and CH_4, C_2H_2, C_2H_4, C_2H_6 may be formed as primary products due to the appreciable mobility of the intermediate species CH, CH_2 and CH_3 on the surface. Below 1500K, where most studies on

the hydrogen-carbon reaction were performed, the mechanism has not been established. Some important questions which have not been answered are: What is the relative importance of gas-phase to surface reactions in the hydrogenation process? How important is atomic hydrogen in the neighbourhood of 1000 K? What intermediate radicals are formed on the carbon surface and how does their mobility affect the rate of the reaction? Actually none of the mechanisms proposed for the reaction below 1200 K considers the possibility of the formation of products intermediate to the formation of methane, for example, C_2 hydrocarbons, and the consequence of their desorption from the surface. Although some studies, particularly at high temperature, have reported the formation of higher hydrocarbon products, it was shown that these were due to the secondary pyrolysis of CH_4. Thermodynamically, at temperatures above 1000 K C_2H_6 and C_2H_4 are less stable than methane and would rapidly disappear in secondary reactions. Observation of them would require measurements at very low conversion.

The primary aim of the present study was to find answers to these questions. Our approach was first a careful search for the formation of products intermediate to methane, so that a clear distinction could be made between primary and secondary products and secondly, a thorough study of the rates of formation of the products over a

range of temperature and pressure so that a kinetic analysis of the processes occurring on the surface and in the gas phase could be achieved.

A further aim of the present studies was an investigation of the effect of O_2 on the rate. Oxygen forms a strongly-bound complex on the surface of carbon. It was reported[46]-[54] that the rate of the reaction of carbon with O_2 was a function of the fraction of the carbon sites covered by strongly-bound complex, and it was suggested that the oxygen-carbon surface complex has an activating effect on the surrounding carbon atoms. The influence of this surface oxide on the hydrogenation of carbon is not known. In the present studies we have compared the rate of the reaction using pure hydrogen with the rate using hydrogen containing 100-1300 ppm O_2. The results showed that the rate is greatly increased by the presence of small amounts of O_2. The results are interpreted as indicating the importance of the surface oxide in the mechanism of the hydrogenation process.

The present studies have been made using a new technique for the study of reaction of gases with carbon which offers some advantages for kinetic analysis.[35] A thin film of carbon is deposited on the surface of the reaction vessel by pyrolysis of methane. The concentration of carbon on the surface, in the range 10^{-5}-10^{-6} gcm^{-2}, may be determined from the optical density of the film using

a He-Ne laser as the analyzing beam. With the thin film pore-diffusion effects are eliminated and a static reaction system provides carefully controlled conditions of reaction time, temperature and pressure. In addition, the carbon formed from methane is virtually free of heavy metal impurities. The system should therefore be suitable for kinetic studies involving an analysis of the time course of the reaction and a measurement of the order of the rate of formation of products.

CHAPTER 2

EXPERIMENTAL

The reaction was studied in a conventional vacuum apparatus shown in Figure 2. The pumping system included a mechanical pump and two mercury diffusion pumps. Provision was made for storage of reactants and for preparing mixtures of reactants.

The reaction vessel was a quartz cylinder, 4.4 cm i.d. and 11.0 cm long with plane fused windows. The volume of the vessel, 182 cm^3, was calibrated before assembling. The geometric surface area was 256 cm^2. The vessel was placed in the center of a Lindberg three-zone tubular furnace, in which the temperature was controlled within ± 1 K. The vessel was used as a static reactor.

The products were analyzed by expansion into a Topler pump from which aliquot samples were taken for analysis by gas chromatograph. At least 2 analyses were made for each experiment. A Hewlett-Packard Model 5790 with FID detector was used for the analysis. The column was Durapak (Phenylisocyanate on Porasil) 6 x 1200 mm maintained at 30°C. Calibration curves were made from mixtures containing about 100 ppm CH_4, C_2H_6, C_2H_4 in pure hydrogen. For all products a good linear relation between sample pressure and peak area was obtained. An example is given in Figure 4. A

Figure 2. Experimental Apparatus

1. 2 mw He-Ne laser beam and power supply
2. Evacuated cylinder
3. Quartz reaction vessel
4. Photodiode (ORIEL 7054)
5. Electrometer
6. Recorder
7. Three-zone controlled furnace
8. G.C. with FID
9. Topler pump
10. Storage bulb
11. Metal valve
12. Manometer
13. Molecular sieve column at 77 K
14. Sampling tube
15. Column for purification of H_2
16. G.C. Column for TCD

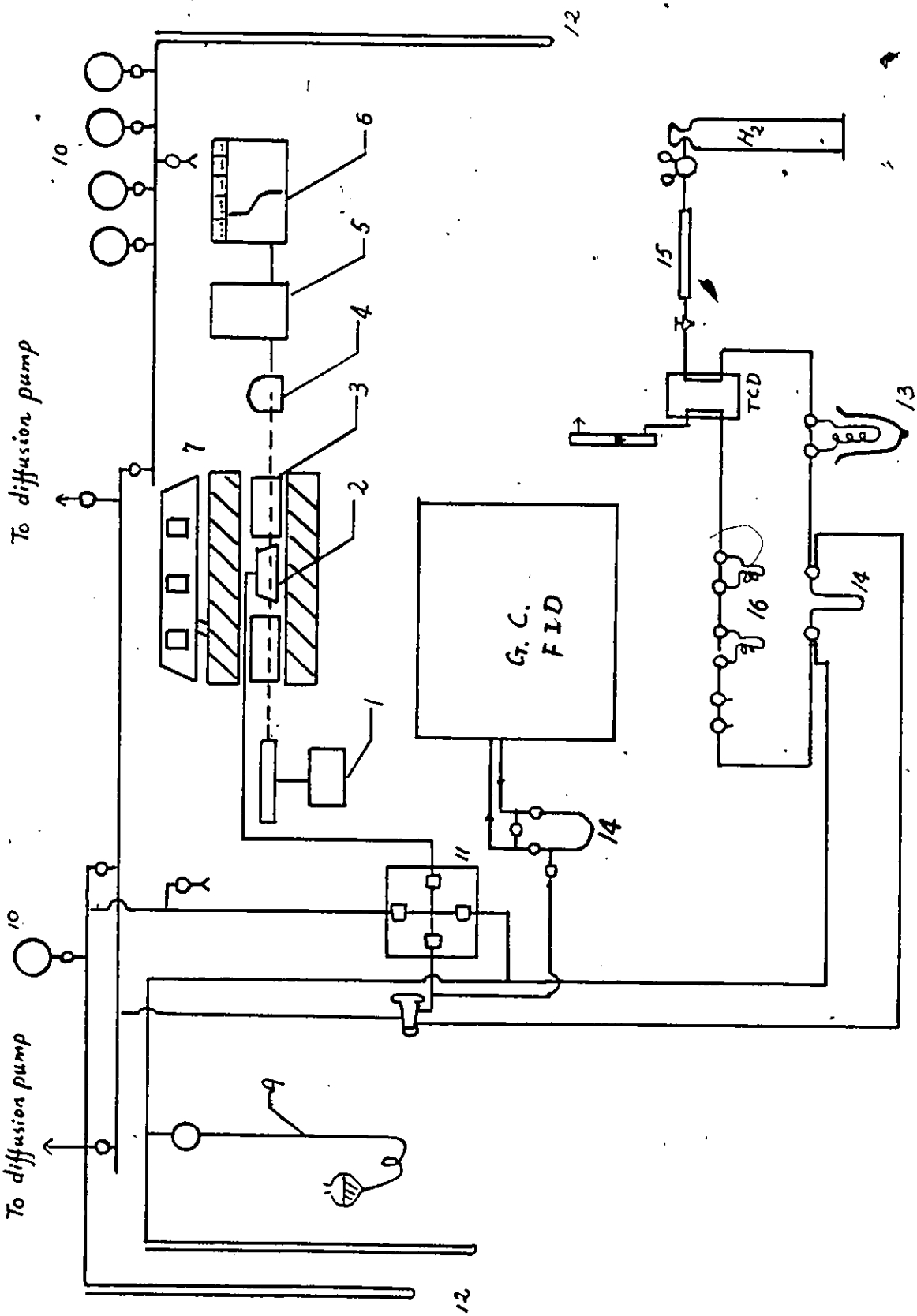
To diffusion pump
To diffusion pump
G. C.
FID
TCD
H_2
1
2
3
4
5
6
7
10
11
12
13
14
15
16

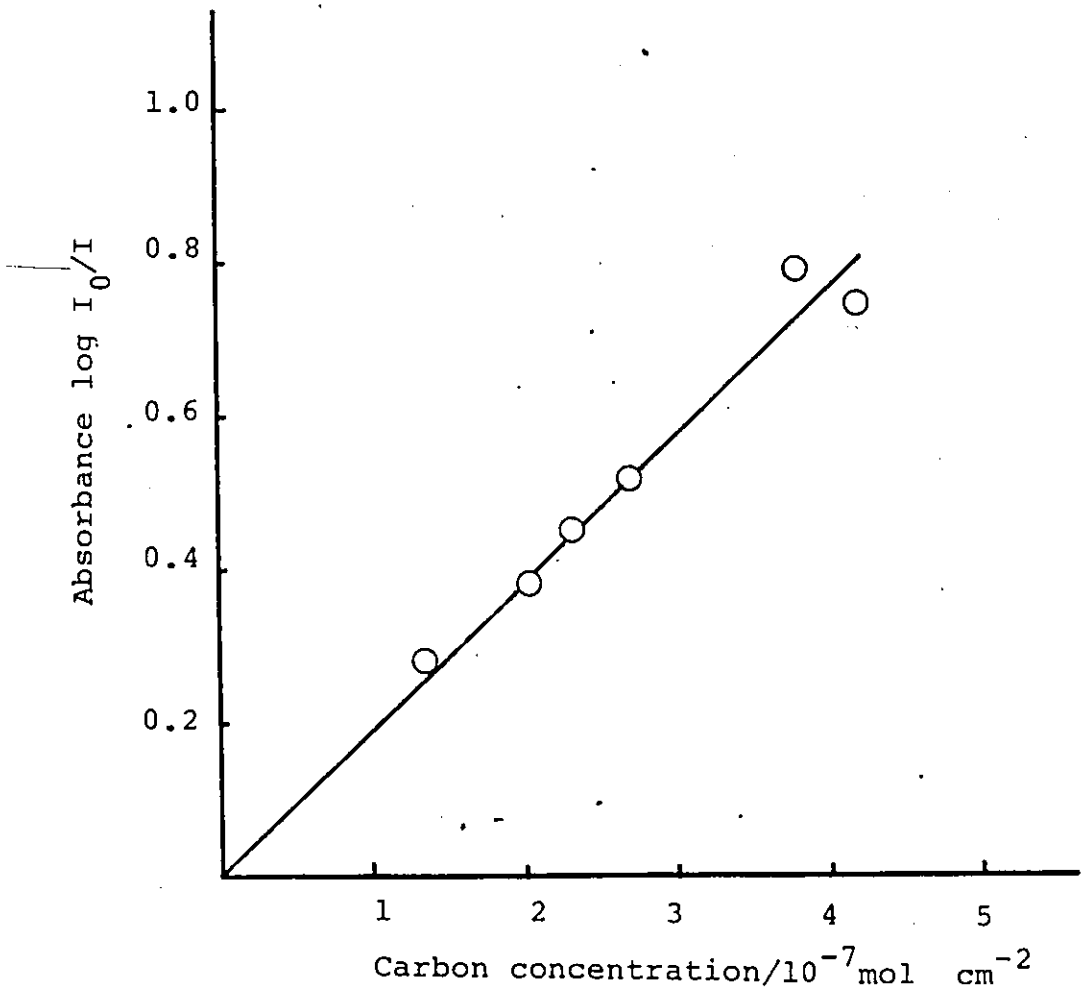

Figure 3. Calibration Curve of Carbon Films

Table 2

RELATION BETWEEN THE ABSORBANCE OF CARBON FILM AND THE CARBON CONCENTRATION mol cm^{-2}

$\log I_o/I$	$M_C/10^{-7}$ mol cm^{-2}
0.743	4.20
0.379	2.03
0.280	1.34
0.515	2.71
0.788	3.78
0.450	2.32

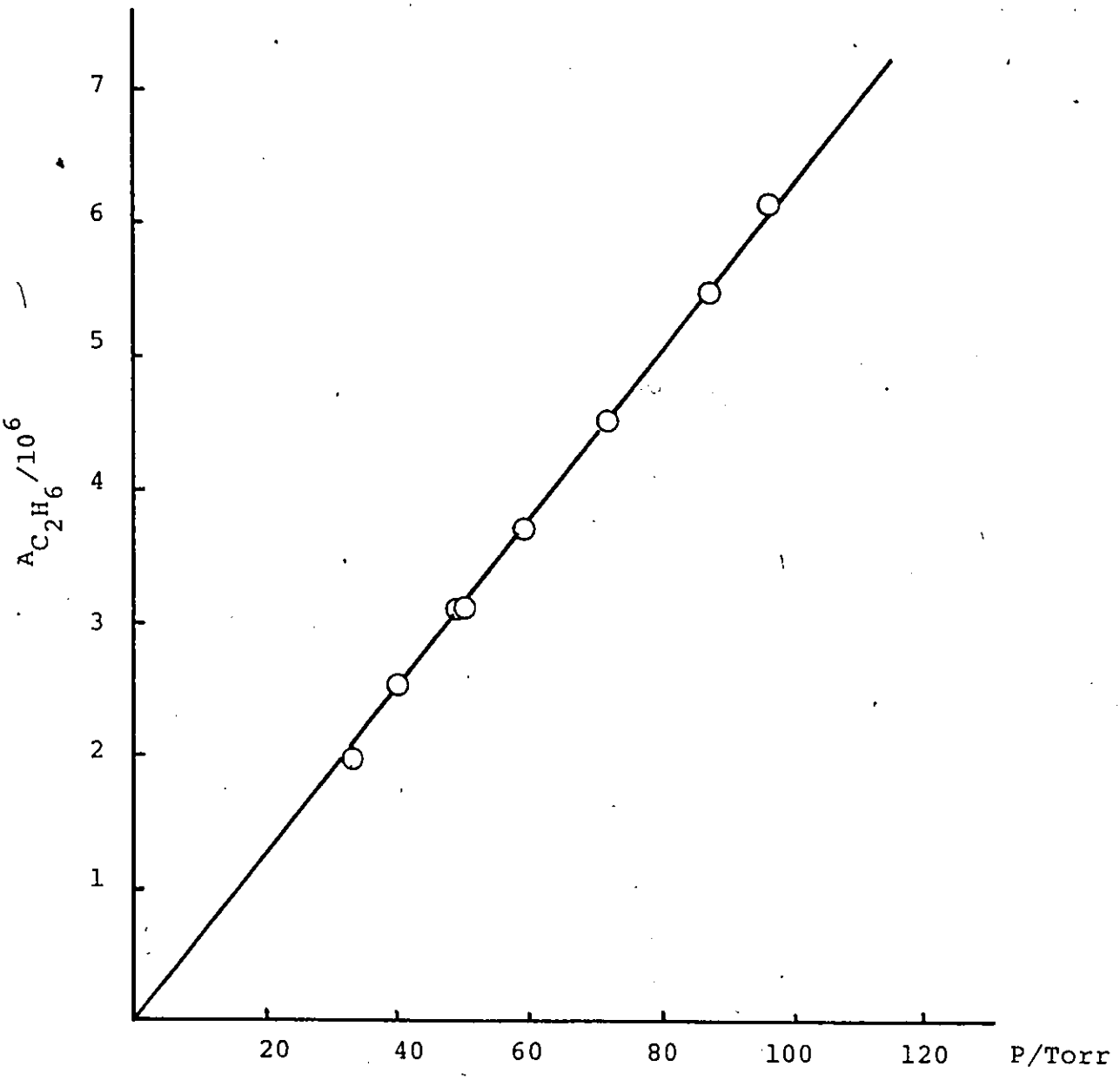

Figure 4. G.C. Calibration Curve for C_2H_6
Concentration of C_2H_6 in H_2 102 ppm

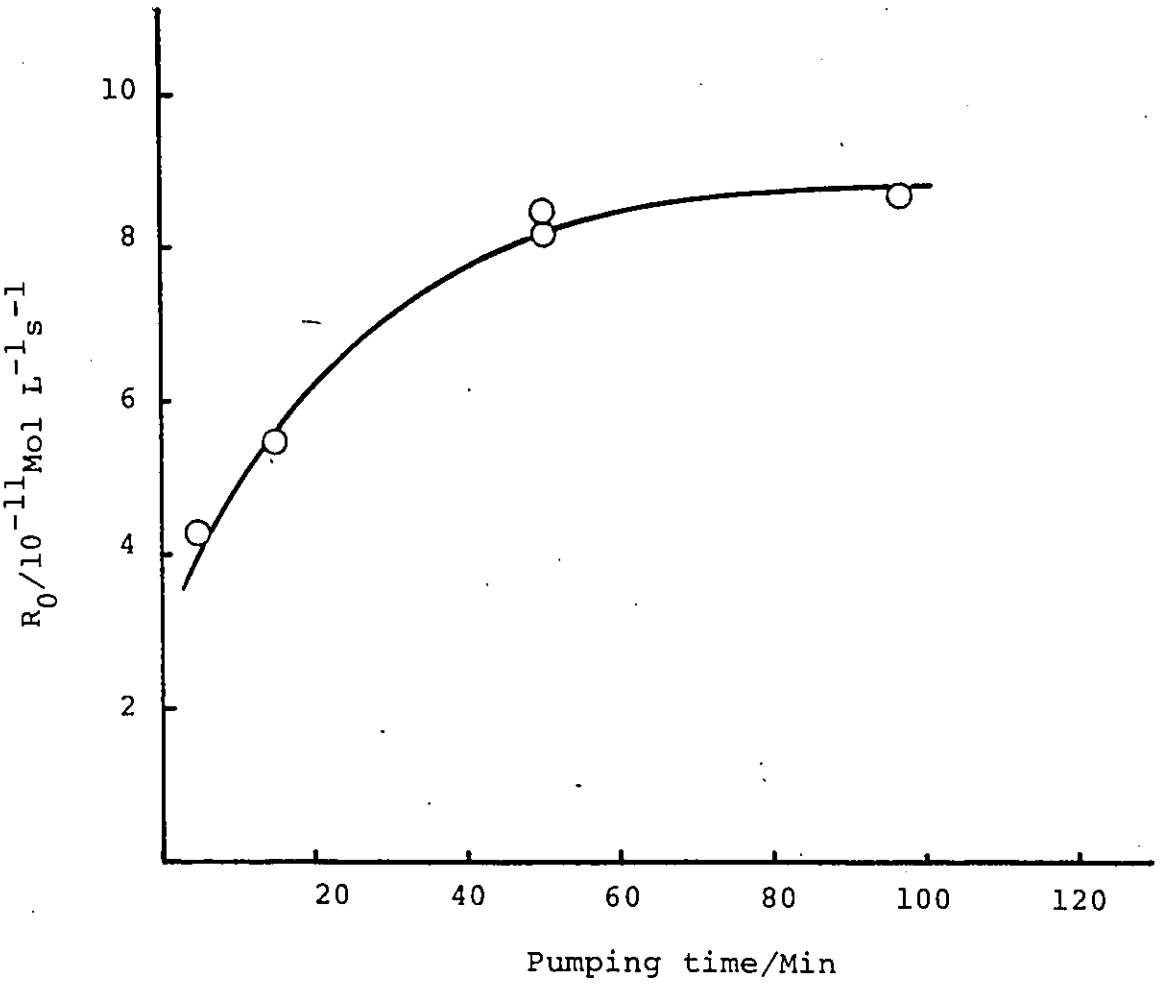

Figure 5. Influence of Pumping Time on the Reactivity of Carbon Film at 1110 K

Table 3

INFLUENCE OF PUMPING TIME ON THE REACTIVITY OF CARBON FILM AT 1110K. P_{H_2} = 109.5 Torr

Pumping time/Min.	$R_o/10^{-11}$ Mol $L^{-1}s^{-1}$
5	4.28
15	5.44
50	8.50
50	8.19
97	8.69

Gow-Mac thermal conductivity detector was used for analysis of CO with a 4 x 1000 mm molecular sieve column at 0°C and for analysis of CO_2 with a 4 x 800 mm silica gel column at 25°C. For measurement of H_2O, as the product of the reaction in the presence of small amounts of O_2, a porapak P column at 120°C was used.

For a series of experiments a carbon film was first produced by the pyrolysis of methane at 1100 K. The thickness of the carbon film produced depends on the initial pressure of CH_4 and the total time of pyrolysis. Most of the carbon films used in the present experiments were made by pyrolysis of 200 Torr of CH_4 for 30 minutes. This procedure produced a carbon film of average concentration 5×10^{-6} g cm^{-2} (4×10^{-7} mol cm^{-2}). Several rate measurements were made with one carbon film since the consumption of carbon in each experiment was very small. When about 5-10% of the carbon had been consumed, the film was removed and a new one prepared. A reproducible carbon surface was obtained by allowing sufficient time for evacuation after each experiment. This time was determined experimentally, as illustrated in Figure 5. Reasons for this behaviour will be discussed later.

The detection and analysis of the carbon deposited on the surface was made by measurement of the attenuation of the intensity of a beam of light. The analyzing beam,

from a 2 mw He-Ne laser (Coherent 80-4 HP) was passed axially through the vessel. The signal was measured with photodiode (ORIEL 7054) and electrometer (Keithley Instruments 600A) and recorded by HP7133A 1 mV recorder. At either end of the furnace the beam passed through evacuated cylinders which minimized convection currents and effectively reduced the light from the furnace. The absorbance of the film was calibrated by complete combustion of carbon to CO_2 at 1110 K using 350 Torr of pure O_2. The calibration curve is shown in Figure 3 and Table 2. The characteristics of the carbon film prepared in this way have been described in previous studies.[34] Measurements of the total surface area by low-temperature adsorption of nitrogen have shown that the surface area of the film for concentrations up to 6×10^{-6} g cm^{-2} is not significantly different from the surface area of the clean quartz vessel. A mean value of ~30 $m^2 g^{-1}$ may be estimated from the geometric area and the total weight of carbon. The films have been examined with an electron microscope[34] and no details or structure were observed at these low concentrations. Assuming a uniform deposit and a density of carbon of 1.9 g cm^{-3}, the average thickness of the film used in the present experiments was about 20 nm.

Methane was Research Grade (99.99%) obtained from Matheson of Canada, Whitby, Ontario and used without further

purification. Hydrogen was purified by passage through a column of Molecular Sieve 5A at liquid nitrogen temperature with a residence time of 1-2 sec. Such treatment is usually sufficient to reduce the oxygen impurity to less than 1 ppm[35] although the present analysis using the TC detector could not detect less than 6 ppm.

CHAPTER 3

RESULTS AND DISCUSSION

3.1 Products of the Reaction

Three products, methane, ethane and ethylene were detected and measured. Yields of the products as a function of time were measured over the temperature range 870-1150K and at pressures of hydrogen from 50-300 Torr. Yield-time curves for methane, ethane and ethylene are shown in Figures 6-8, corresponding to the data in Tables 4-6. Methane was the main product and the C_2 hydrocarbons were always minor. Traces of acetylene and propane were observed under some conditions, but no higher hydrocarbons were detected. The yield of ethylene attained a maximum value, which approached 10% of the yield of methane, at an early stage of the reaction and fell rapidly thereafter. At high temperatures the yield of ethane fell rapidly with time and was less than the yield of ethylene, but at low temperatures the yield increased with time in a manner analogous to that of methane and became greater than that of ethylene. The rate of formation of methane decreased slowly with increasing time of reaction and appeared to approach a limiting value. This value was much lower than the equilibrium concentration of methane at these conditions (2×10^{-5} mol L^{-1} at 177 Torr and 1111 K). The decrease in

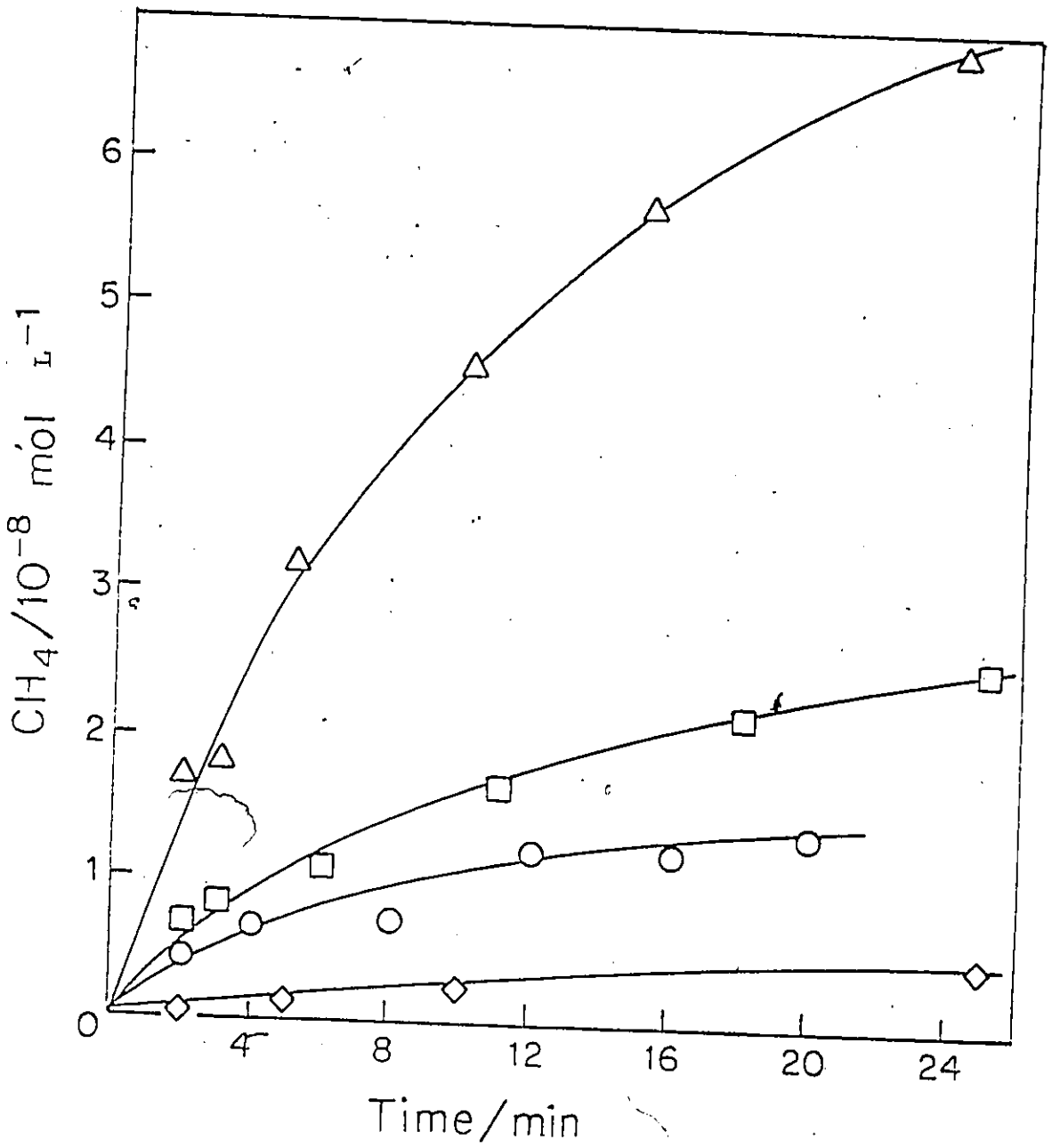

Figure 6. Yield of Methane as a Function of Time. Pressure of Hydrogen 177 Torr

◇ - 908 K
O - 1010 K
□ - 1061 K
Δ - 1111 K

Table 4

YIELD OF CH_4 AS A FUNCTION OF TIME

PRESSURE OF HYDROGEN 177 Torr

T/K	Reaction Time/min.	Yield of $CH_4/10^{-8}$ mol L^{-1}
1111	2	1.70
	3	1.81
	5	3.18
	10	4.61
	15	5.70
	24	6.84
1061	2	0.68
	3	0.82
	6	1.07
	11	1.67
	18	2.15
	25	2.54
1010	2	0.63
	4	0.66
	8	0.73
	12	1.24
	16	1.20
	20	1.37
908	2	0.058
	5	0.126
	10	0.249
	25	0.484
	40	0.488

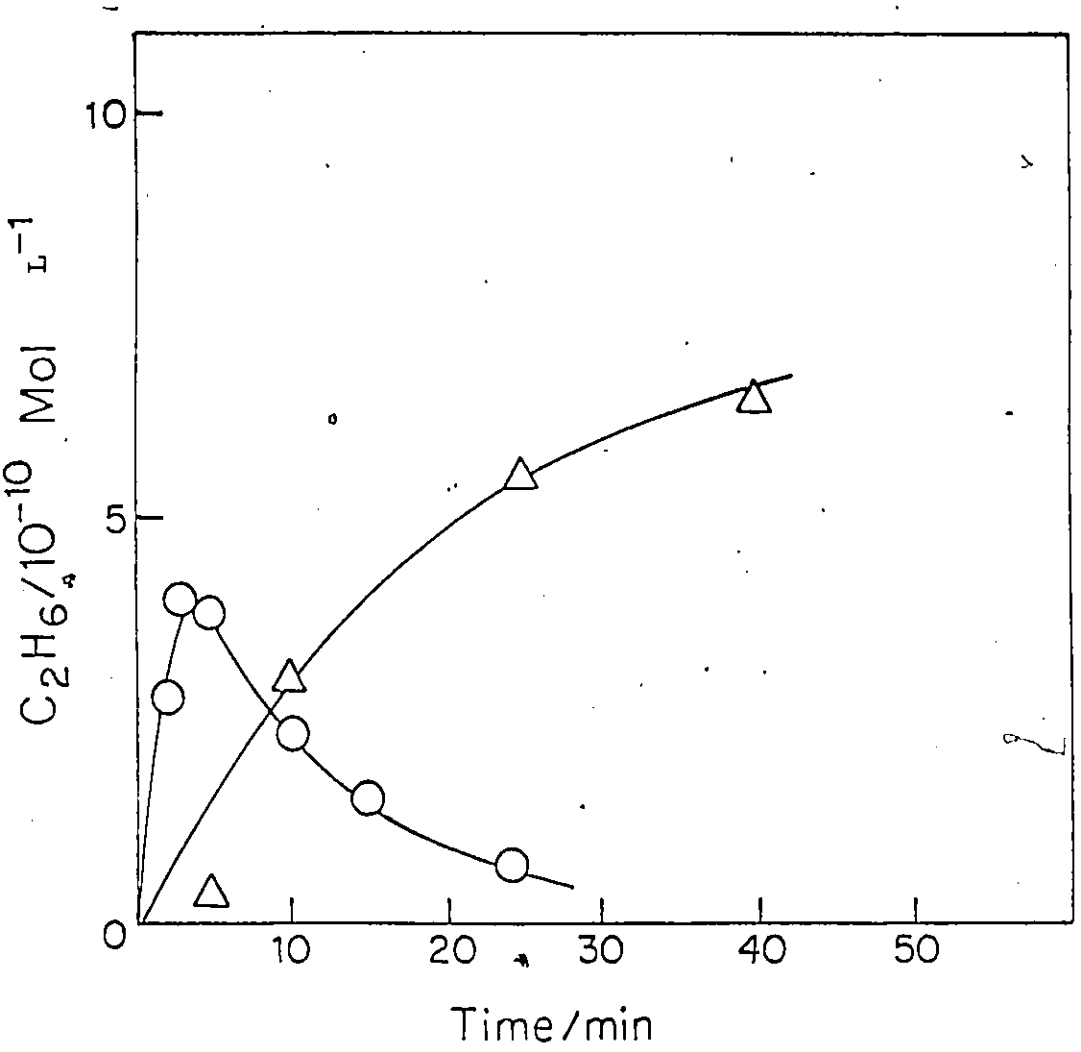

Figure 7. Yield of Ethane as a Function of Time. Pressure of Hydrogen 177 Torr

Δ - 908 K
O - 1111 K

Table 5

YIELD OF ETHANE AS A FUNCTION OF TIME

P_{H_2} = 177 Torr

T/K	Reaction Time/min.	Yield of $C_2H_6/10^{-10}$ mol $\cdot L^{-1}$
1111	3	3.98
	2	2.81
	5	3.79
	10	2.34
	15	1.53
	24	0.76
908	5	0.35
	10	3.00
	25	5.61
	40	6.51

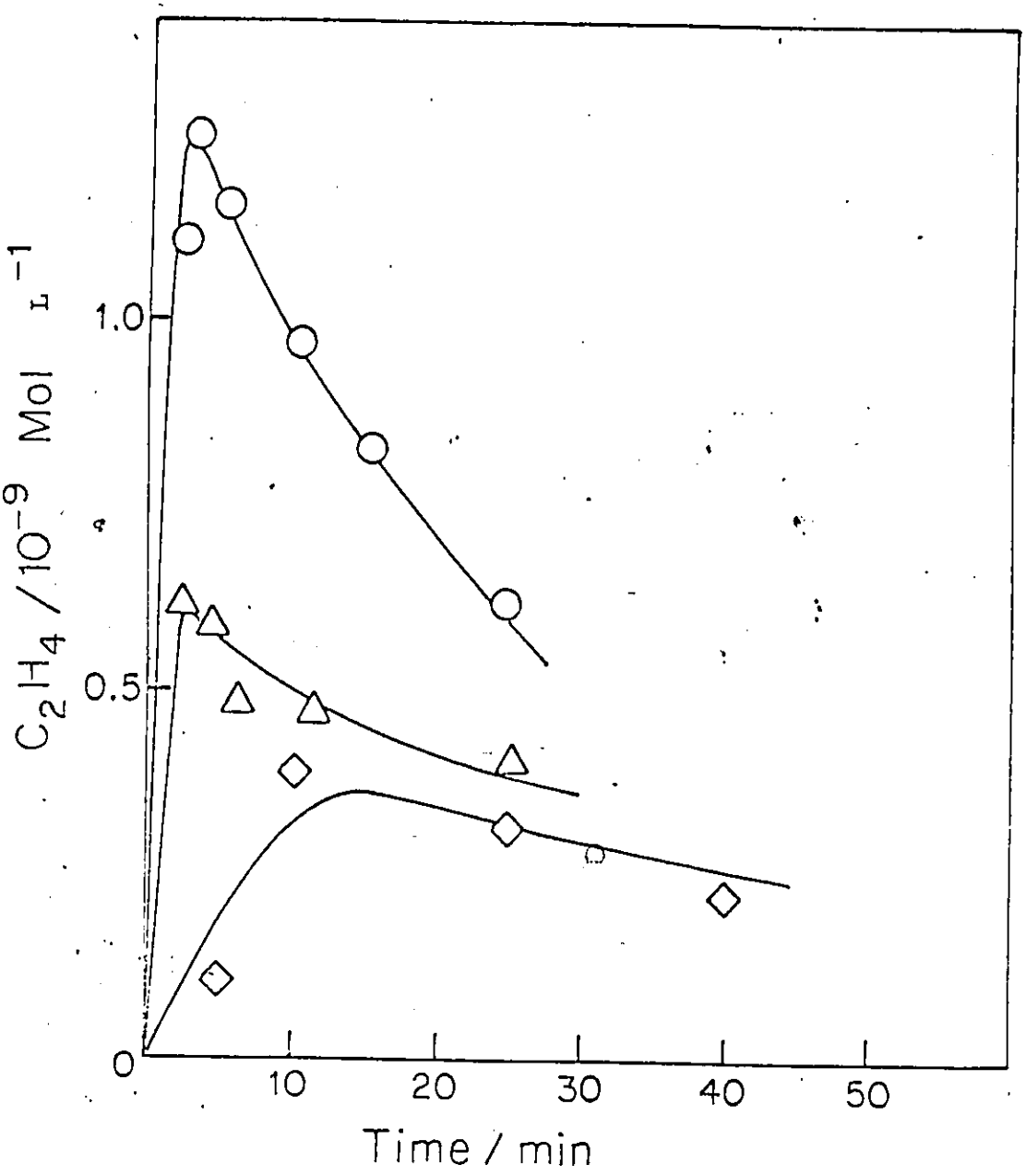

Figure 8. Yield of Ethylene as a Function of Time. Pressure of Hydrogen 177 Torr

◇ - 908 K
Δ - 1061 K
O - 1111 K

Table 6

YIELD OF C_2H_4 AS A FUNCTION OF TIME

PRESSURE OF HYDROGEN 177 Torr

T/K	Reaction Time/min.	Yield of $C_2H_4/10^{-9}$ mol L^{-1}
1111	2	1.10
	3	1.24
	5	1.15
	10	0.962
	15	0.796
	24	0.604
1061	2	0.619
	3	0.586
	6	0.479
	11	0.456
	25	0.411
908	5	0.112
	10	0.390
	25	0.312
	40	0.229

rate therefore does not signify an approach to equilibrium and in the present experiments the reverse formation of carbon from methane is probably not important. The reason for the observation of a limiting rate will be discussed later.

The ratios CH_4/C_2H_4 and CH_4/C_2H_6 as a function of time are shown in Figure 9 and Figure 10 for three temperatures. The fact that these ratios increase with time of reaction at high temperatures suggests that methane is formed by secondary reaction of C_2 hydrocarbons. Although there is some uncertainty in the measurement of these rates, it appears that the values extrapolate to a finite value at zero time. This suggests that a certain fraction of the methane is a primary product and may be formed directly on the surface. In the low temperature region these ratios changed very little with time of reaction. The secondary reactions of C_2 hydrocarbons leading to methane are therefore relatively unimportant in this region.

Because of the rapid disappearance of ethane and ethylene it was not possible to measure an initial rate of formation for these products. The initial rate of formation of methane was estimated by extrapolation of the rate as a function of time. A summary of the initial rates is given in Table 9. A log-log plot of these rates as a function of the initial pressure of hydrogen is shown in Figure 11. The order of the rate is about 0.5 ~ 0.6 over

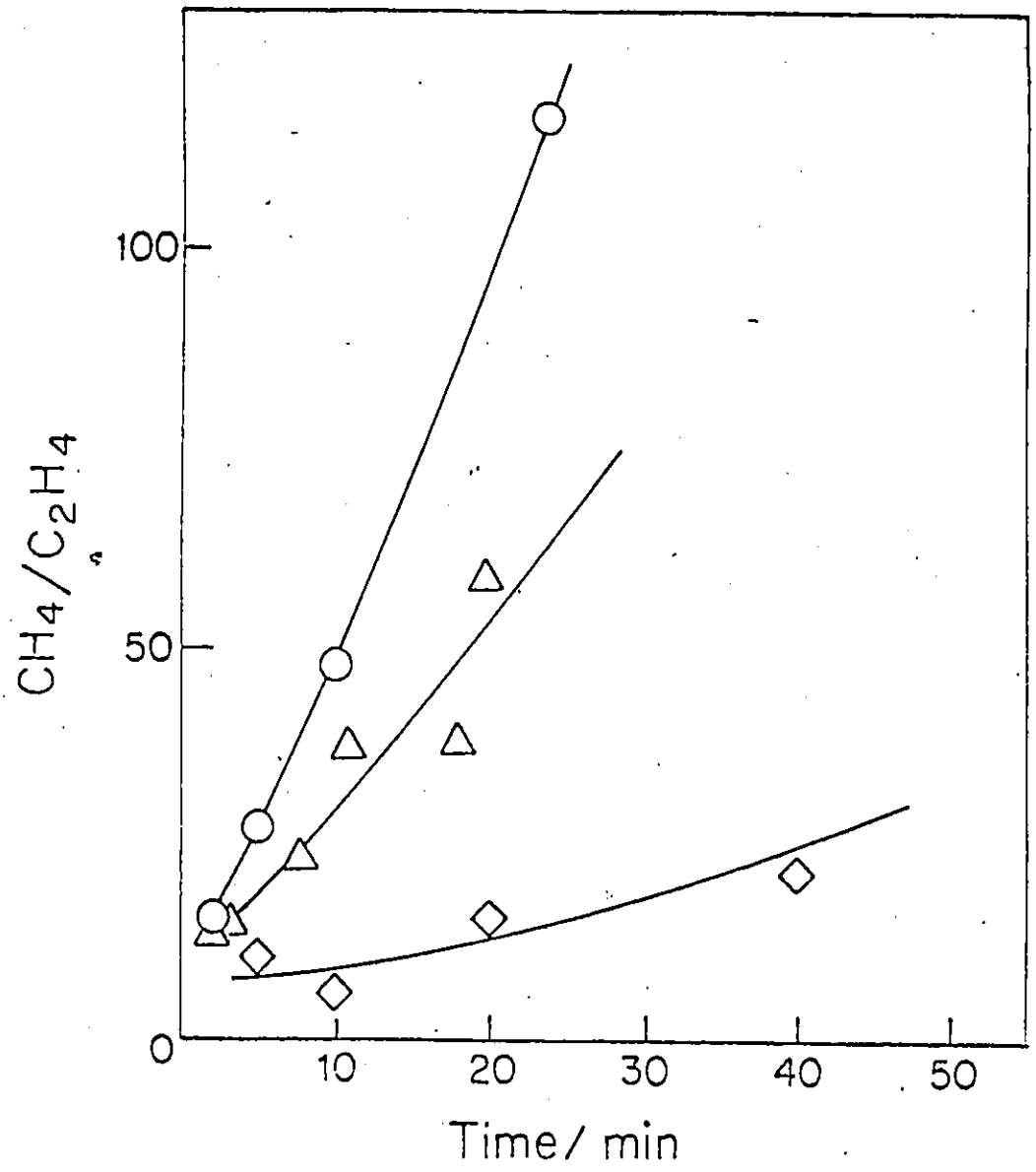

Figure 9. The ratio CH_4/C_2H_4 as a function of Time. Pressure of Hydrogen 177 Torr

◇ - 908 K
Δ - 1061 K
O - 1111 K

Table 7

THE RATIO CH_4/C_2H_4 AS A FUNCTION OF TIME

PRESSURE OF HYDROGEN 177 Torr

T/K	Time/min.	CH_4/C_2H_4
1111	2	15.9
	5	27.6
	10	47.8
	15	72.5
	24	116.3
1061	2	11.4
	3	14.3
	6	23.2
	11	37.9
	18	37.6
	25	58.5
908	5	11.1
	10	6.4
	25	15.4
	40	21.2

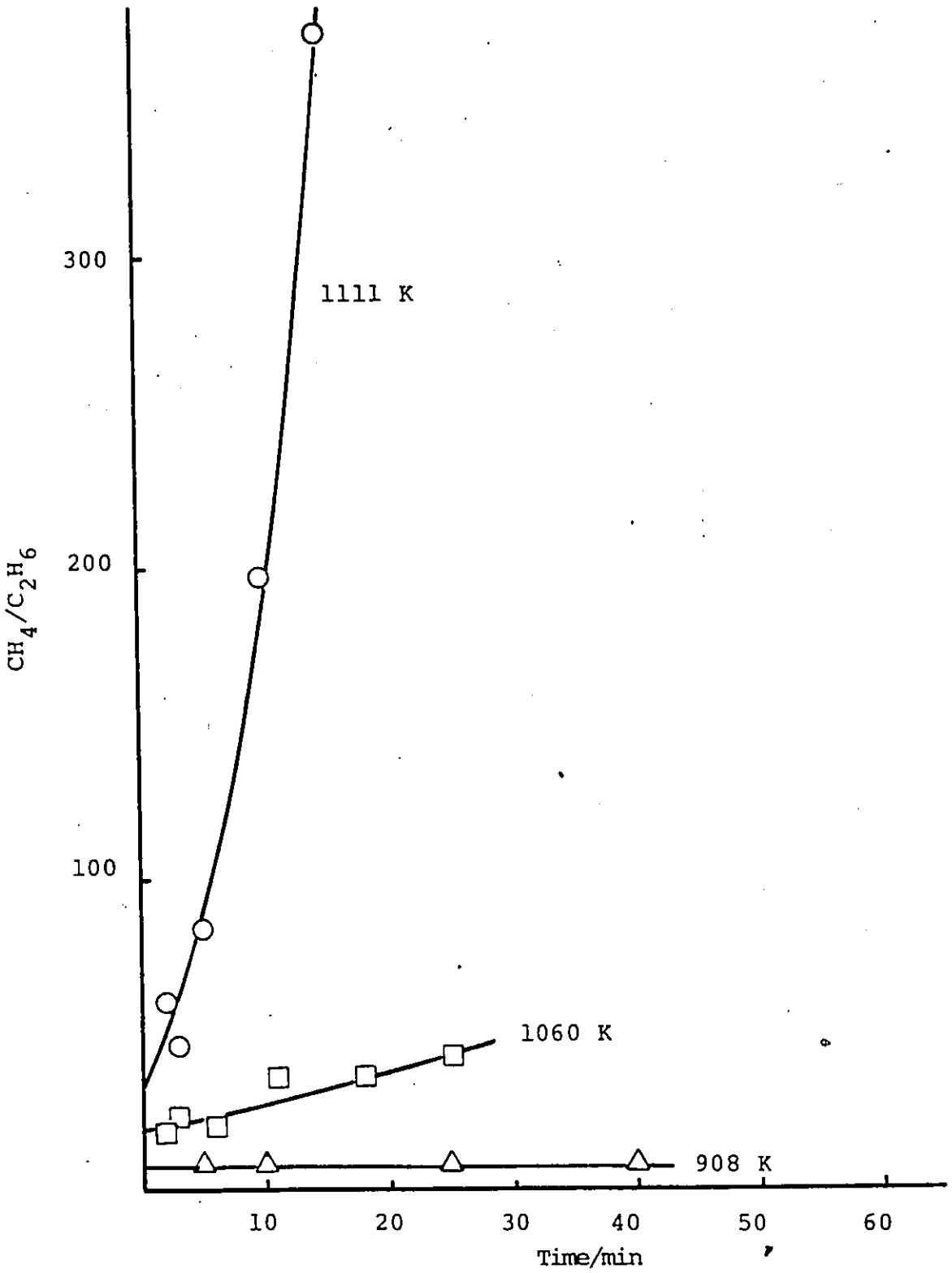

Figure 10. Ratio of CH_4/C_2H_6 as a function of reaction Time

O - 1111 K
□ - 1060 K
Δ - 908 K

Table 8

THE RATIO OF CH_4/C_2H_6 AS A FUNCTION OF TIME

PRESSURE OF HYDROGEN 177 Torr

T/K	Time/min.	CH_4/C_2H_6
1111	2	60.5
	3	45.5
	5	83.9
	10	197
	15	372
	24	900
908	5	8.2
	10	8.3
	25	8.6
	40	7.5
1061	2	18.2
	3	23.0
	6	19.9
	11	35.5
	18	35.6
	25	42.1

Table 9

INITIAL RATE OF FORMATION OF CH_4 AGAINST HYDROGEN PRESSURE

T/K	Pressure of H_2/Torr	$R_0/10^{-11}$ mol $L^{-1}s^{-1}$
1111	309.5	18.4
	177.0	14.2
	104.0	10.5
	54.0	6.27
1061	177.0	5.68
	307.0	8.60
	234.0	7.69
	109.0	6.18
	109.0	4.90
	75.0	4.62
961	177.0	3.47
	177.0	3.28
	306.0	4.58
	224.0	3.68
	120.5	2.52
	90.0	2.33
	109.0	2.32
910	177.0	2.85
	213.0	2.92
	105.0	2.26

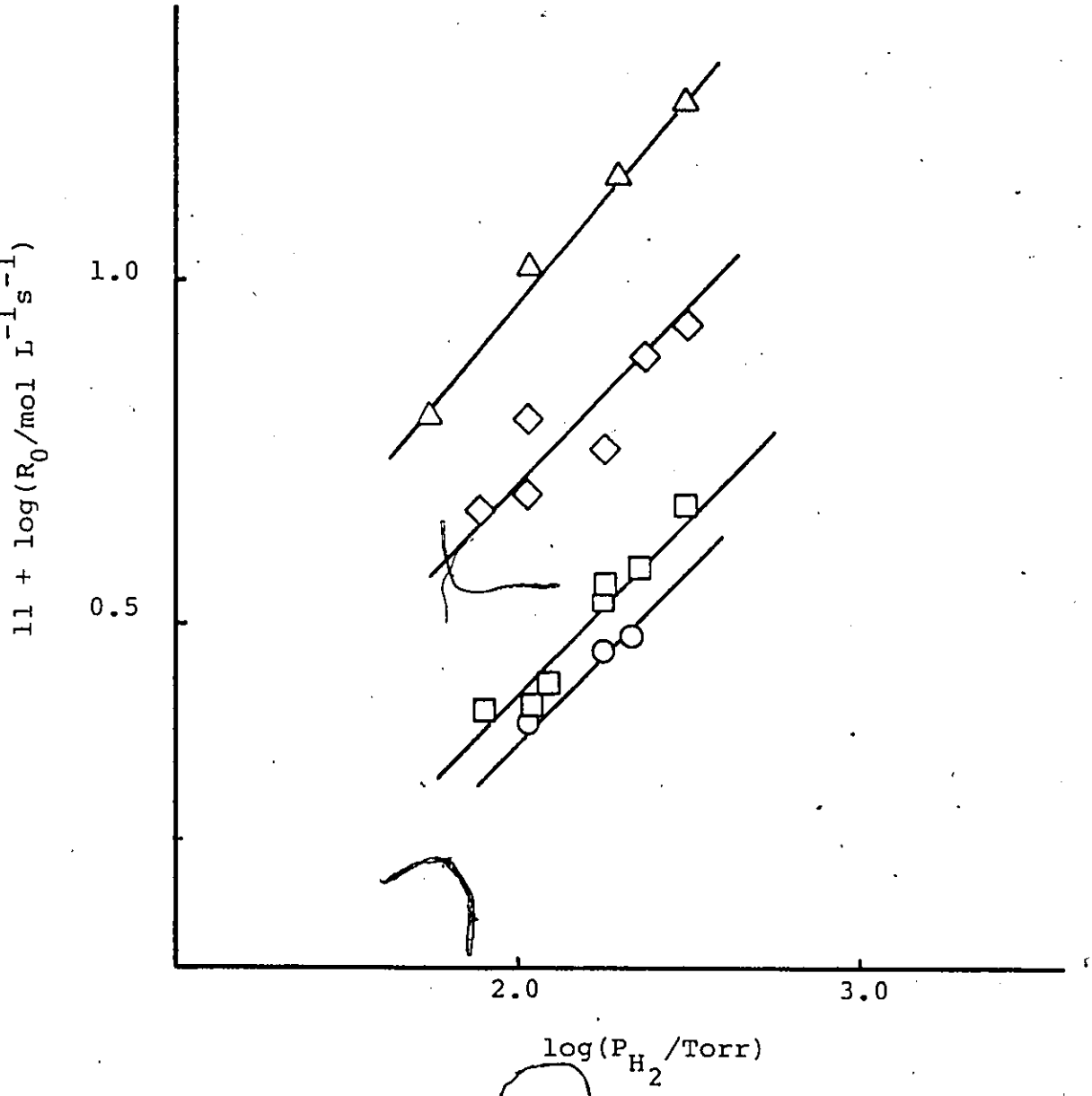

Figure 11. Logarithm of the Initial Rate of Formation of Methane Against Logarithm of the Pressure of Hydrogen

○ - 910 K
◇ - 961 K
□ - 1061 K
△ - 1111 K

the range of temperature 910-1111 K. The temperature dependence of the initial rate at a pressure of hydrogen of 177 Torr is shown in Figure 12. The dependence of the rate on temperature shows two distinct regions with different activation energies. In the high temperature region, 1050-1150 K, the activation energy is 51 kcal/mol while in the low temperature region, 1010-819 K, the activation energy is only 6 kcal/mol.

3.2 Mechanism of the Reaction

The observed change in activation energy indicates a fundamental change in the mechanism of the reaction over the range of temperature studied. Such changes are often observed in heterogeneous reactions. In some cases, a gradually increasing activation energy with increasing temperature has been observed and this behaviour has been called the compensation effect.[40] Several interpretations of this have been offered, but in general terms, processes with higher activation energy become increasingly important as the temperature is increased. The effect is common with surface reactions because these reactions usually involve a complex series of concurrent and consecutive elementary processes whose relative rates continuously change as the temperature is increased. In the present reaction there appear to be two regions, each with a fairly well-defined

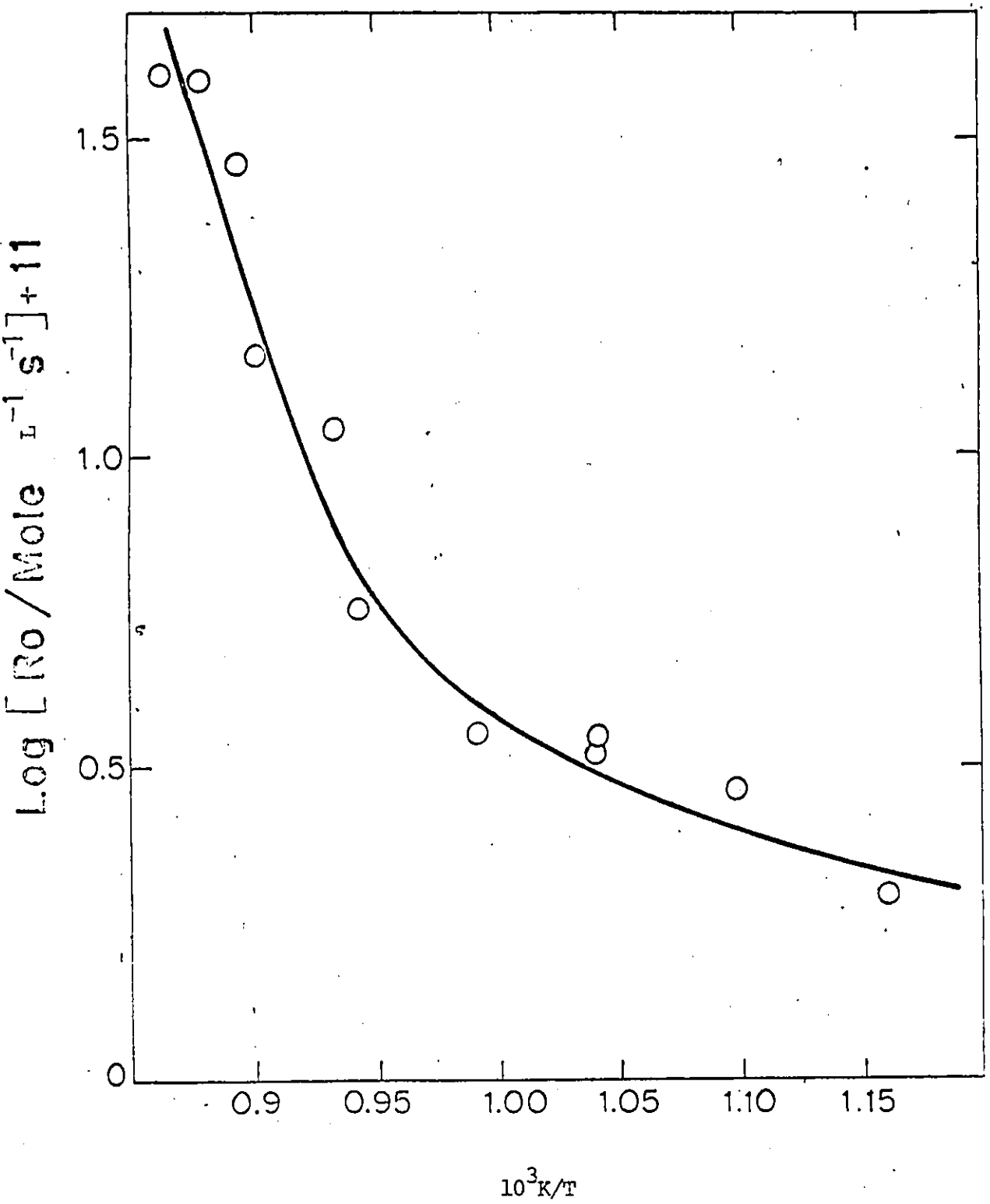

Figure 12. Logarithm of the Initial Rate of Formation of Methane as a Function of 1/T

Table 10

TEMPERATURE DEPENDENCE OF INITIAL RATE OF FORMATIION OF CH_4 HYDROGEN PRESSURE 177 Torr

T/K	$R_0/10^{-10}$ mol $L^{-1}s^{-1}$
1111	1.42
1061	0.560
1010	0.357
1138	3.89
1121	2.84
1072	1.08
961	0.347
961	0.328
911	0.284
862	0.199
1163	3.95

activation energy. In the low-temperature region, from 900-1010 K, the activation energy is 6.5 kcal/mol while in the high temperature region, from 1050-1150, the activation energy is 51 kcal/mol. A similar change in activation energy in this temperature region was reported by Corney and Thomas,[28] Barrer[1] and Breisacher and Marx.[29] The large increase in activation energy suggests that the change in mechanism may involve a transition from mainly heterogeneous to mainly homogeneous processes. The reactions occurring in each of these regions will be considered separately.

A. Heterogeneous Reaction

In the low temperature region, the ratios CH_4/C_2H_4 and CH_4/C_2H_6 (Figure 9 and 10) were essentially constant with time of reaction. It may be concluded that both products are formed directly through reactions occurring on the surface and subsequent reactions in the gas phase are negligible. The mechanism for hydrogenation proposed by Zielke and Gorin[12] may be reasonably modified to allow for the formation of C_2 hydrocarbons as well as methane. In this sequence of reactions, neighbouring carbon atoms in the graphite structure are hydrogenated until CH_3 groups are attained. Further reaction of the CH_3 group with hydrogen gives methane. If the intermediate structures resembling

ethylene and ethane are allowed a certain probability for desorption as molecules, the present results are qualitatively explained. The mechanism of Zielke and Gorin, with these modifications, may be written as follows:

(1) 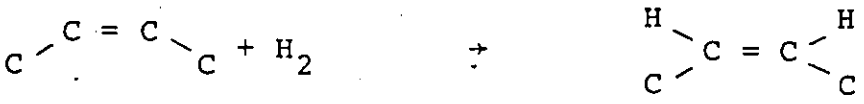

(2) 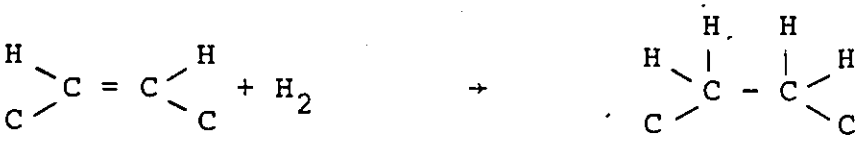

(3) 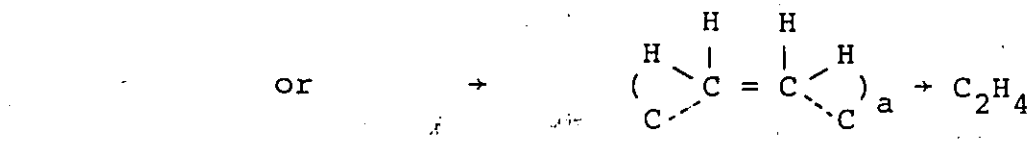

(4) 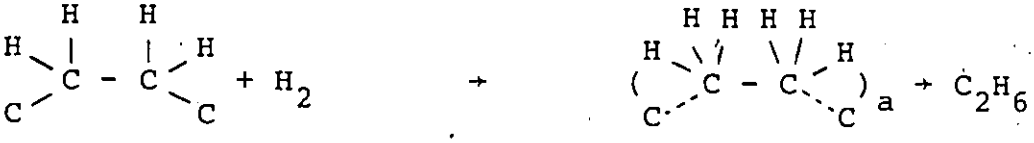

(5) 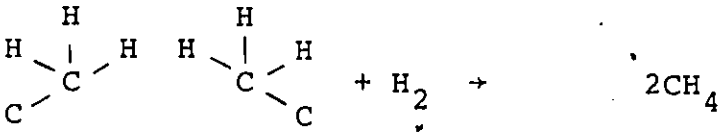

Here the hydrogenation is pictured as a simple addition of a molecule of hydrogen to the carbon surface with the possibility of desorption at any stage.

Since this mechanism was proposed, further knowledge has

accumulated on the nature of the adsorbed species on the carbon surface.[41] For example, it has been suggested that atoms and radicals may have a degree of mobility on the surface.[42] To allow for this the simplified scheme written above should be modified so that at each stage of hydrogenation the radical may migrate over the lattice. Combination of radicals during this process may form a molecule which may desorb with a probability which will depend on the temperature. For example,

$$(CH)_a + H_2 \rightarrow (CH_2)_a + H \quad (6)$$

$$(CH_2)_a + H_2 \rightarrow (CH_3)_a + H \quad (7)$$

$$(CH_2)_a + (CH_2)_a \rightarrow (C_2H_4)_a \rightarrow C_2H_4 \quad (8)$$

$$(CH_3)_a + H_2 \rightarrow CH_4 + H \quad (9)$$

$$(CH_3)_a + (CH_3)_a \rightarrow (C_2H_6)_a \rightarrow C_2H_6 \quad (10)$$

Thus the C_2 hydrocarbons need not be formed by hydrogenation of neighbouring carbon atoms, but a similar distribution of products could be obtained by either scheme. According to this mechanism, ethylene, ethane and methane are all primary products whose distribution depends on the competition between abstraction from hydrogen or dimerization of the intermediate radicals. The relative amount of the products also depends on the rate of desorption of the product molecule. In this regard, it is significant that acetylene was not detected at these temperatures, but has been reported

at higher temperatures. This may mean that the CH radicals have less mobility than the more hydrogenated radicals and the dimerization of CH does not compete with reaction with hydrogen. Alternatively, acetylene may be strongly adsorbed and further hydrogenation competes with desorption. With the mechanism proposed by Blackwood,[17][18] in which CH_4 is formed directly from the hydrogenation of the CH_2 radical, it is difficult to explain the fact that ethane is a primary product.

The overall activation energy for this series of hydrogenation steps will be a complex function involving the difference between the heat gained following the adsorption processes and the energy required for rearrangement and desorption. These values are not known for the reactions outlined above, but the adsorption processes could be sufficiently exothermic to allow a low overall activation energy, as observed.

B. Homogeneous Reactions

(a) Secondary Reaction of Ethane

The most noticeable distinguishing feature between the low-temperature and high-temperature regions is the relative importance of the products methane and ethane. In the low temperature region, ethane is an important product, but it gradually decreases in importance as the temperature is

increased and becomes negligible at the highest temperature. The decrease in ethane is balanced by an increase in methane. This change may be accounted for by the secondary thermal dissociation of ethane.

$$C_2H_6 \rightarrow 2CH_3 \qquad (11)$$

The rate of reaction (11) is slow in the low temperature region but in the high temperature region is sufficiently rapid to prevent accumulation of ethane in the gas phase. The rate constant for this homogeneous dissociation k_{11} is well established.[43] At 1111 K and a pressure of 177 Torr of ethane, the measured ratio k_{11}/k_{11}^{∞} was about 0.58.[83] This ratio represents the fall-off in k_{11} in the presence of a strong collider, the parent molecule ethane. In the present experiments, H_2 is the bath gas and the ratio k_{11}/k_{11}^{∞} would therefore be lower for a comparable pressure. From the results on the collisional efficiency of H_2, presented in Part 2, the ratio k_{11}/k_{11}^{∞} should be lower by a factor of about 0.1. Thus at 1111 K and 177 Torr of H_2, k_{11} may be estimated as $1.1 \times 10^{-2}\ s^{-1}$. The rate of dissociation of ethane may be expressed as

$$-\frac{d[C_2H_6]}{dt} = k_{11}[C_2H_6]$$

At the maximum yield of ethane under these conditions, 4×10^{-10} mol L^{-1}, the rate of dissociation is therefore

$$-\frac{d[C_2H_6]_m}{dt} = 4.3 \times 10^{-12} \text{mol } L^{-1}s^{-1}$$

This rate should be equal to the initial rate of formation of ethane. The measured rate of formation of C_2H_6 at two minutes reaction time (the shortest reaction time) is 2.3×10^{-12} mol $L^{-1}s^{-1}$. The initial rate would be slightly higher. If methane is formed solely by hydrogen abstraction from hydrogen by methyl radicals following dissociation of ethane, the rate of formation of methane at the maximum concentration of ethane would be 8.6×10^{-12} mol $L^{-1}s^{-1}$. The observed rate at this time (three minutes) is 9.2×10^{-11} mol $L^{-1}s^{-1}$. In other words, at 1111 K the yield of methane, formed through the homogeneous thermal dissociation of the product ethane in the gas phase, is about 8-10% of the total methane formed in the reaction, and is in agreement with the ratio CH_4/C_2H_6 at the initial time.

In the low temperature region the rate of dissociation of ethane is negligible compared to the observed rate of formation of methane. At 908 K, k_{11} in the presence of 177 Torr of H_2 was estimated as 1.0×10^{-5} s^{-1}. The yield of ethane at 10 minutes is 3.9×10^{-10} mol L^{-1} (Figure 7) and the rate of dissociation of ethane is therefore

$$-\frac{d[C_2H_6]}{dt} = 3.9 \times 10^{-15} \text{ mol } L^{-1}s^{-1}$$

The rate of formation of methane at this time is 3.0×10^{-12} mol $L^{-1}s^{-1}$. In this region, therefore, secondary dissociation of ethane is not sufficiently rapid to account for the rate of formation of methane.

(b) Secondary Reactions of Methane and Ethylene

The effect of additions of small amounts of methane and ethylene to the reactant hydrogen was investigated to test for the importance of these products in secondary reactions.

A series of experiments was made at 1111 K with a total pressure of 177 torr of hydrogen containing 41 ppm CH_4, corresponding to a concentration of 1.1×10^{-7} mol L^{-1}. The rate of formation of methane is not altered by the presence of methane in an amount comparable to that formed during a reaction. The rates of formation of the other products are also unchanged. Homogeneous secondary dissociation of methane is therefore not important under these conditions, as expected from the measured rate of the thermal dissociation of methane.[44] Experiments were made at 1111 and 908 K using hydrogen containing two different concentrations of ethylene: 9 ppm and 43 ppm. At each temperature the ethylene was rapidly consumed. At

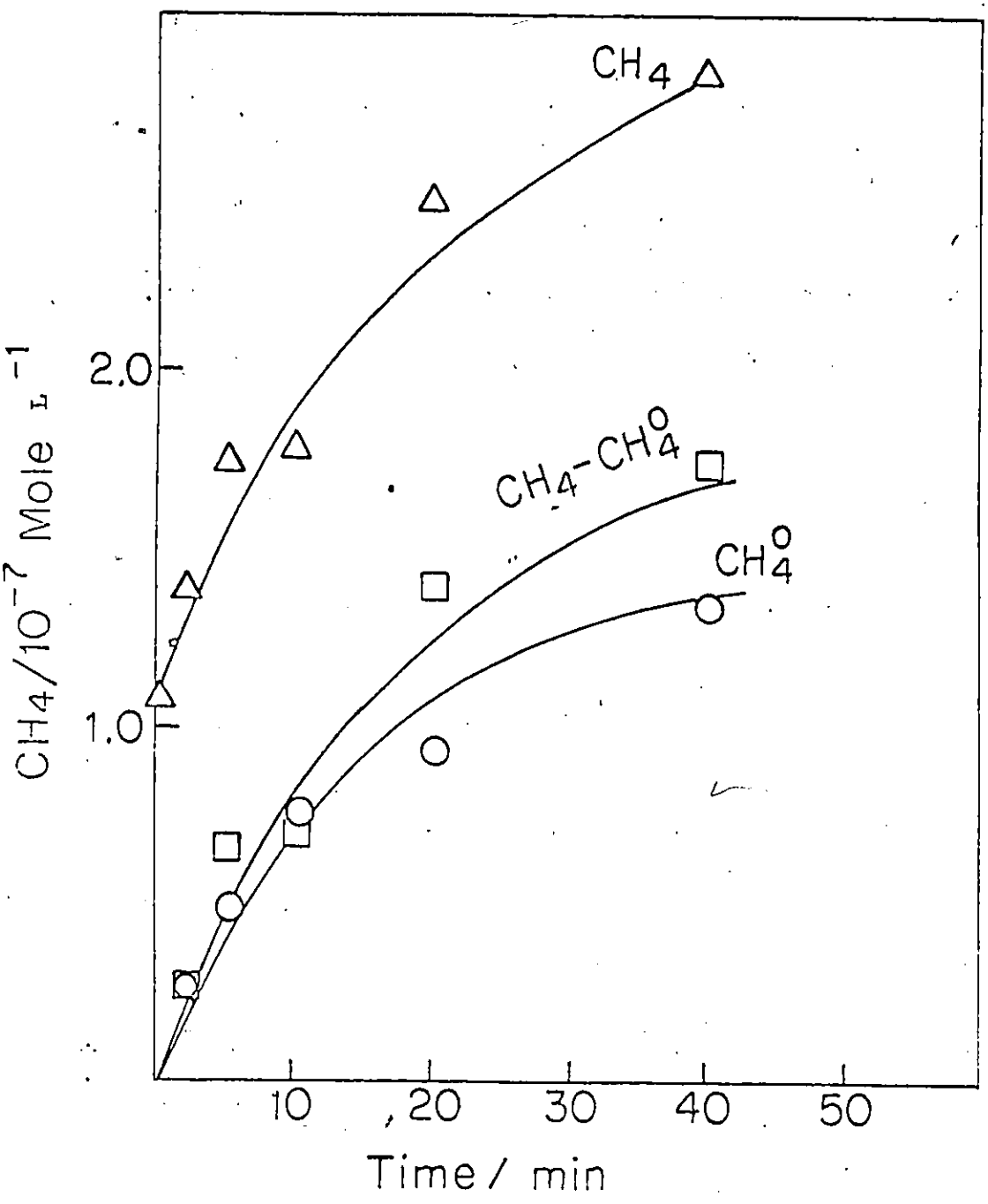

Figure 13. Yield of Methane as a Function of Time. Pressure of Hydrogen 177 Torr

O - Pure hydrogen
Δ - Hydrogen + 41 ppm CH_4

Table 11

YIELD OF CH_4 AS FUNCTION OF TIME AT 1111 K

PRESSURE OF HYDROGEN 177 Torr
INITIAL CONCENTRATION OF CH_4 IN H_2 41 ppm

Time/min.	$CH_4/10^{-7}$ mol L^{-1}
0	1.09
2	1.40
5	1.76
10	1.79
20	2.59
40	2.84

Figure 14. Yield of Products as a Function of Time. Pressure of Hydrogen 177 Torr with 43 ppm C_2H_4. 1111 K

O - CH_4

□ - C_2H_4

Δ - C_2H_6

■ - ΣC_2 (Equation (12))

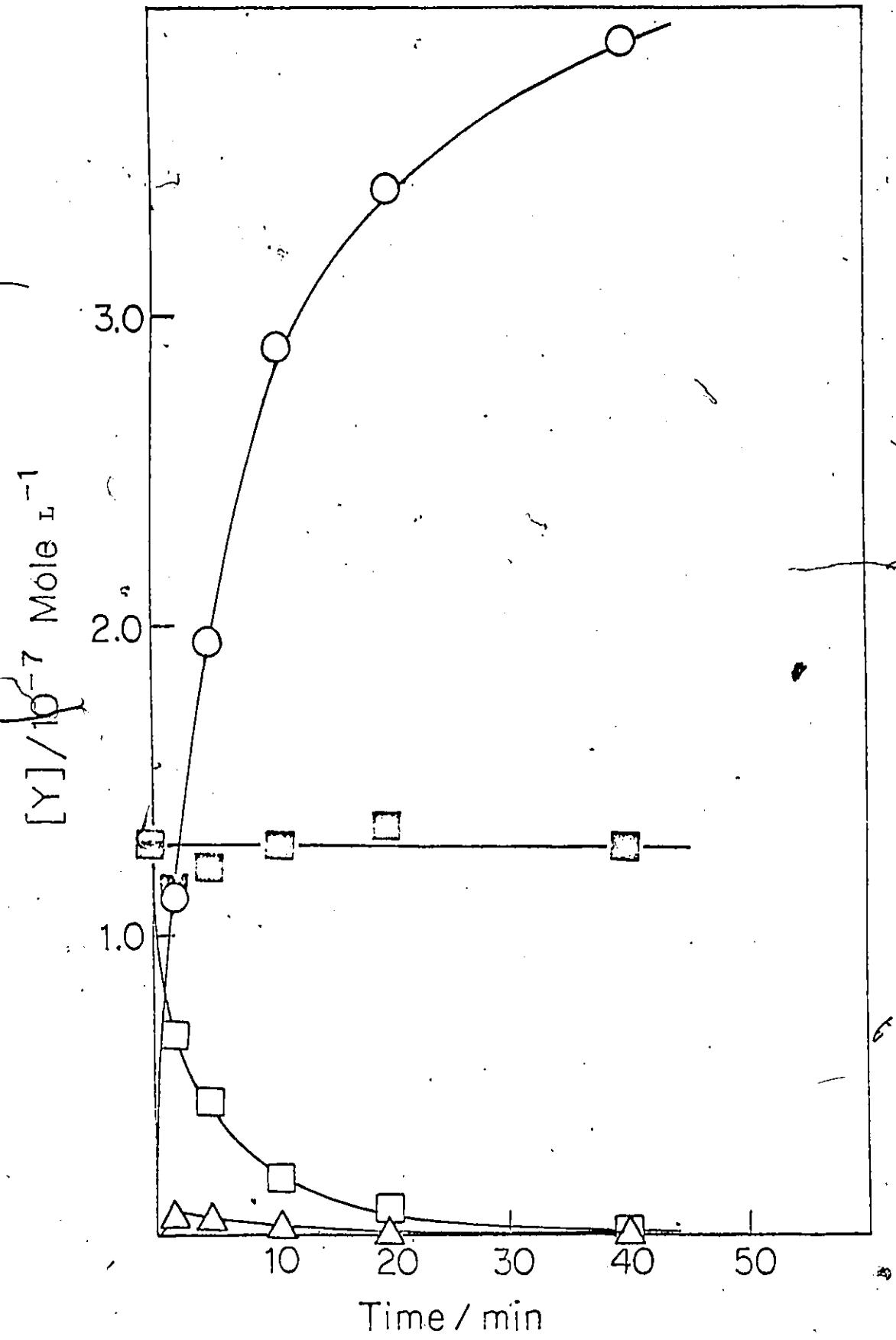
3.0
2.0
1.0
[Y] / 10⁻⁷ Mole L⁻¹
10
20
30
40
50
Time / min

Table 12

YIELD OF PRODUCTS OF THE REACTION OF CARBON WITH HYDROGEN CONTAINING 43 ppm C_2H_4 AT 1111 K
PRESSURE OF HYDROGEN 177 Torr

Time/min.	$CH_4/10^{-7}$ mol L^{-1}	$C_2H_4/10^{-7}$ mol L^{-1}	$C_2H_6/10^{-7}$ mol L^{-1}	$\Sigma C_2/10^{-7}$ mol L^{-1}
0	0	1.09	0	1.09
2	1.12	0.666	0.056	1.15
5	1.94	0.441	0.048	1.21
11	2.90	0.184	0.027	1.28
20	3.43	0.085	0.012	1.35
40	3.88	0.015	0.015	1.29

Figure 15. Yield of Products as a Function of Time. Pressure of Hydrogen 177 Torr with 43 ppm C_2H_4. 908 K

o - CH_4

□ - C_2H_4

Δ - C_2H_6

■ - ΣC_2 (Equation (12))

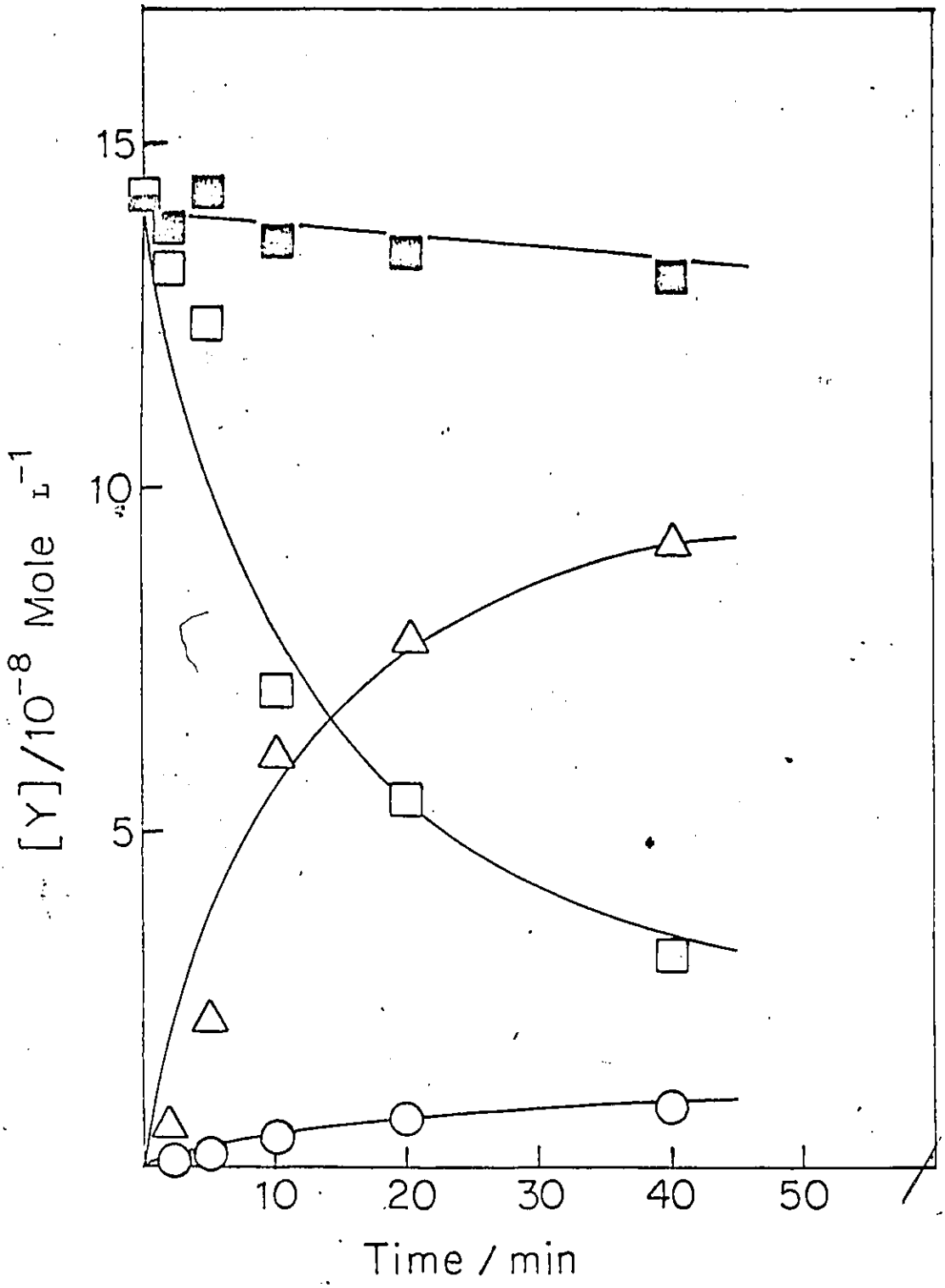
15
10
5
[Y] / 10⁻⁸ Mole L⁻¹
10
20
30
40
50
Time / min

Table 13

YIELD OF PRODUCTS OF THE REACTION OF CARBON WITH HYDROGEN CONTAINING 44 ppm C_2H_4 AT 908 K
PRESSURE OF HYDROGEN 177 Torr

Time/min.	$CH_4/10^{-4}$ mol L^{-1}	$C_2H_4/10^{-7}$ mol L^{-1}	$C_2H_6/10^{-7}$ mol L^{-1}	$\Sigma C_2{}^*/10^{-7}$ mol L^{-1}
0	0	1.35	0	1.35
2	1.40	1.32	0.070	1.38
5	2.44	1.24	0.221	1.43
10	4.77	0.698	0.613	1.35
20	7.46	0.548	0.781	1.33
40	9.29	0.311	0.912	1.31

$$\Sigma C_2 = \frac{1}{2}(CH_4 - CH_4^0) + (C_2H_6 - C_2H_6^0) + (C_2H_4 - C_2H_4^0)$$

1111 K (Figure 14) ethylene was converted almost entirely to methane with very little ethane. On the other hand, at 908K (Figure 15) ethylene was converted mainly to ethane with very little methane. A carbon balance for the reaction is given by the following expression:

$$\Sigma C_2 = \frac{1}{2}(CH_4 - CH_4^*) + (C_2H_6 - C_2H_6^*) + (C_2H_4 - C_2H_4^*) \quad (12)$$

where the starred quantity refers to the yield from pure hydrogen. This sum is shown in both figures. It is clear that ethylene is rapidly hydrogenated under these conditions.

To test the relative importance of homogeneous and heterogeneous reactions in the hydrogenation process, a further series of experiments was made with hydrogen containing 43 ppm ethylene in the absence of the carbon film. At 1111 K the rate of conversion of ethylene to methane was almost identical to that found in the presence of carbon (Figure 16). At 908 K the disappearance of ethylene was much faster in the absence of carbon. These results provide convincing evidence of the importance of the homogeneous hydrogenation reaction in the high temperature region.

Further experiments on hydrogenation of C_2H_4 in the presence of a large excess H_2 in the gas phase at 1100-1200 K have been performed and the results will be presented

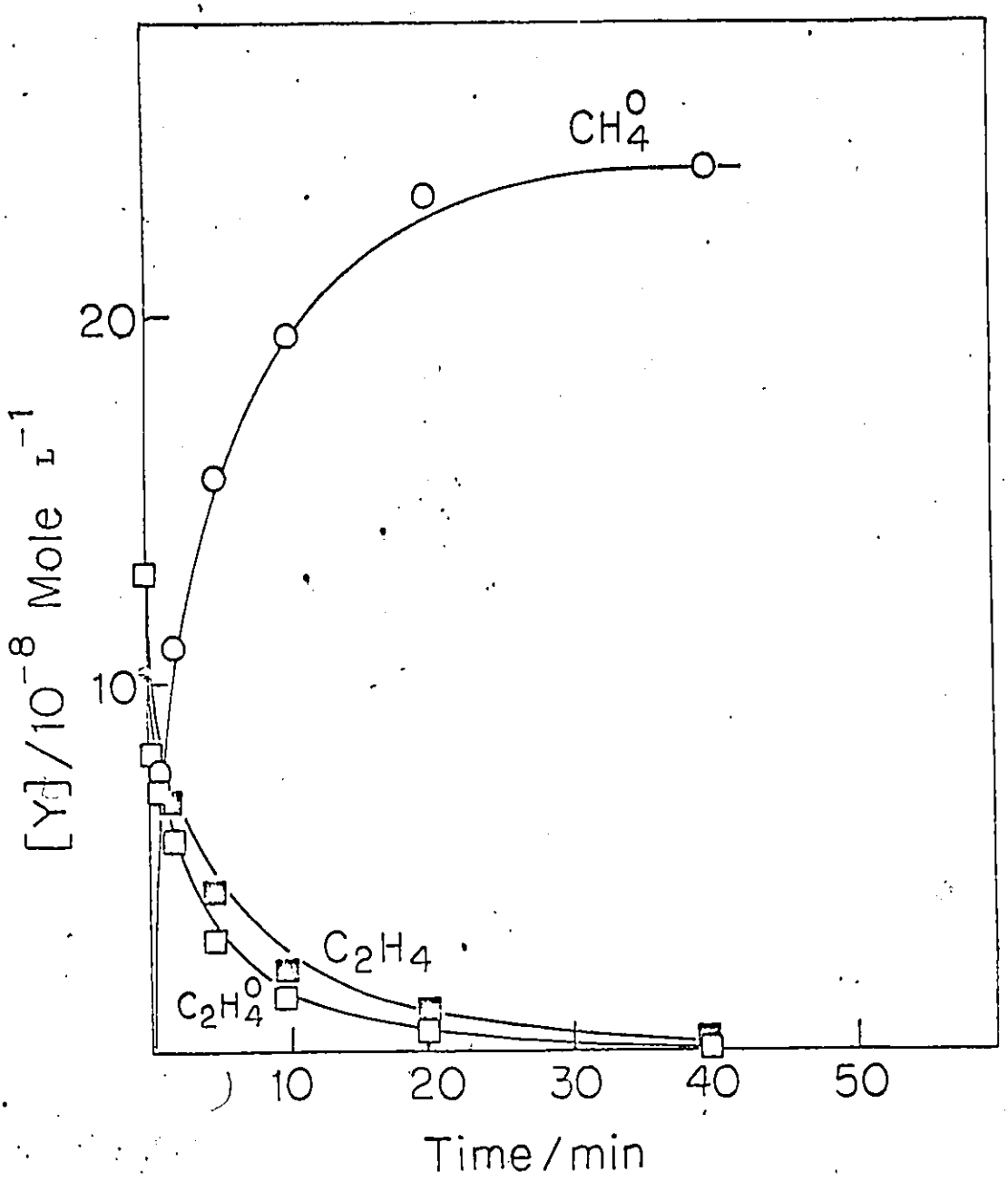

Figure 16. Yield of Products as a Function of Time. 1111 K. Pressure of Hydrogen 177 Torr with 43 ppm C_2H_4. Filled Symbols Refer to Experiments with the Carbon Film. Open Symbols Refer to Experiments Without the Carbon Film

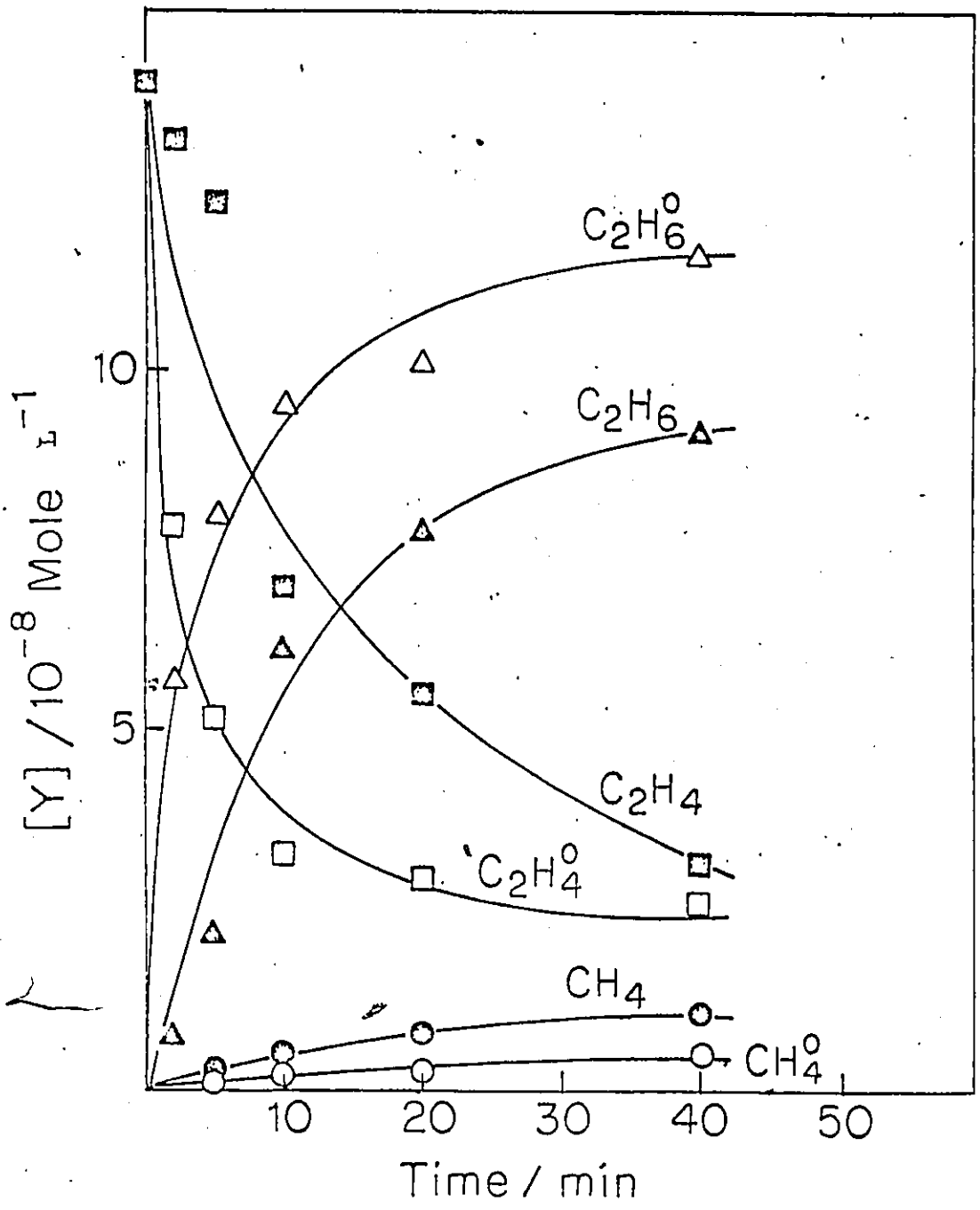

Figure 17. Yield of Products as a Function of Time. 908 K. Pressure of Hydrogen 177 Torr with 43 ppm. C_2H_4. Filled Symbols Refer to Experiments with the Carbon Film. Open Symbols Refer to Experiments Without the Carbon Film

Table 14

YIELD OF PRODUCTS AS A FUNCTION OF TIME WITHOUT THE CARBON FILM

T/K	Reaction Time/min.	$CH_4/10^{-7}$mol L^{-1}	$C_2H_6/10^{-7}$mol L^{-1}	$C_2H_6/10^{-7}$mol L^{-1}
1111	0	0	0	1.09
	1	0.755	0.0897	0.714
	2	1.10	0.0836	0.574
	5	1.56	0.0546	0.293
	10	2.33	0.0211	0.0436
	40	2.40	0.0050	0.0075
908	0	0	0	1.34
	2	0.0073	0.568	0.781
	5	0.0073	0.799	0.514
	10	0.0145	0.945	0.325
	20	0.0173	1.01	0.292
	40	0.0347	1.16	0.257

in Part Two of this thesis. It will be shown that the thermal dissociation of hydrogen provides a sufficient radical concentration for the homogeneous hydrogenation of ethylene under these conditions.

(c) The Mechanism of Carbon Hydrogenation Involving Atomic Hydrogen

As discussed earlier, the major portion of the methane formed is not the result of homogeneous reactions but rather arises through processes occurring on the carbon surface. Neither ratio CH_4/C_2H_4 nor CH_4/C_2H_6, extrapolates to zero at zero time. The value of $(CH_4/C_2H_4)^o$ was about 10 at all temperatures and values of $(CH_4/C_2H_6)^o$ were about 10, 20 and 30 at 908 K, 1060 K and 1111 K respectively. From Figure 10, it was observed that the rate of formation of methane increased very rapidly at temperatures above about 1010 K. This rapid increase in rate of the surface reaction must indicate the occurrence of a new initiation process. The observed activation energy of 51 kcal mol^{-1} in the high temperature region suggests that the thermal dissociation of hydrogen provides this initiation since the temperature coefficient for production of H atoms would be one-half the dissociation energy for the H_2 molecule. Hydrogen atoms may react directly with the carbon surface or with radicals adsorbed on the surface leading

to an increased rate of formation of products. The following represents such a series of reactions:

$$(CH)_a + H \rightarrow (CH_2)_a \quad (21)$$

$$(CH_2)_a + H \rightarrow (CH_3)_a \quad (22)$$

$$(CH_3)_a + H \rightarrow (CH_4)_a \rightarrow CH_4 \quad (23)$$

The reactions with hydrogen atoms would involve little activation energy[36][37][38] and the overall activation energy therefore should be close to one-half the heat of dissociation of hydrogen[45] or 52 kcal mol^{-1}. The rate of formation of CH_4 would depend on the concentration of hydrogen atoms. If H atoms are in equilibrium with H_2, the concentration of H atoms may be expressed as $[H] = K^{1/2} [H_2]^{1/2}$. The order of the rate of formation of CH_4, therefore, would be 0.5 with respect to H_2. The observed order with respect to H_2 was 0.5 ~ 0.6 (Figure 11). The final step in the formation of CH_4, reaction (23) may occur through reaction with an adsorbed H_2 molecule:

$$(CH_3)_a + H_2 \rightarrow (CH_4)_a + H \rightarrow CH_4 \quad (24)$$

A molecular beam study on the reaction between a carbon surface and molecular hydrogen showed that the sticking probability of molecular hydrogen on the carbon surface

was very low, less than 10^{-12}.[38] On the other hand, the sticking probability of a hydrogen atom on the carbon surface is between $10^{-2} \sim 10^{-4}$,[38] depending on the conditions. At 1100K and a pressure of 177 Torr, the equilibrium ratio $H/H_2 \approx 10^{-8}$. The rates of reaction (24) and (23) may, therefore, be comparable. Assuming the methyl radical attains a steady state concentration, the order with respect to H_2, based either on (23) or (24), would be 0.5.

The ethane and ethylene may be formed by the reactions

$$(CH_2)_a + (CH_2)_a \rightarrow (C_2H_4)_a \rightarrow C_2H_4$$
$$(CH_3)_a + (CH_3)_a \rightarrow (C_2H_6)_a \rightarrow C_2H_6$$

The ratios C_2H_4/C_2H_6 at zero time were about 1, 2 and 3 at 908 K, 1060 K and 1111 K respectively. The fact that the ratio C_2H_4/C_2H_6 increases with temperature suggests the mobility of CH_2 radicals on the surface increases with temperature relative to that of CH_3 radicals. The mobility of the radicals on the carbon surface increases in the following order

$$CH < CH_2 < CH_3 < H$$

H atoms on the surface are generally assumed to be mobile at all temperatures.

At high temperature the surface CH radicals may become sufficiently mobile to permit the formation of acetylene. C_2H_2 was reported[38][22-24] in appreciable yield only at temperatures above 2000 K.

It may therefore be concluded that at temperatures above 1100K thermal dissociation of hydrogen provides an important source of radicals which increase the rate of surface hydrogenation and the rate of secondary hydrogenation in the gas phase. Initiation by dissociation of hydrogen may be augmented by dissociation of ethane. The concentration of methyl radicals may be calculated from the following expression

$$[R] = \left[\frac{k_{11}[C_2H_6]}{k_t}\right]^{1/2}$$

where k_t is a radical termination rate constant. At 1111 K and 177 Torr of hydrogen, assuming a value of 10^{10} L mol^{-1}s^{-1} for k_t, [R] will equal the equilibrium concentration of hydrogen atoms when $[C_2H_6] = 10^{-8}$ mol L^{-1}. From Figure it may be seen that this concentration of ethane is not achieved at this temperature and initiation is therefore largely due to dissociation of hydrogen.

(d) Inhibition by Products

This mechanism provides a general picture of a product distribution involving methane, ethane and ethylene formed in surface reactions followed by further hydrogenation in the gas phase at sufficiently high temperatures. The mechanism however does not account for the decrease in the yield of ethylene and ethane with time beyond the maximum value or the decrease in the rate of formation of methane at longer times. In these experiments, neither of the reactants, carbon or H_2, was appreciably consumed.

Furthermore, the series of experiments with addition of methane and ethylene to the reactant hydrogen showed that neither of these products had an inhibiting effect on the hydrogenation reaction. This was clear in the case of ethylene by the sum ΣC_2, given by Equation (12), which indicates that the products from pure hydrogen are not reduced when small amounts of ethylene were added to the reactant.

A possible explanation of this effect may be an inhibition of the reaction on the surface before the products are desorbed. In the series of reactions represented by (6) to (10) further addition of radicals or atoms at any of the intermediate stages may occur to give higher molecular weight products. This may be regarded as a surface polymerization process and could lead to the formation of

ring compounds, partially hydrogenated, which might remain strongly adsorbed on the surface. Such compounds could remove active carbon atoms and inhibit the reactions leading to formation of ethylene. In this connection, it may be significant that during the course of the experiments it was observed that a reproducible surface was obtained only after sufficient evacuation time after each reaction, as shown in Figure 5. In fact, the rate measured immediately after an experiment was lower than the original rate, but returned to the original value as the evacuation time was increased. Attempts were made to trap with liquid nitrogen the material removed by pumping. Analysis showed the presence of small amounts of C_2 and C_3 hydrocarbons but no higher molecular weight compounds. These observations suggest that during the course of the reaction, higher molecular weight compounds may be formed on the surface which desorb slowly at the reaction temperature and after desorption decompose in the furnace to give lower molecular weight compounds. Such products may be unsaturated ring compounds which might be strongly adsorbed on the carbon surface.

3.3 The Effect of the Surface Oxide on the Reactivity of the Carbon Film

The importance of a strongly-bound surface oxide complex in the carbon-oxygen reaction has been discussed many times.[47]-[54] The role of the complex in the kinetics of the carbon-oxygen reaction is not well understood but results[51][55][56] have been reported which show that the rate of reaction depends on the fraction of carbon covered by the complex. It was suggested that the complex has an activating effect on the surrounding carbon atoms.

In the present experiments it was found that a carbon film kept at 1111 K under vacuum for several days appeared to show higher reactivity than usual, but returned to its normal reactivity after treatment with hydrogen at this temperature. The reason for this increased reactivity of the carbon film may be related to the adsorption of a small amount of oxygen accumulated in the system, with the consequent formation of the strongly-bound complex on the carbon surface. The present experiments were designed to investigate the effect of the surface oxide complex on the reaction between carbon and hydrogen.

The reaction of the carbon film with hydrogen, which contains a small amount of oxygen in the range from 30 to 1300 ppm, was studied at temperatures from 832 to 1114 K and at a total pressure of 177 Torr. Figure 18 shows the

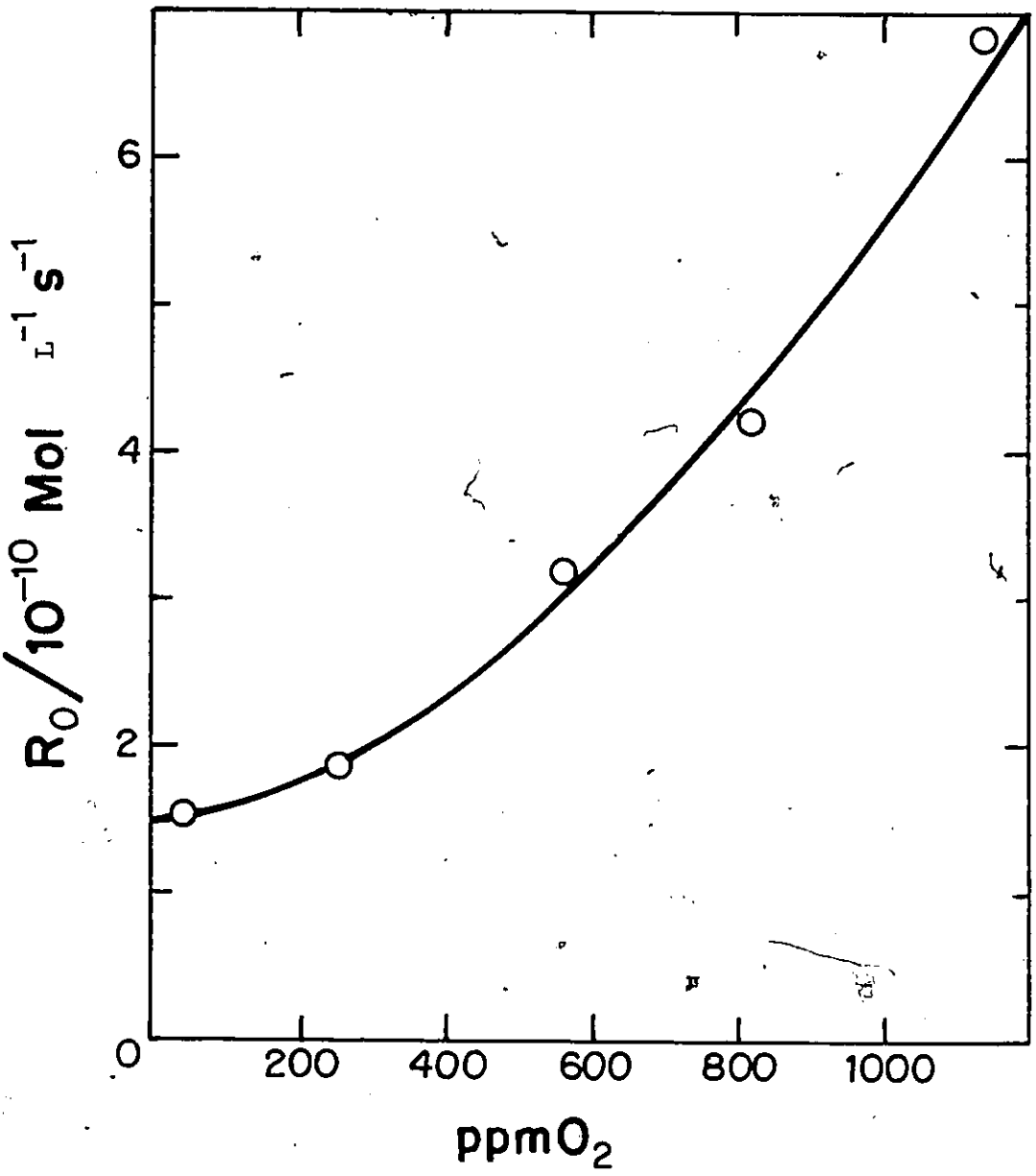

Figure 18. The Rate of Formation of Methane as a Function of Concentration of Oxygen in Hydrogen at 1111 K and Total Pressure of 177 Torr

Table 15 (Figure 18)

INFLUENCE OF OXYGEN ON THE REACTIVITY

(1111 K 177 Torr)

Concentration of O_2 in H_2 (ppm)	Initial Rate of Formation of CH_4 $R_0/10^{-10}$ mol $L^{-1}s^{-1}$
30	1.54
246	1.85
553	3.17
816	4.21
1130	6.81

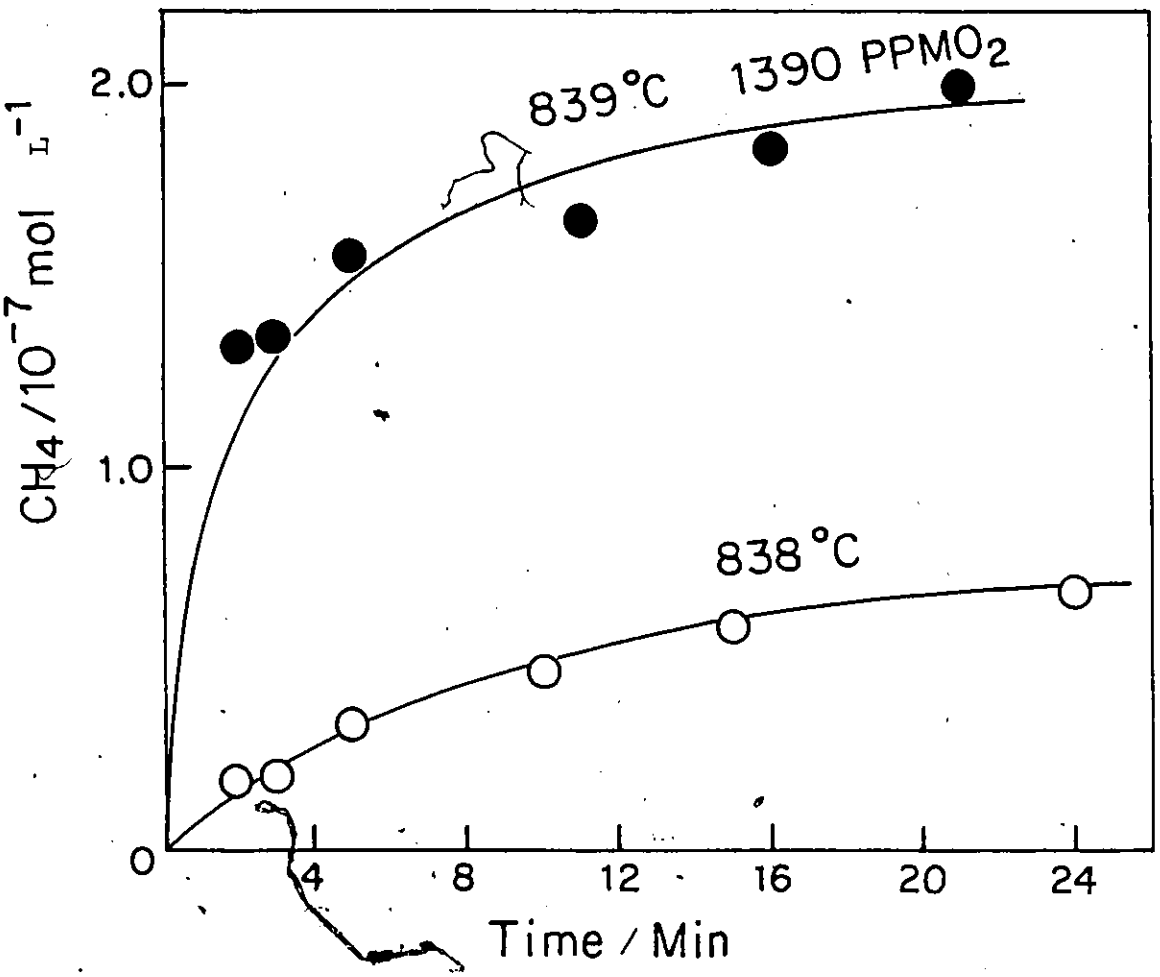

Figure 19. Methane Yield-Time Curves at 1112 K and Total Pressure of 177 Torr. Open Symbols Refer to the Reaction with Pure Hydrogen. Filled Symbols Refer to the Reaction with Hydrogen Containing 1390 ppm O_2

Table 16 (Figure 19)

YIELD OF CH_4 AS A FUNCTION OF TIME

Temp. = 1112 K
Total Pressure = 177 Torr
Concentration of O_2 in H_2
1390 ppm

Time/min.	Yield $CH_4/10^{-7}$ mol L^{-1}
2	1.31
3	1.34
5	1.54
11	1.64
16	1.83
21	1.99

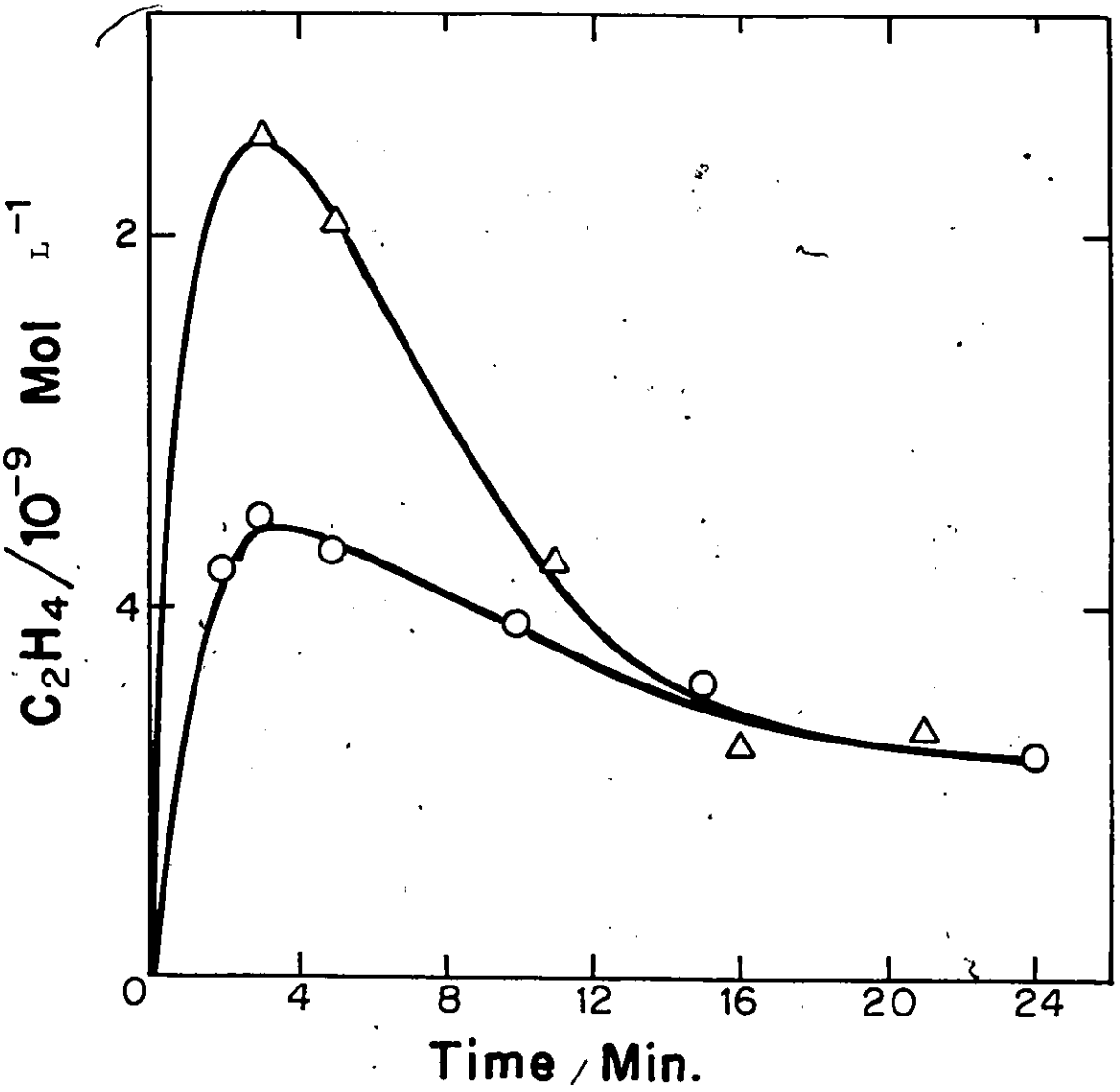

Figure 20. Yield of C_2H_4 as a Function of Time at 1112 K, 177 Torr

Δ - Represents the Reaction with Hydrogen Containing 1390 ppm O_2

0 - Represents the Reaction with Pure Hydrogen

Table 17 (Figure 20)

YIELD OF C_2H_4 AS A FUNCTION OF TIME

Temp. = 1112 K
Total Pressure = 177 Torr
Concentration of O_2 in H_2
1390 ppm

Time/Min.	Yield of $C_2H_4/10^{-9}$ mol L^{-1}
2	2.08
3	2.27
5	2.03
11	1.13
16	0.63
21	0.68

Pure H_2

Time/Min.	Yield of $C_2H_4/10^{-9}$ mol L^{-1}
2	1.10
3	1.24
5	1.15
10	0.96
15	0.80
24	0.60

dependence of the initial rate of methane formation on the oxygen concentration in hydrogen at 1111 K and at a total pressure of 177 Torr. Figures 19 and 20 show the yield-time curves of the products CH_4 and C_2H_4 with pure hydrogen and with hydrogen containing 1390 ppm O_2. These results clearly show that these small amounts of oxygen have a positive effect on the rate of the reaction of carbon with hydrogen. In addition to the hydrocarbon products (CH_4, C_2H_4, C_2H_6), water and CO were also observed from the reaction with mixtures of hydrogen containing 1390 ppm O_2. The product CO_2 was not detected. The yield-time curves for H_2O and CO at 1115 K and 934 K are shown in Figure 21. The yield of H_2O, about 2200 ppm from the mixture of 1390 ppm O_2 formed rapidly at the beginning of the reaction, is unchanged within experimental error over the course of the reaction. This fact points out that the reaction between H_2 and O_2 is very fast at these temperatures and that most of the O_2 converts immediately into H_2O. The CO yield-time curve at 1115K shows a fast initial rate of formation which rapidly falls with time, causing the yield to pass through a maximum, at which the concentration of CO in the gas phase is about 110 ppm. After the maximum, the yield of CO falls until a limiting concentration of about 15 ppm CO is attained.

The CO yield-time curve at 1115 K can be considered in four stages: a) the initial rate; b) at the maximum

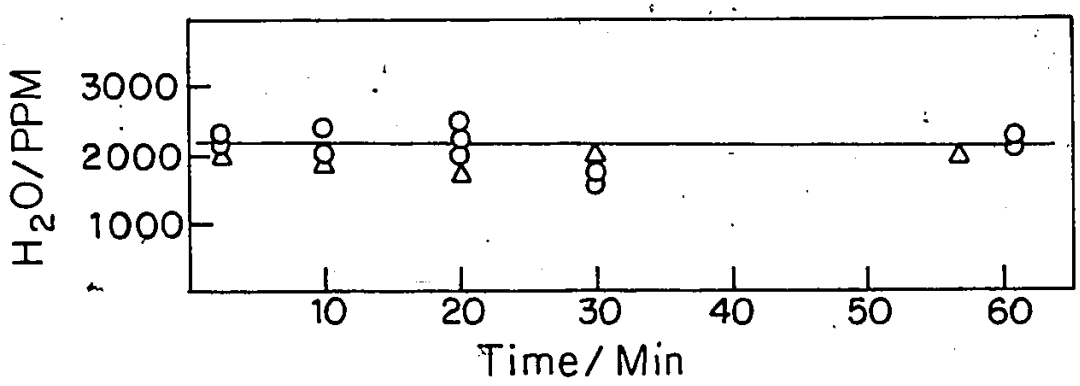

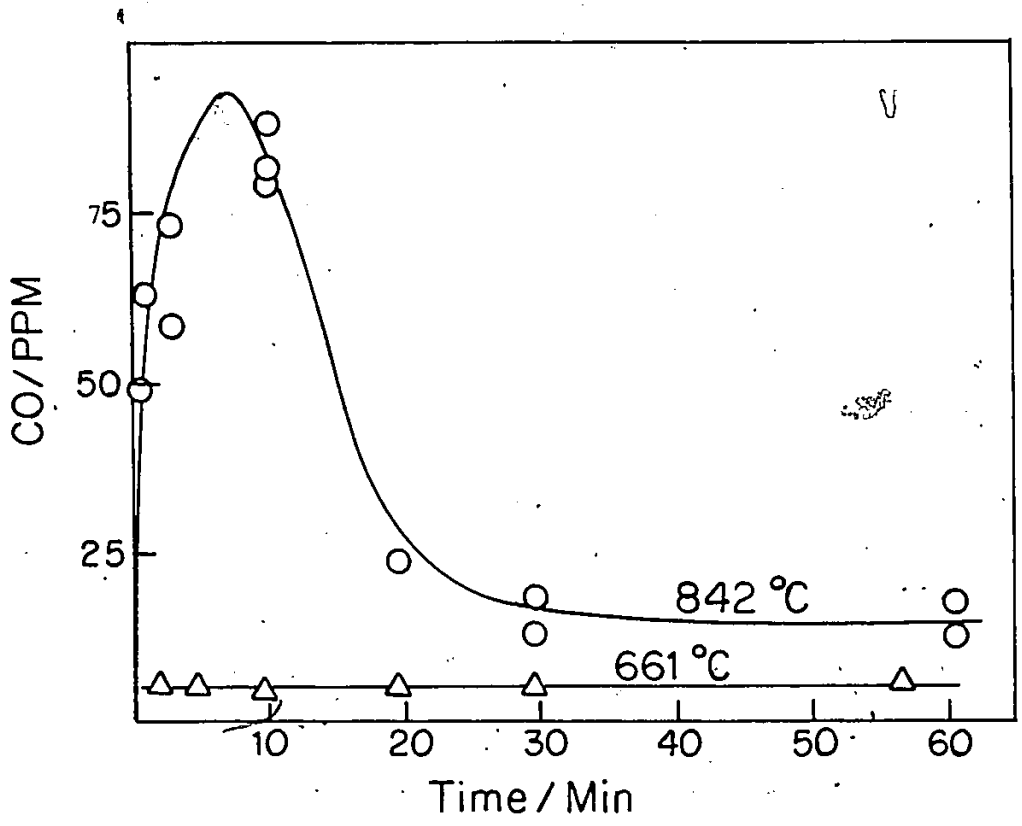

Figure 21A. Yield of H_2O as a Function of Time.
Figure 21B. Yield of CO as a Function of Time.

Table 18 (Figure 21)

YIELD OF H_2O AND CO AS A FUNCTION OF TIME

Temp. 1115 K
Total Pressure 484 ~ 520 Torr
Concentration of O_2 in H_2
1390 ppm

Time/Min.	CO/ppm	H_2O/ppm
1	63.1	-
1	48.5	-
3	73.3	2200
3	58.3	2300
10	87.9	-
10	81.1	2000
10	79.1	2370
20	23.3	-
20	-	2200
20	-	2000
20	-	2500
30	12.6	1500
30	18.0	1740
61	12.1	2100
61	13.5	2300

Table 19 (Figure 21)

YIELD OF H_2O AND CO AS A FUNCTION OF TIME

Temp. 934 K
Total Pressure 468 - 405 Torr
Concentration of O_2 in H_2
1400 ppm

Time/Min.	CO/ppm	H_2O/ppm
3	5.3	2000
5	4.4	1850
10	4.4	1960
20	5.3	1690
30	5.3	1900
57	6.8	1900

concentration of CO in the gas phase; c) the fall in yield with time; d) the equilibrium concentration of CO. The interpretation of the reaction occurring in each of these stages will be considered in the following paragraphs.

In the initial stage it appears from Figure 21 that most of the oxygen reacts rapidly with hydrogen to form H_2O and only a small part of the O_2 undergoes adsorption on the carbon surface with possible formation of the surface complex, [C-O]. Because the yield of H_2O does not change during the reaction this initial partition of the O_2 in the gas phase between formation of H_2O and adsorption on the surface must occur in a time short compared to the measured time. The partial pressure of O_2 in the gas phase should therefore instantly drop to a very low value. The adsorbed O_2 does not react further with H_2 to give water, but rather undergoes a slow desorption to release CO. This behaviour is characteristic of the strongly-bound surface complex. In these experiments the initial concentration of O_2 is about 1390 ppm O_2. Formation of 2200 ppm H_2O corresponds to consumption of 1100 ppm O_2. Therefore about 290 ppm O_2 may be adsorbed on the carbon surface. The concentration of complex on the surface may be expressed as mol cm^{-2} taking the surface area of the carbon film as equal to the area of the vessel[34] (as discussed in Chapter 2), and assuming one molecule of O_2 gives two molecules of complex. In these experiments

the concentration of complex is 1.02×10^{-9} mol cm^{-2}. The initial rate of desorption of CO can be estimated from the yield-time curve to be 2.4×10^{-9} mol $L^{-1}s^{-1}$. If this rate is expressed in terms of the concentration of complex

$$R^{o}_{CO} = k_d \, [C \ldots O]_o \qquad (3\text{-}1)$$

where R^{o}_{CO} is the initial rate of CO desorption, k_d is the rate constant of desorption, and $[C \ldots O]_o$ is the surface concentration of complex at initial time. k_d is therefore $2.31 \times 10^{-3}s^{-1}$ at 1115 K. Using the frequency factor $3 \times 10^{12}s^{-1}$ suggested by Olander,[37] the activation energy of desorption can be estimated to be about 80 kcal mol^{-1}. The total concentration of carbon on the surface in these experiments was 4×10^{-7} mol cm^{-2}. The ratio of the number of carbon atoms covered by the complex to the total number of atoms of carbon is therefore $1.02 \times 10^{-9} / 4 \times 10^{-7} = 2.6 \times 10^{-3}$. This ratio is in agreement with similar estimates based on measurements of the surface area of the carbon used.[48] Because the CO disappears during the course of the reaction, it must be concluded that reaction with H_2 occurs in the gas phase. The concentration of CO in the gas phase is too low to allow a significant rate of adsorption onto the carbon surface.

At the maximum concentration of CO in the gas phase, the rate of desorption of CO will equal the rate of disappearance of CO. The reaction between H_2 and CO may be expressed as

$$-\frac{d[CO]}{dt} = k_r[CO][H_2]^n$$

and therefore

$$k_d[C...O]_m = k_r[CO]_m[H_2]^n \qquad (3\text{-}2)$$

where the rate of disappearance of CO is assumed to be first order with respect to CO but of unknown order with respect to H_2. In Equation (3-2), $[C ... O]_m$ represents the surface concentration of complex at the time of maximum concentration of CO in the gas phase.

We define θ as the ratio of the concentration of complex [C ... O] on the surface at any time to the concentration at the initial time $[C ... O]_o$.

$$\theta = [C ... O]/[C ... O]_o$$

At the maximum gas-phase concentration of CO, according to Equation (3-2), θ may be expressed as follows:

$$\theta_m = \frac{[C \ldots O]_m}{[C \ldots O]_o} = \frac{k_r[CO]_m[H_2]^n}{R^o_{CO}} = \frac{k_r[H_2]^n}{R^o_{CO}}[CO]_m \qquad (3\text{-}3)$$

It will be shown in the next paragraph that the term $k_r[H_2]^n$, which is independent of reaction time, can be evaluated from the third region of the yield-time curve for CO. From this value, the maximum concentration of $[CO]_m$ in the gas phase and the initial rate of desorption of CO, θ_m can be calculated to be 0.13.

After the maximum concentration of CO in the gas phase, the rate of desorption of CO decreases rapidly since the surface concentration of complex is greatly depleted ($\theta < 0.1$). The observed rate of disappearance of CO may, to a good approximation, be due solely to the reaction between H_2 and CO.

$$-\frac{d[CO]}{dt} = k_r[CO][H_2]^n$$

or

$$-\frac{d \log[CO]}{dt} = k_r[H_2]^n$$

At constant temperature and pressure of H_2, $k_r[H_2]^n$ should be a constant. The smoothed curve obtained in this region was plotted as log[CO] as a function of time. From the linear portion a rough estimate for $k_r[H_2]^n$ was obtained

of $1.1 \times 10^{-3} s^{-1}$ at 1115 K. This value was used for the calculation of θ_m in the preceeding paragraph.

The final region of the CO yield-time curve shows that the concentration of CO approached a limiting value (15 ppm). This may indicate the establishment of various equilibria involving gas phase reactions and heterogeneous reactions of CO. If, in this region where the coverage is low, it is assumed that the coverage of the surface by the complex does not change with time and is proportional to the CO concentration in the gas phase, then the relative surface concentration of complex θ may be estimated as follows

$$\theta = \frac{[CO]}{[CO]_m} \cdot \theta_m = \frac{15 \text{ ppm}}{110 \text{ ppm}} \times 0.13 = 0.018$$

Now the variation of θ over the course of the reaction is illustrated in Figure 22. This variation can be compared with the variation in the rate of formation of CH_4 in the presence of 1390 ppm O_2. Both functions decrease rapidly in the early stage of the reaction while θ approaches the final limiting value. The rate of CH_4 formation also tends to a limiting value, which is comparable with the rate of the reaction with pure hydrogen. Thus the rate of formation of CH_4 appears to be related to θ, the relative surface concentration of complex.

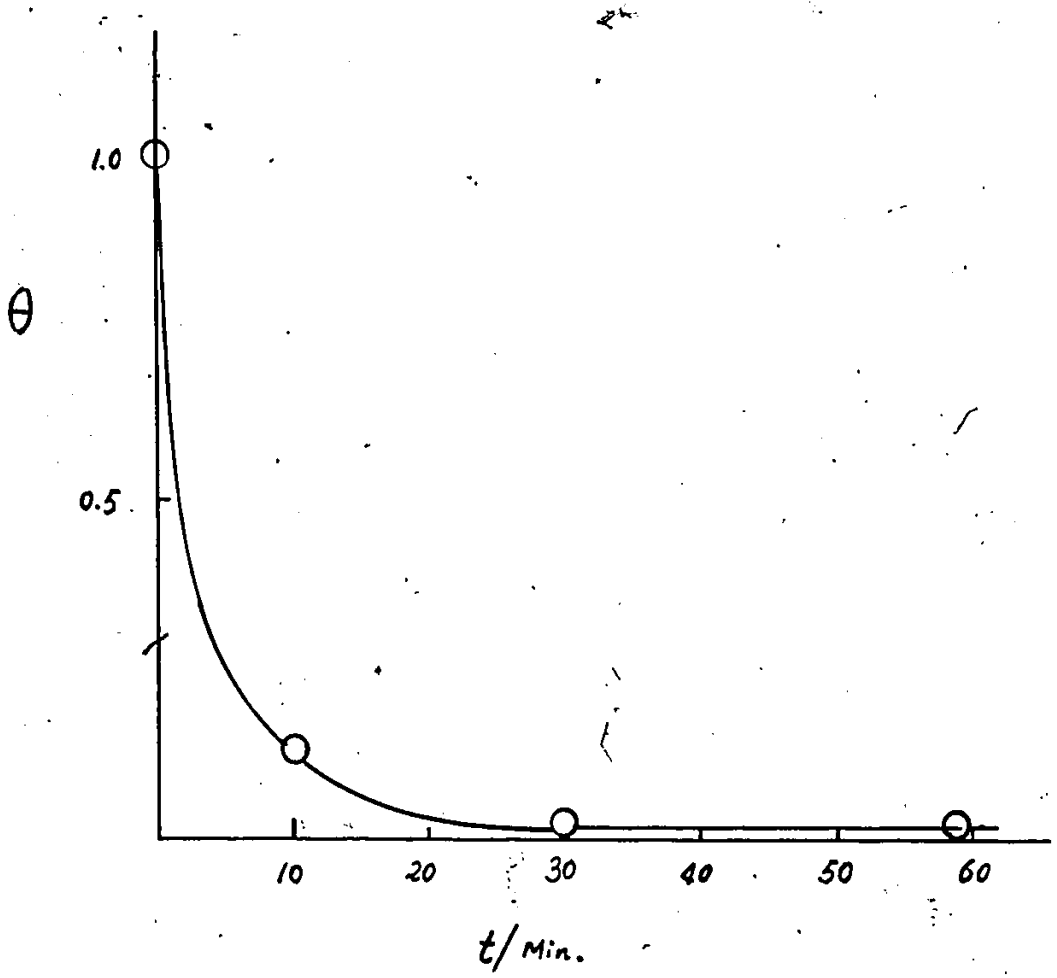

Figure 22. Relative Concentration of Surface Complex as a Function of Reaction Time

The present results, Figures 23 and 24, show that the relation between the rate and the concentration of complex may not be a simple linear function of O_2, in other words, a first-order dependence on the concentration of complex. In Figure 18, the rate of formation of CH_4 increased sharply with the initial concentration of O_2 in the gas phase. If the concentration of complex on the surface is proportional to the initial concentration of O_2 in the reacting mixture then the rate of formation of CH_4 is strongly dependent on the surface concentration of the complex. This strong dependence is compatible with the suggestion that the complex has an activating effect on the surrounding carbon atoms.[33] One complex could activate several surrounding carbon atoms. Although the dependence of the rate on the concentration of complex on the surface cannot be quantitatively determined from the present experiments, the results are in agreement with this previous interpretation from the studies of the reaction between C and O_2.

The initial rate of formation of CH_4 in mixtures with 1390 ppm O_2 was measured over the temperature range 832 to 1114 K. Figure 25 shows, as an Arrhenius plot, the temperature dependence of the initial rate of CH_4 formation. The apparent activation energy decreases with increasing temperature. The temperature dependence of the ratio of the initial rate of formation of CH_4 in the presence and absence of O_2, R_{O_2}/R, at a total pressure of

Table 20 (Figures 23 & 24)

THE ORDER OF THE RATE OF CH_4 FORMATION WITH RESPECT TO PARTIAL PRESSURE OF O_2

Temp. 1111 K
Total Pressure 177 Torr

$[O_2]/10^{-6}$	$4 + \log[O_2]$	$R_0/10^{-10}$ mol $L^{-1}s^{-1}$
246	0.390	1.85
553	0.743	3.17
816	0.912	4.21
1130	1.052	6.81

Temp. 934 K
Total Pressure 177 Torr

$[O_2]/10^{-6}$	$4 + \log[O_2]$	$R_0/10^{-11}$ mol $L^{-1}s^{-1}$
232	0.365	2.37
456	0.659	6.61
722	0.859	11.7
1090	1.037	33.5
1400	1.146	42.4

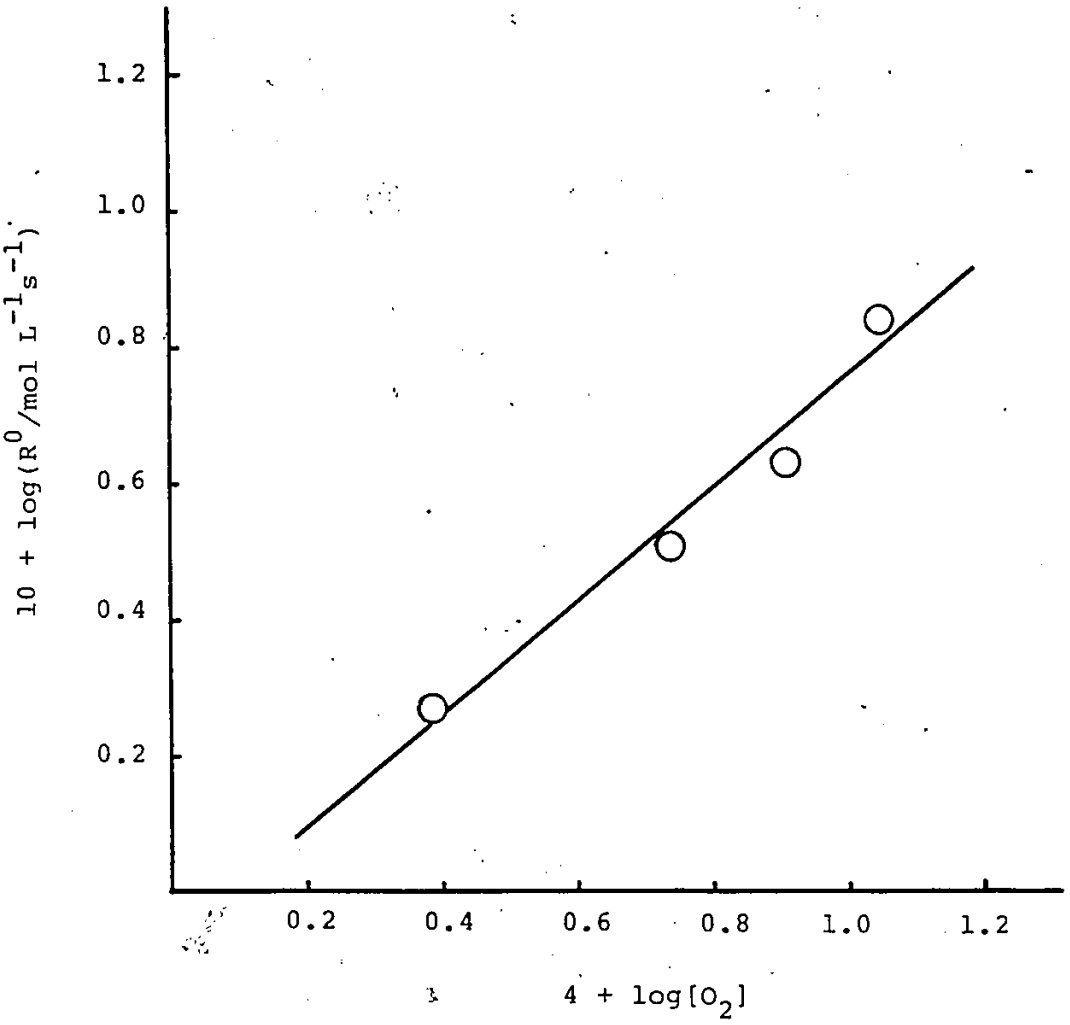

Figure 23. The Order of Rate of Formation of Methane with Respect to Partial Pressure of O_2 in H_2 at 1111 K with Total Pressure 177 Torr

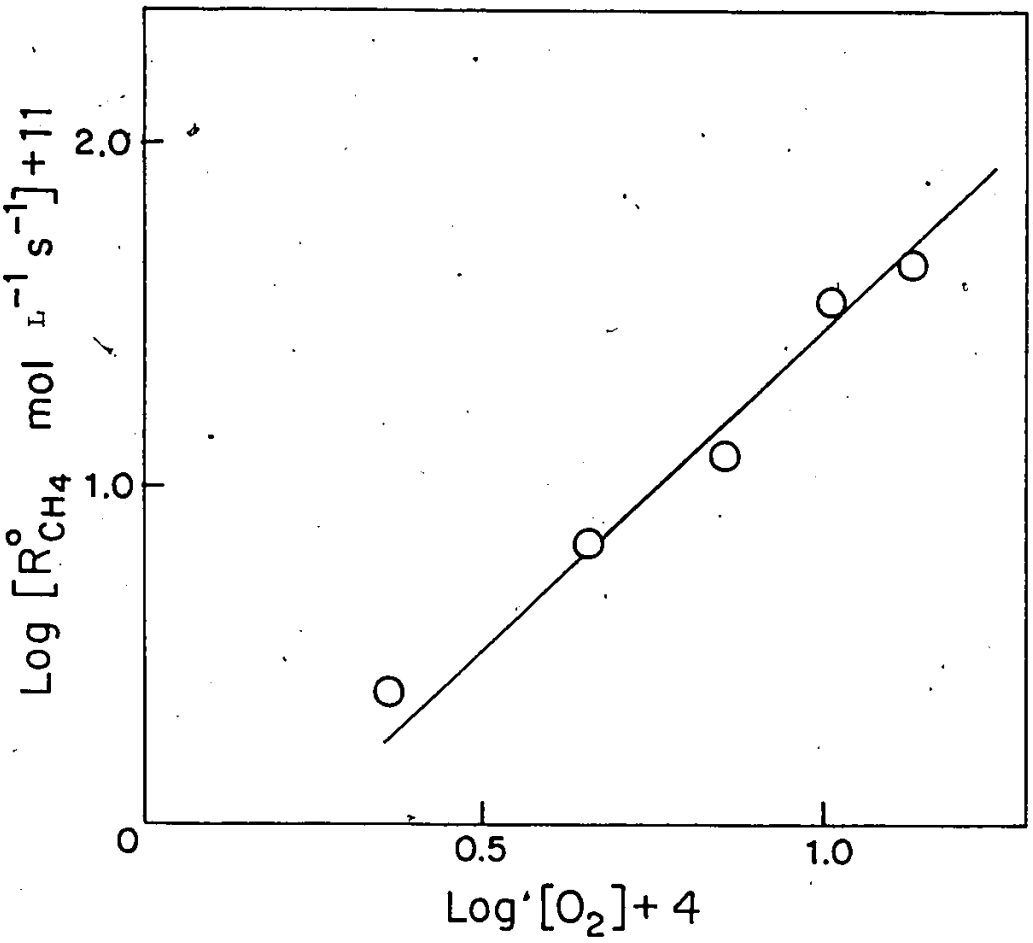

Figure 24. The Order of Rate of Formation of Methane with Respect to Partial Pressure of O_2 in H_2 at 934 K and Total Pressure of 177 Torr

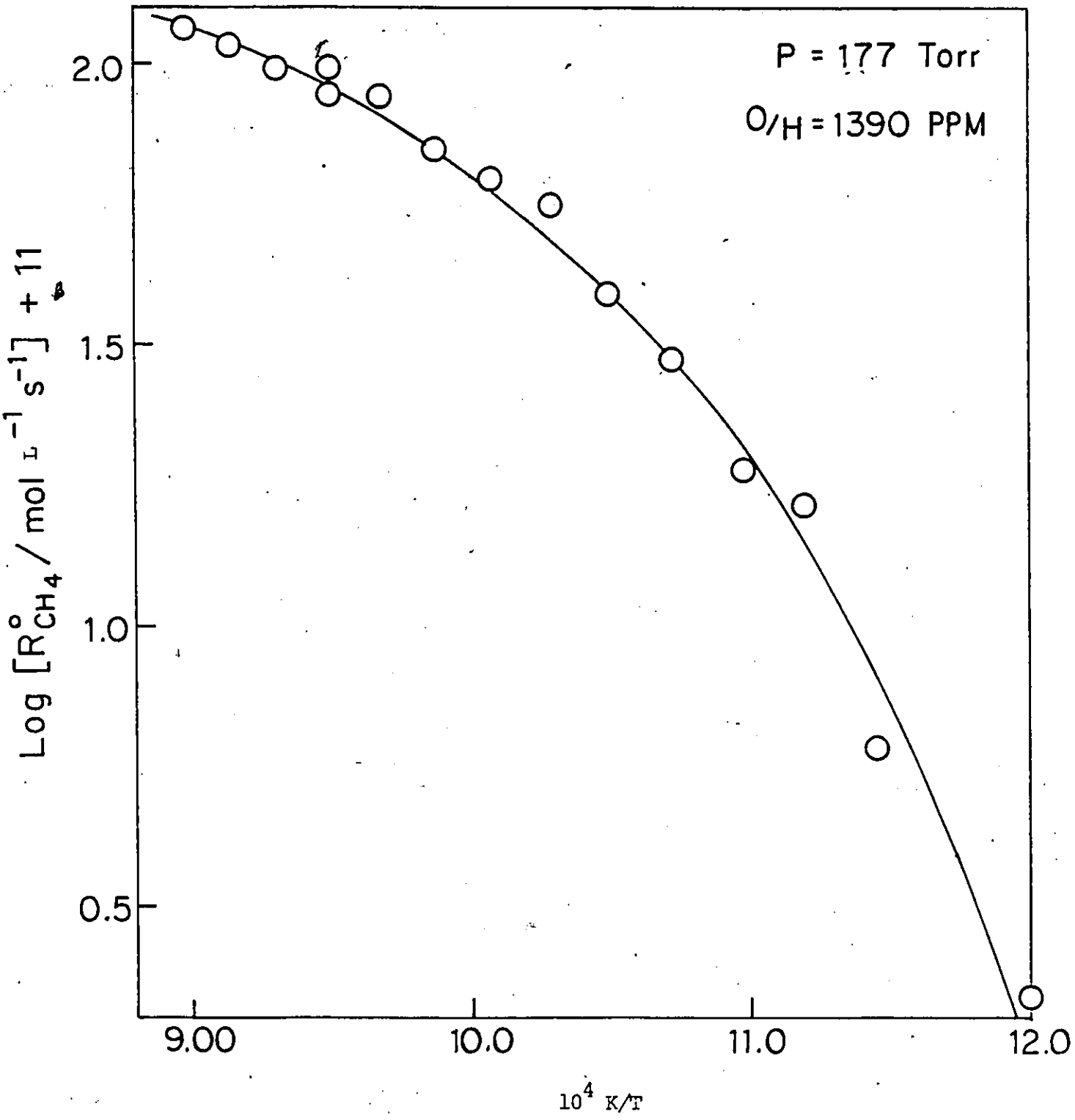

Figure 25. Temperature Dependence of the Rate of Formation of CH_4 for the Reaction with Hydrogen Containing 1390 ppm O_2 at Total Pressure of 177 Torr

Table 21 (Figure 25)

TEMPERATURE DEPENDENCE OF RATE OF CH_4 FORMATION

O_2/O_2+H_2 = 1390 ppm

P_{H_2} = 177 Torr

T/K	$R_{O_2}/10^{-11}$ mol $L^{-1}s^{-1}$
832	2.20
872	8.24
893	16.7
911	19.4
932	29.8
952	38.5
972	58.2
993	62.2
1012	70.4
1033	87.0
1054	88.0
1053	98.3
1074	36.8
1094	106
1114	116.5

177 Torr, is shown in Figure 26. The maximum value of the ratio R_{O_2}/R occurs at a temperature of about 1000 K. This variation in the effect of O_2 on the rate of the reaction may be examined in terms of the properties of the (C ... O) complex. Studies of the temperature-programmed desorption of the complex have shown that by 1000 K desorption is rapid and the equilibrium concentration of complex on the surface would rapidly decrease at higher temperatures. Any effect on the rate by the complex would then decrease as its concentration on the surface decreased. The decrease in the ratio at low temperatures is not easily explained. In the present experiments the concentration of complex on the surface is qualitatively indicated by the difference between the amount of O_2 initially added and the yield of H_2O recovered. This amount appears not to change significantly from the low temperature limit to the temperature of the maximum in the ratio R_{O_2}/R. The decrease in the ratio with temperature may then reflect competition between various surface processes, such as migration and desorption, which contribute to the final formation of methane. The suggestion concerning the mechanism of the oxidation process itself proposed by Olander[57] may be relevant to these observations. They proposed two kinds of active sites A and B on the carbon surface. The O_2 is chemisorbed only on the A-type sites, forming the bound CO complex and at the same time, releasing the partner oxygen atom as a

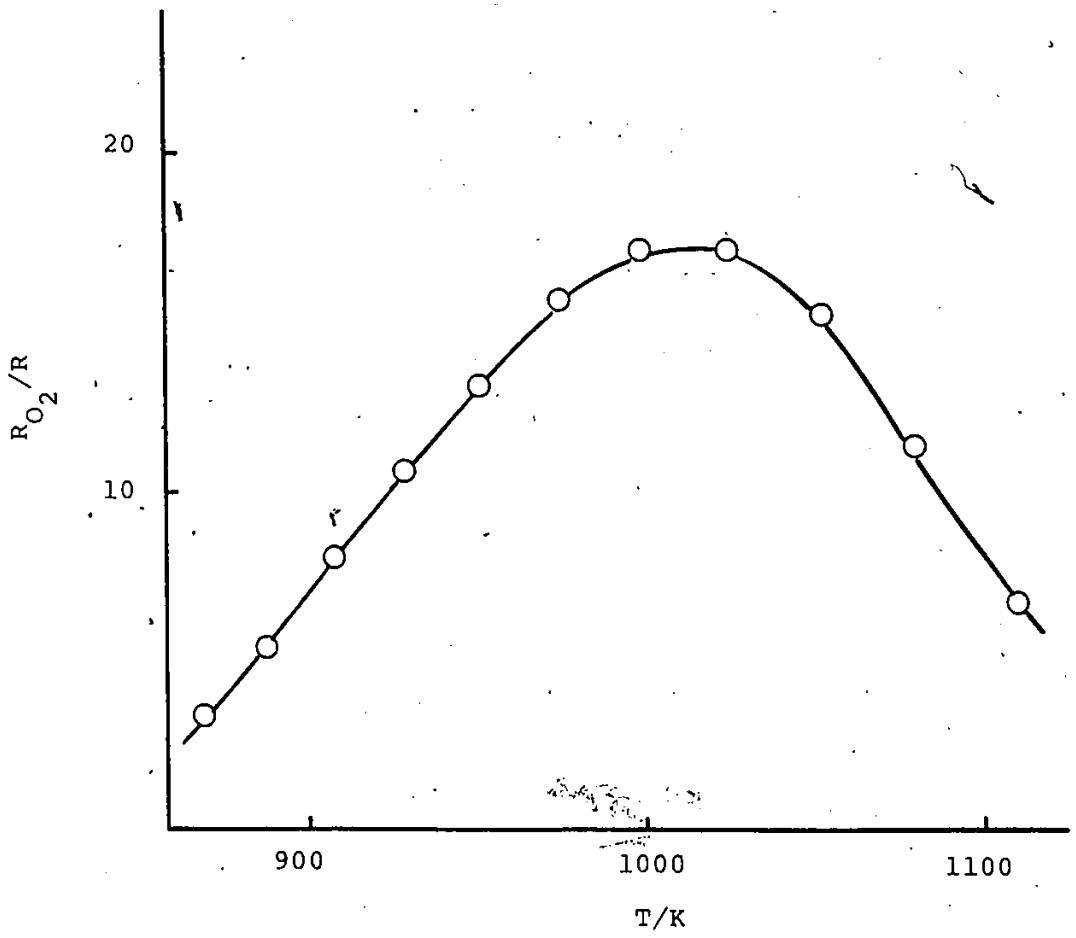

Figure 26. The Temperature Dependence of the Ratio of the Initial Rate of Formation of CH_4 in the Presence and Absence of 1390 ppm Oxygen, R_{O_2}/R, at a Total Pressure 177 Torr

mobile adsorbed species. This species migrates over the surface until it reaches a B-type site where it reacts to form a bound CO complex. In this interpretation the reaction which occurs on the B-type sites will depend on the mobility of the adsorbed oxygen atoms. The mobility will increase with increasing temperature and hence the concentration of complex will increase with temperature. The present results are consistent with such a general picture of the formation of the complex, but cannot be assumed to provide confirmation. In summary, the results of these experiments show clearly the significant effect of the presence of the surface complex of oxygen on the rate of the reaction between H_2 and carbon. The details of the mechanism of this effect are still speculative. Further experiments with other systems will be necessary before a clear picture emerges.

PART TWO

KINETICS OF THE THERMAL REACTIONS

$$C_2H_5 + H_2 \rightarrow C_2H_6 + H$$

$$C_2H_6 + H \rightarrow C_2H_5 + H_2$$

$$C_2H_6 \rightarrow 2CH_3$$

LIST OF REACTIONS IN PART TWO

[1] $H_2 \rightleftharpoons 2H$

[2] $H + C_2H_4 + M \rightleftharpoons C_2H_5 + M$

[3] $C_2H_5 + H_2 \rightleftharpoons C_2H_6 + H$

[4] $C_2H_6 \rightleftharpoons 2CH_3$

[5] $CH_3 + H_2 \rightleftharpoons CH_4 + H$

[6] $C_2H_5 + H \rightarrow C_2H_6$

[7] $H + C_2H_5 \rightarrow 2CH_3$

[8] $C_2H_4 + H_2 \rightarrow C_2H_5 + H$

[9] $C_2H_4 \rightarrow C_2H_3 + H$

[10] $C_2H_5 + C_2H_5CHO \rightleftharpoons C_2H_6 + C_2H_5CO$

[11] $H + O_2 \rightarrow OH + O$

[12] $C_2H_5 + C_2H_4 \rightarrow C_2H_6 + C_2H_3$

CHAPTER 4

INTRODUCTION

During the study of the reaction of carbon with hydrogen reported in Part I, the importance of concurrent, gas-phase hydrogenation reactions was noted. Part II will present the results of kinetic studies on the hydrogenation of ethylene and the decomposition of ethane in the gas phase at temperatures in the neighbourhood of 1000 K. These studies involve the kinetics of the elementary reactions

$$C_2H_5 + H_2 \rightarrow C_2H_6 + H \qquad (3)$$

$$H + C_2H_6 \rightarrow C_2H_5 + H_2 \qquad (-3)$$

$$C_2H_6 + M \rightarrow 2CH_3 + M \qquad (4)$$

In addition, the weak collisional effects of hydrogen in the thermal unimolecular dissociation of C_2H_6 have been measured.

Most of the measurements of rate constants for reactions of small hydrocarbon radicals have been obtained at temperatures below about 850 K where the radicals have a reasonable lifetime for kinetic studies. Rate constants for reactions of hydrogen and other atoms have been obtained at higher temperatures above 1500 K from shock

tube studies. There is a scarcity of data in the temperature region around 1000 K and yet many thermal reaction systems involving these radicals have been studied at these temperatures and higher. It is important to have reliable measurements of rate constants for elementary reactions, not only for qualitative understanding of mechanisms, but for quantitative modelling studies. Many rate constants are obtained by extrapolation of measurements made at lower temperatures. Serious errors may be introduced in this procedure if the reaction shows non-Arrhenius behaviour.[58] The evidence for such behaviour in the reactions of small hydrocarbon radicals has been discussed. There has been a suggestion that the Arrhenius plot for the reaction analogous to (-3) for methane is strongly curved and further, there is good evidence that the reaction of methyl radicals with ethane provides a curved Arrhenius plot. Clark and Dove[59] suggested that reaction (-3) also has a curved Arrhenius plot, although the curvature is thought to be quite small. Such behaviour is of great fundamental importance in the kinetics of gas phase reactions. The question has not been satisfactorily resolved and improved determination of such rate constants is therefore an important goal of kinetic studies.

Only four measurements of the rate constant of reaction (3) have been reported.[60-63] These measurements

were conducted over a narrow temperature range or at a single temperature and were all made relative to the rate constant for combination of ethyl radicals.

Halstead and Quinn[62] studied the kinetics of the thermal hydrogenation of ethylene at 823 K by a detailed product analysis. Analysis of the kinetics gave a value for the rate constant for reaction (3).

Baldwin, et al.[63] obtained the rate constant for reaction (3) at 673 K through kinetic studies on the oxidation of C_2H_5CHO. In their experiment the ratio of rate constants for reactions

$$C_2H_5 + C_2H_5CHO \rightarrow C_2H_6 + C_2H_5CO \qquad (10)$$

$$C_2H_5 + H_2 \rightarrow C_2H_6 + H \qquad (3)$$

was measured.

Reid and LeRoy[61] made a quantitative study of the reaction of ethyl radicals with molecular hydrogen in the gas phase over the temperature range 513-593 K. The mercury (6^3P_1) photosensitized decomposition of hydrogen in the presence of ethylene was used to generate ethyl radicals.

Boddy and Steacie[60] studied the reaction of deuterated ethyl radicals with hydrogen in the temperature range 375-515 K.

A summary of these data is given later in Table 25 and Figure 33. All these measurements were made below 823 K. New measurements at temperatures about 1000 K should therefore be valuable in establishing this rate constant in a higher temperature region.

Measurements of the rate constant for reaction (-3) have been reported by a variety of techniques for many years, and several summaries have recently appeared.[64] Most of the measurements have been conducted over a narrow temperature range and occasionally at a single temperature. The main problem encountered in these measurements is the determination of the concentration of hydrogen atoms. During the past few years the technique of atomic resonance absorption has been successfully applied to measurements of the concentration of hydrogen atoms in several systems.[65] This provides a direct measurement of the instantaneous concentration of H atoms but has been applied only at temperatures above 1000 K. Rate constants for reactions both producing[66] and consuming[67] hydrogen atoms have been obtained. At lower temperatures, however, the measurements of rate constants for reaction of hydrogen atoms with ethane have, except for studies using ESR detection,[68] relied on a relative measure of the hydrogen-atom concentration.

In systems involving atoms and radicals the concentration of hydrogen atoms is seldom controlled by their rate of mutual combination, either homogeneously or heterogeneously and other reactions consuming hydrogen atoms must be used as a reference. For example, the rate constant for reaction (-3) at 990-1430 K was determined by Fenimore[69] from flame studies relative to the rate constant of the reference reaction

$$H + O_2 \rightarrow OH + O \qquad (11)$$

This reaction has also been used as reference in studies of the inhibition of ethane in the H_2/O_2 reaction at 813 K.[70]

At slightly lower temperatures, 500-750 K, Marshall, Purnell and co-workers have shown that in a flow system at low pressure with reactant ethane[71] the combination reaction

$$H + C_2H_5 \rightarrow 2CH_3 \qquad (7)$$

is the main competing process for removal of hydrogen atoms and provides a reference reaction with known rate constant.

At lower temperatures, Yang[72] measured rate constants for several abstraction reactions of H atoms relative to the addition reaction with propylene.

Several measurements,[74][68] which are based on the direct reaction between H atoms and ethane, require a knowledge of the stoichiometry of the reaction, that is, the number of hydrogen atoms, n, reacting per ethane molecule consumed. This has usually been assumed to be 4.0, the value corresponding to the situation where methane is the sole product. If, however, ethane may be reformed subsequent to the initial reaction, n could be less than 4 and the assumed stoichiometric ratio should be corrected.

There is fairly good agreement among these various methods but there is no doubt that better accuracy is needed to give confidence to modelling studies and to assess the extent of curvature in the Arrhenius expression over the temperature range covered by the measurements.

A new system for the measurement of rate constants for radical reactions at temperatures in the neighbourhood of 1000 K has been explored in this work. The method is based on the premise that at these temperatures, with moderate pressures of hydrogen, an equilibrium concentration of hydrogen atoms can be maintained in the system. A small quantity of reactant in concentration of a few ppm, is added to the hydrogen and the rate of consumption of reactant and appearance of the products is measured. It is assumed that the equilibrium between hydrogen molecules and atoms is not significantly perturbed by the

addition of the reagent. In the present study, this assumption is tested through a measurement of the order of the rate of the reaction. The present studies describe the kinetics of the reaction with reactants ethylene and ethane. In the former case an equilibrium concentration of ethyl radicals is attained by addition of hydrogen atoms to ethylene and the rate-controlling step is the abstraction reaction of ethyl radicals with hydrogen, reaction (3).

$$C_2H_5 + H_2 \rightarrow C_2H_6 + H \qquad (3)$$

With the reactant ethane there are two possible pathways for the initial disappearance of C_2H_6 in the presence of excess of H_2: first, the reaction between hydrogen atoms and ethane, reaction (-3), leading to formation of C_2H_4, second, the dissociation of ethane to methyl radicals, reaction (4), which convert into CH_4 through further hydrogenation. Measurement of k_4 in the present system provides data on the relative collisional efficiency of hydrogen in a unimolecular dissociation.

CHAPTER 5

EXPERIMENTAL

The reactions were studied in the same system, with minor modifications, as described in Chapter 2. A second vessel, similar to the one described earlier, was packed with quartz tubes to give a S/V = 7.5 cm^{-1} and was used to test for the importance of surface reactions. Mixtures of H_2 - C_2H_4 and H_2 - C_2H_6 were prepared by a two-step dilution with pure H_2 to obtain the desired concentration of C_2H_4 or C_2H_6 in H_2 of between 10-100 ppm. During the dilutions the reading of pressure was made with at least 3 significant figures. After a mixing period of 12 hours the composition of the mixture was homogeneous and invariant. Ethylene (99.98%), ethane (99.99%) and xenon were Research Grade obtained from Matheson of Canada, Whitby, Ontario. Hydrogen was purified by passage through a Molecular Sieve 5A Column at liquid nitrogen temperature with a residence time of 1~2 sec. as described earlier.

The products were analyzed as described in Chapter 2. The reactants and products, ethane, ethylene and methane, were measured for reaction times from 1-40 min. Experiments covered the temperature range 850-1200 K. The total pressure ranged from 30 Torr to 300 Torr.

CHAPTER 6

KINETICS OF THE REACTION $C_2H_5 + H_2 \rightarrow C_2H_6 + H$ FROM 1111-1200 K

(a) Products

The primary product of hydrogenation was ethane, but at the temperature of the reaction, secondary decomposition was rapid and ethane was quantitatively converted to methane. Yields of CH_4, C_2H_6 as a function of time at 1111 K together with the corresponding concentration of C_2H_4 remaining are shown in Figures 27-29. Particularly from Figure 28 it is clear that ethane is an intermediate product and even at the lowest temperature its yield is small. It became undetectable above about 1200 K. It should be noted that equilibrium in this system corresponds to almost complete conversion of ethylene to methane. The reaction was therefore followed by the disappearance of ethylene and the appearance of methane.

(b) Measurement of Rates

The rate of the reaction in the unpacked vessel was measured at 1111 K for five concentrations of ethylene in hydrogen ranging from 9-36 ppm. At each concentration the rate was measured at three to five total pressures

Figure 27. Variation in Mole Fraction of Reactant and Products at 1111 K and Total Pressure of 182 Torr

□ - C_2H_4

O - CH_4

Δ - C_2H_6

Open Symbols Refer to Unpacked Vessel (S/V ~ 1 cm^{-1}) and Filled Symbols Refer to Packed Vessel (S/V ~ 7 cm^{-1})

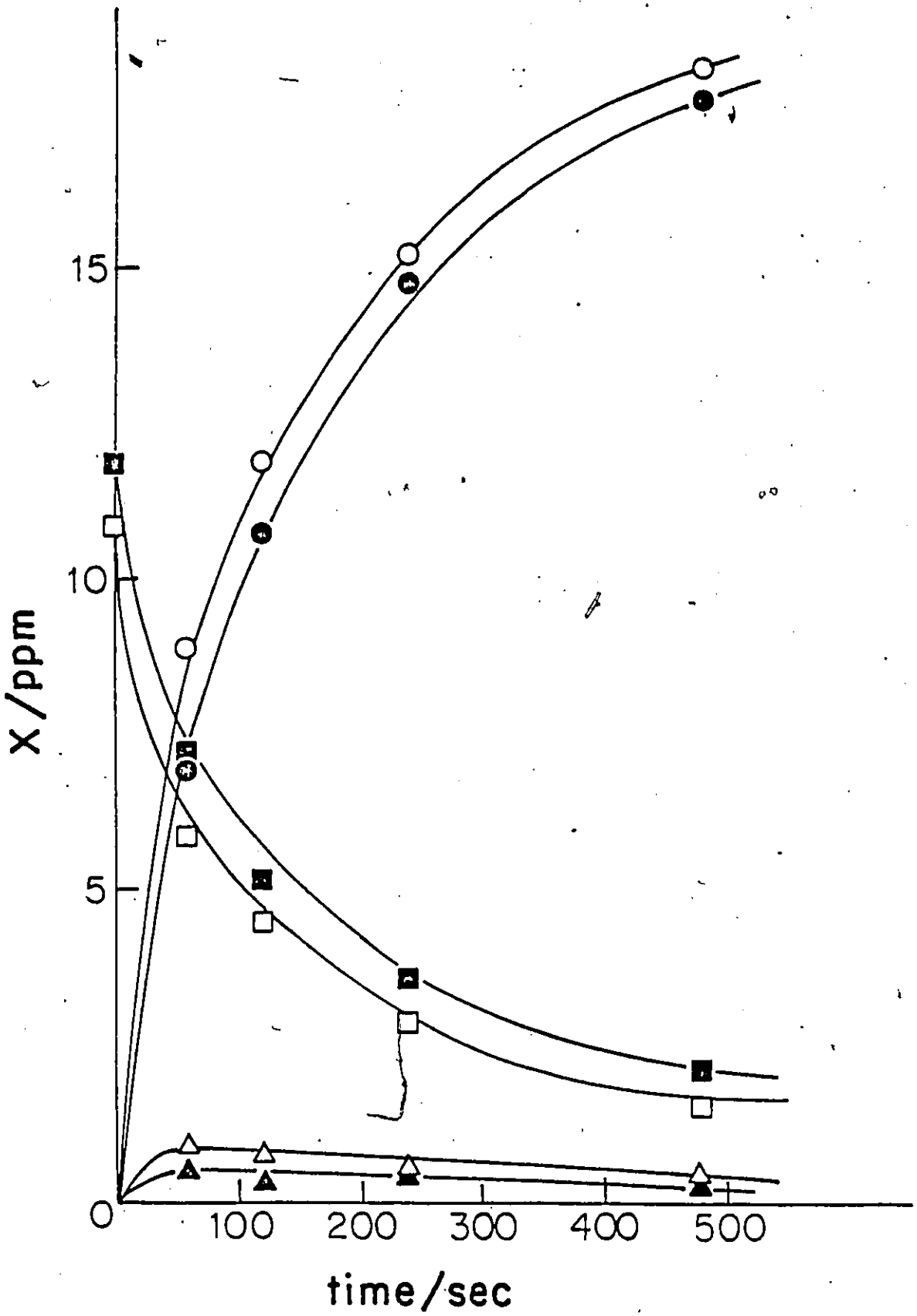
15
10
5
0
X /ppm
100
200
300
400
500
time/sec

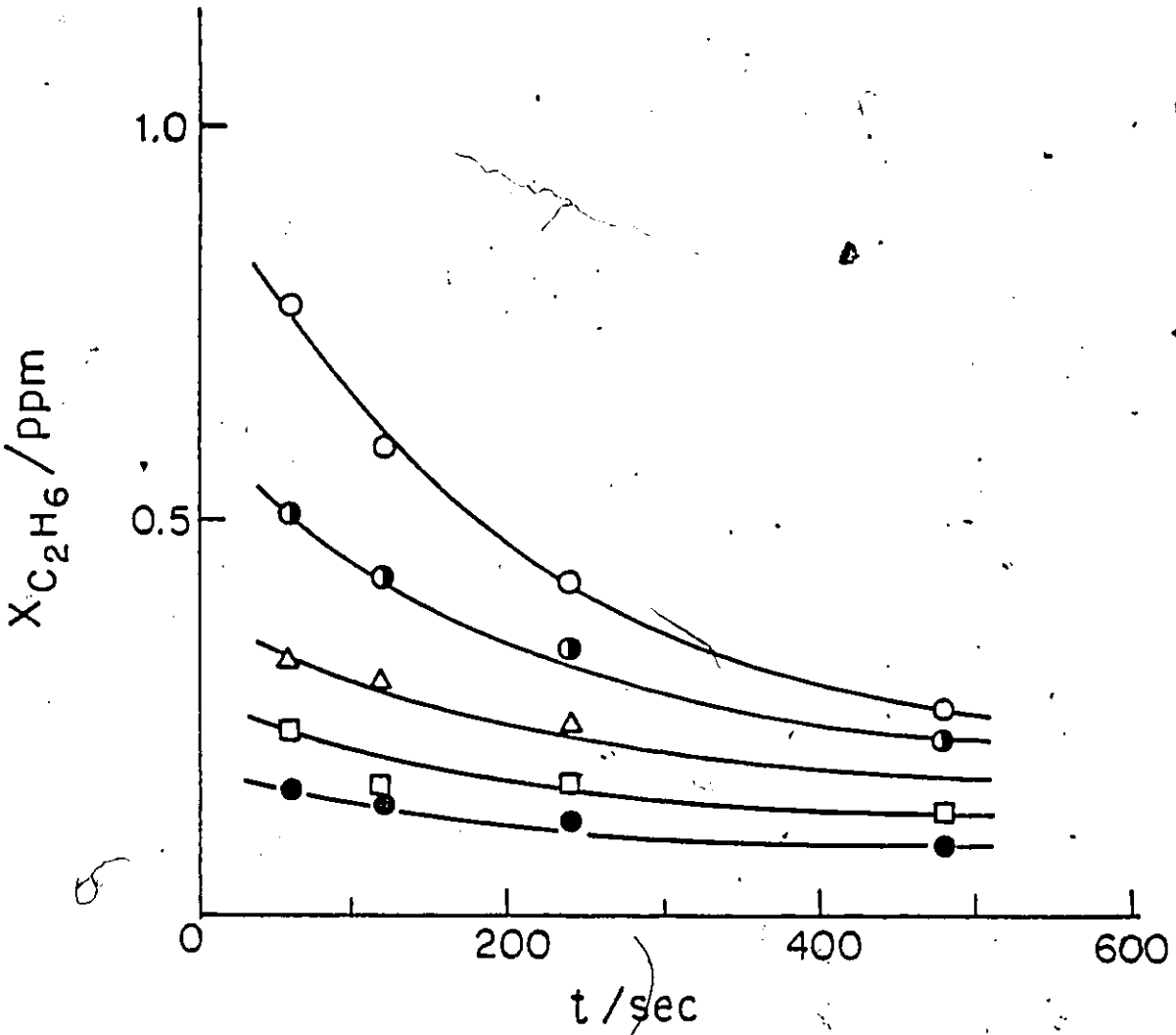

Figure 28. Mole Fraction of Ethane as a Function of Time at Various Temperatures. Initial Concentration of Ethylene: 9.33 ppm; Total Pressure: 182 Torr

○ - 1111 K
◑ - 1131 K
□ - 1171 K
● - 1192 K
△ - 1151 K

Figure 29. Mole Fraction of Ethylene as a Function of Time at 1111 K, with Initial Concentration of Ethylene of 19.2 ppm. Total Pressure:

△ - 85.5 Torr
◇ - 117 Torr
□ - 149 Torr
○ - 182 Torr

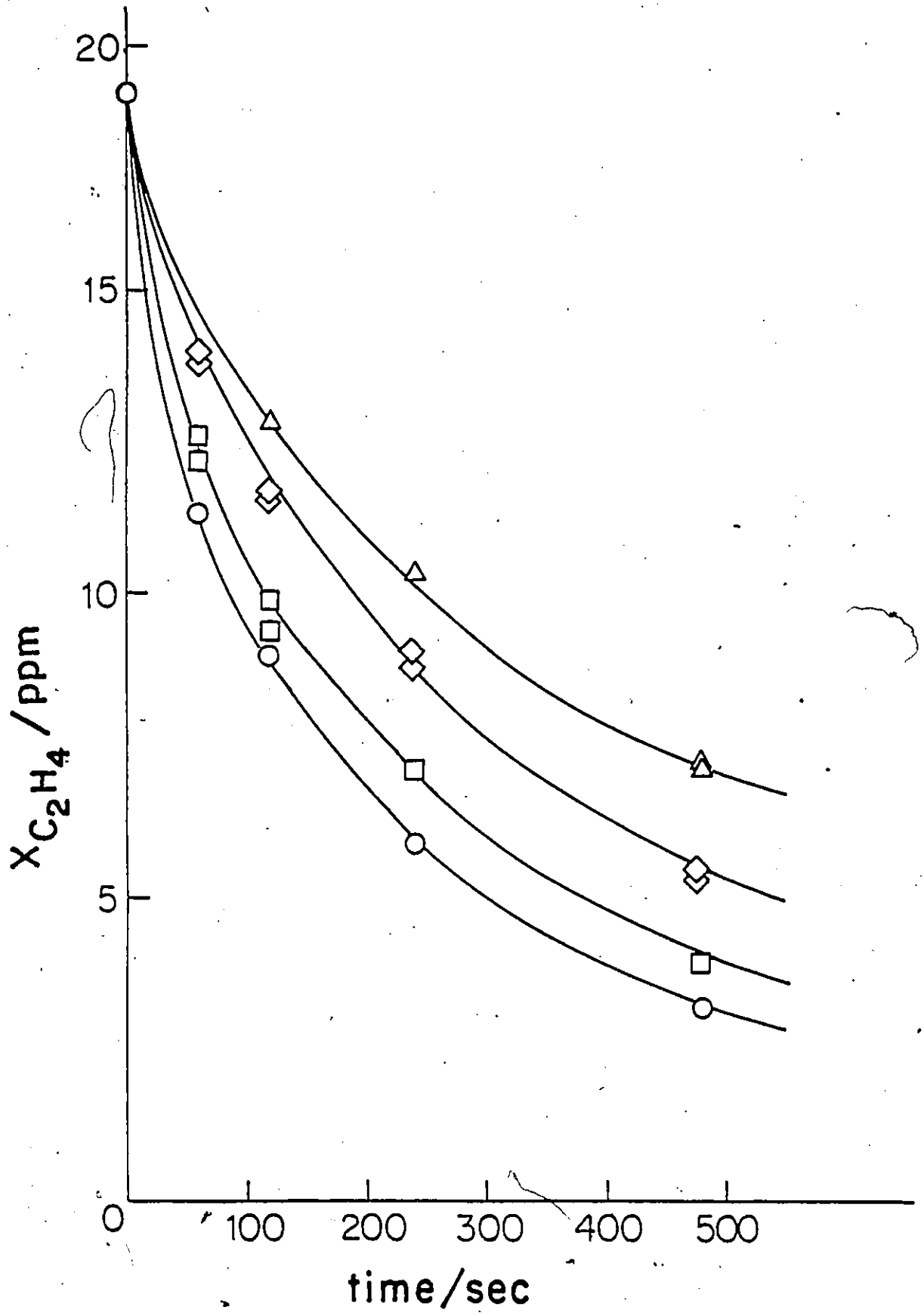
20
15
10
5
0
100
200
300
400
500
$X_{C_2H_4}$ /ppm
time/sec

ranging from 100-300 Torr. At a total pressure of 182 Torr the rate was measured at several temperatures over the range 1111-1192 K. In addition, the total order of the rate with respect to both reactants was measured at 1192 K. It is evident from Figures 27-29 that the measurement of initial rates from the data required an extrapolation to zero time. The procedure adopted for this was the following. The data were fitted to integrated equations for orders of 0.5, 1.0, 1.5 and 2.0. The best linear extrapolation was obtained with the function 1/X against time. This function was therefore used for all the data. A summary of the measurements of initial rates is given in Table 22. For comparison, initial rates were estimated directly from the yield-time plots or from the function log X against time. These estimates were within 25% of the values given in Table 22. It should be emphasized that the function used to estimate the initial rates is not particularly significant in terms of the mechanism of the reaction during the initial stages.

(c) Determination of the Order of the Rate with Respect to Both Reactants

The dependence of the rate on the initial concentration of the reactant is the characteristic of most importance to the mechanism. The rate of disappearance of ethylene may be written

Table 22

Initial Rates of Reaction of Ethylene and Values for k_3

T/K	Pressure/ Torr	$X_{C_2H_4}$/ ppm	$-\frac{d}{dt}[C_2H_4]$/ mol $L^{-1}s^{-1}x10^{-10}$	$K_1^{1/2}$/ (mol $L^{-1})^{1/2}x10^{-9}$	K_2/ (mol $L^{-1})^{-1}x10^4$	k_3/ L mol $^{-1}s^{-1}x10^6$
1071	182	10.84	2.64	1.51	3.19	1.31
1111	117	10.84	1.42	3.48	1.72	1.91
		19.2	1.75			1.32
		27.3	2.65			1.42
		36.6	4.26			1.70
	182	9.33	2.82			1.39
		10.84	3.49			1.56
		19.2	5.23			1.32
		27.3	8.37			1.49
		36.6	11.0			1.46
	308	10.84	14.8			1.73
		19.7	19.3			1.24
		27.3	28.9			1.34
		36.6	39.3			1.36
1131	182	9.33	3.44	4.89	1.39	1.64
1151	182	9.33	4.59	7.00	0.966	2.05
		10.84	5.89			2.18
1171	182	9.33	6.26	10.02	0.729	2.62
1181	182	10.84	8.28	12.8	0.640	2.84
1192	119	9.33	3.18	18.1	0.556	3.31
	182	9.33	8.97			2.98
	248	9.33	19.5			3.22

Packed Reaction Vessel $S/V = 7.0\ cm^{-1}$

1111	116	11.85	1.91	3.48	1.72	1.61
		18.46	2.03			1.22
		27.9	2.33			
	182	11.85	3.63			1.49
		18.46	4.10			
		27.9	7.17			1.26
	274	11.85	7.60			1.09
		18.46	8.63			
		27.9	15.8			0.97
	325	11.85	11.4			1.07

$$- R_{C_2H_4} = k[H_2]^m [C_2H_4]^n \qquad (6\text{-}1)$$

where k represents an overall rate constant and m and n represent the order of the rate with respect to hydrogen and ethylene, respectively. Designating the mole fraction of each reactant by X and making the approximation that $X_{H_2} = 1$.

$$- R_{C_2H_4} = k[P]^{m+n} X^n_{C_2H_4} \qquad (6\text{-}2)$$

where P is the total pressure.

A log-log plot of the initial rate as a function of $X_{C_2H_4}$ is shown in Figure 30 for four total pressures. The concentration of hydrogen is essentially constant for each total pressure and the slope of these plots therefore gives directly a value for n. From these data the average value of n is 1.0 ± 0.1. A similar plot was then made for conditions where the concentration of ethylene was constant and the total pressure was varied. These results are shown in Figure 31. The slope of these plots, all equal to 2.4 ± 0.1, gives the total order m+n. A similar plot using the data obtained at 1192 K (Table 22) gives a value for m+n = 2.5. The value of m is therefore 1.5 ± 0.1. An Arrhenius plot of the initial rate, which is shown in Figure 32A, gives an activation energy of 33 Kcal/mole.

Figure 30. Logarithm of the Initial Rate of Reaction of Ethylene as a Function of the Logarithm of the Initial Mole Fraction of Ethylene for Various Total Pressures at 1111 K

◇ - 307 Torr; slope = 0.95
Δ - 274 Torr; slope = 0.97
O - 183 Torr; slope = 0.98
□ - 117 Torr; slope = 1.03

Open Symbols Refer to Unpacked Vessel (S/V ~ 1 cm^{-1}) and Filled Symbols Refer to Packed Vessel (S/V ~ 7 cm^{-1}).

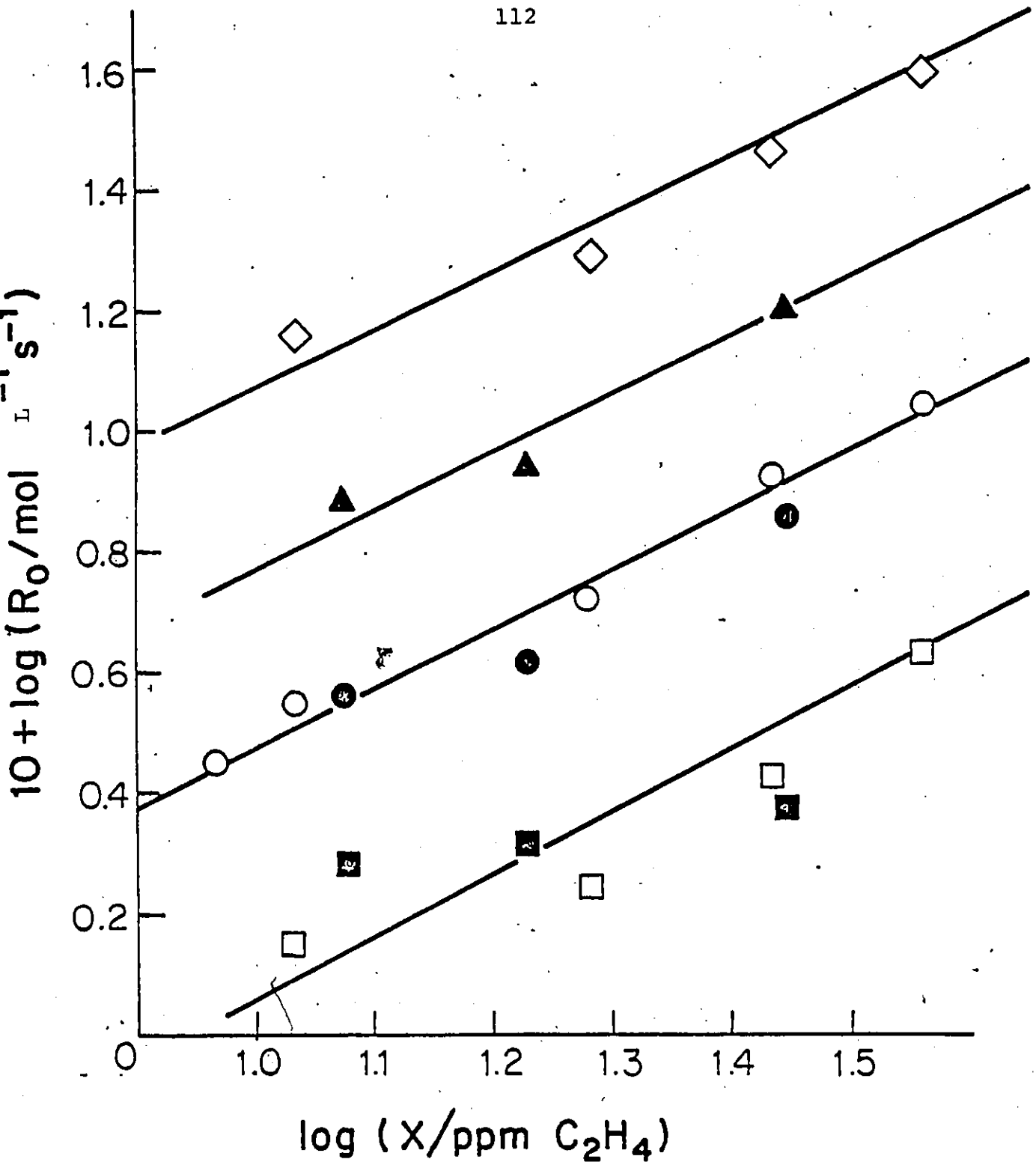
1.6
1.4
1.2
1.0
0.8
0.6
0.4
0.2
0
1.0
1.1
1.2
1.3
1.4
1.5
10 + log (R0/mol L-1 s-1)
log (X/ppm C2H4)

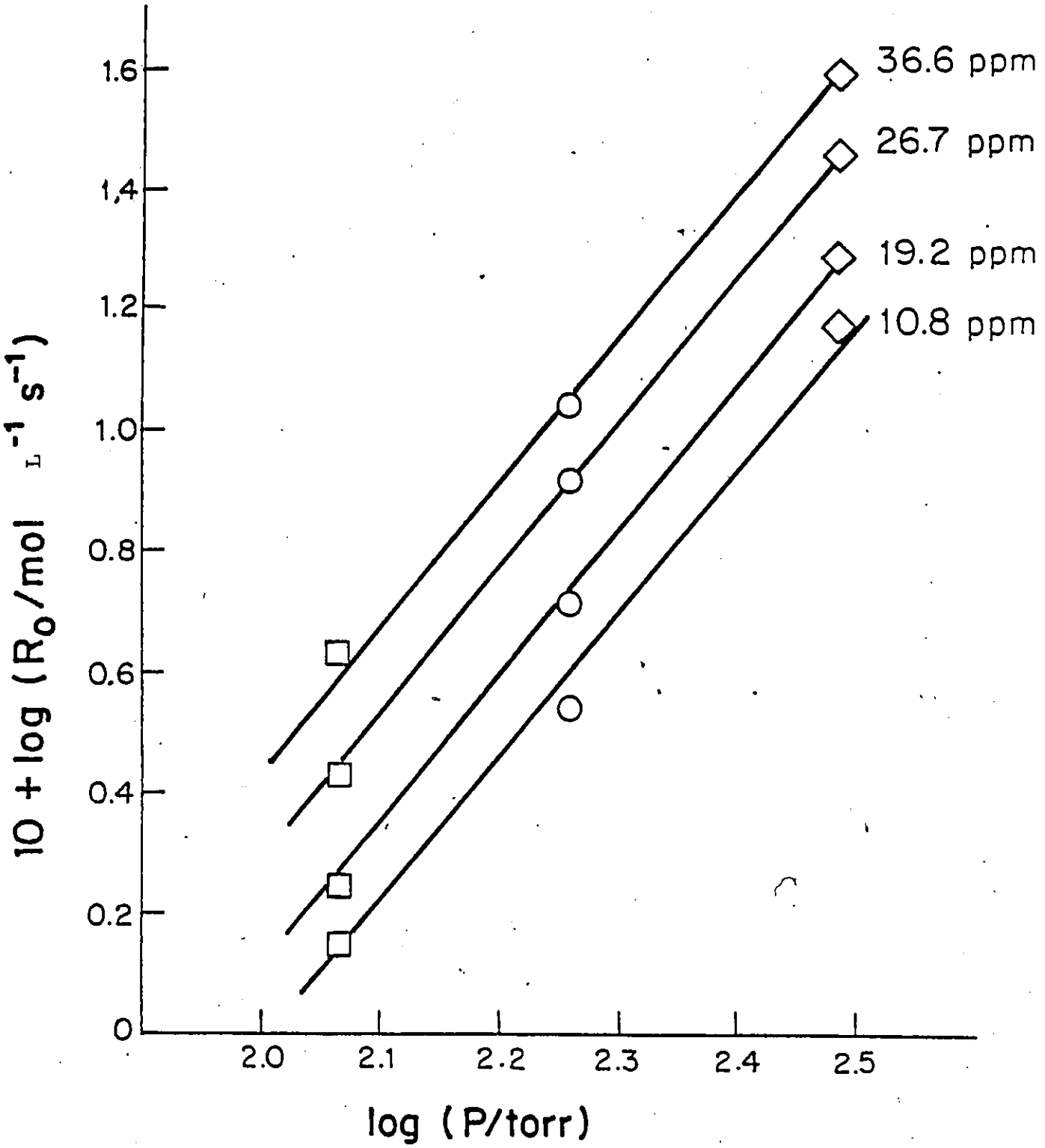

Figure 31. Logarithm of the Initial Rate of Reaction of Ethylene as a Function of the Logarithm of the Total Pressure at 1111 K for Various Initial Concentrations of Ethylene

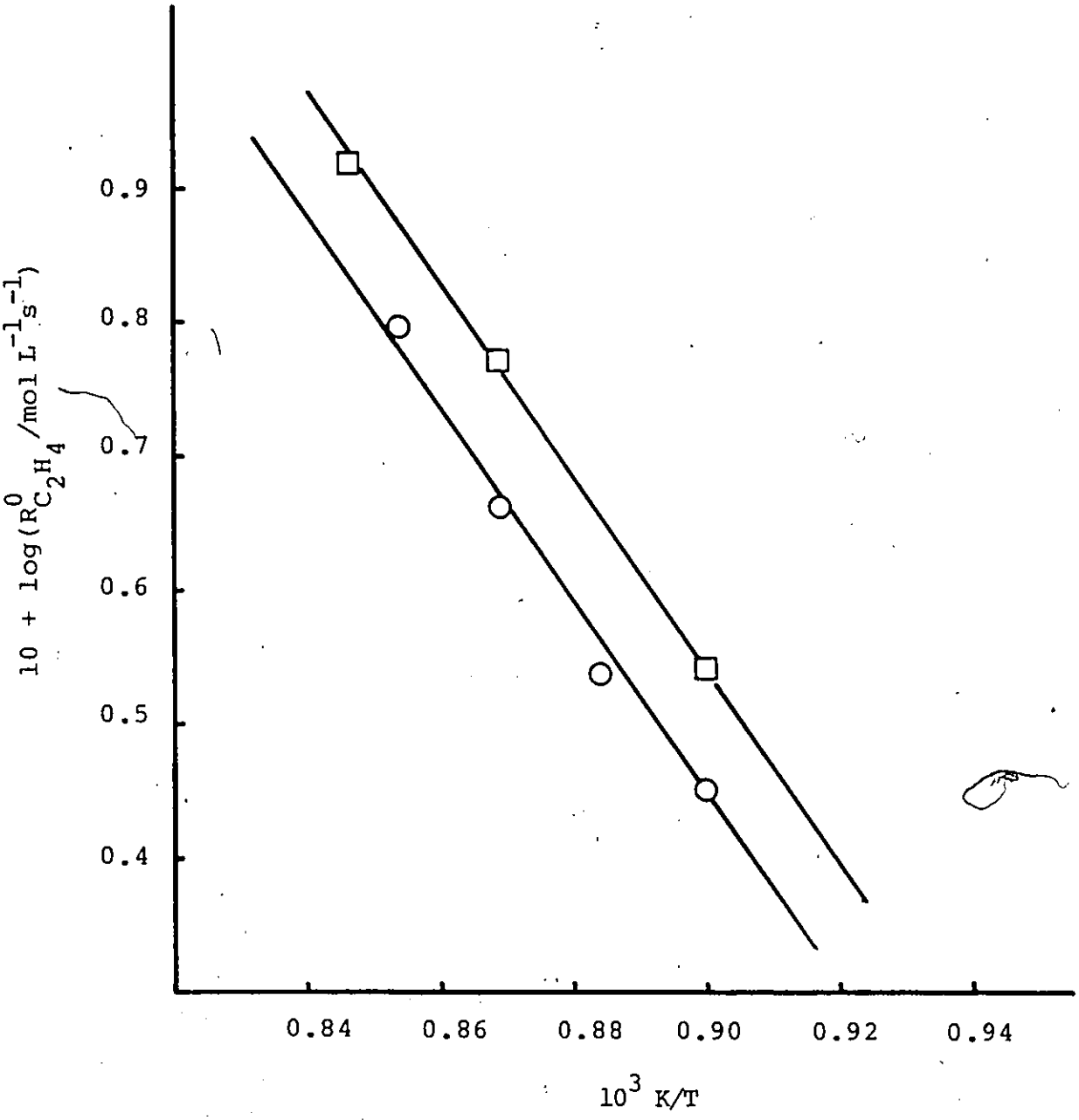

Figure 32A. Arrhenius Plot for Initial Rate of C_2H_4 at Total Pressure 182 Torr

o - 9.33 ppm C_2H_4

□ - 10.84 ppm C_2H_4

(d) Measurements in the Packed Vessel

In the packed vessel, rates were measured at total pressures of 116.0, 182.0, 274.0 and 325.0 Torr for each of three mixtures 12.0, 18.5, 28.0 ppm ethylene at 1111 K. The results are included in Table 22 and are shown as the filled symbols in Figure 27 and 30. It is evident, particularly from Figure 30, that the rates were not significantly altered in the packed vessel. It may be concluded that heterogeneous processes are not important in the rate-determining steps of the reaction except to a slight extent at the highest pressures.

(e) Mechanism of the Reaction

These results may be interpreted through a simple set of reactions where the H-atom concentration in the system is determined by the equilibrium between molecules and atoms

$$H_2 \rightleftharpoons 2H \quad (1)$$

$$H + C_2H_4 + M \rightleftharpoons C_2H_5 + M \quad (2)$$

$$C_2H_5 + H_2 \rightarrow C_2H_6 + H \quad (3)$$

$$C_2H_6 \rightarrow 2CH_3 \quad (4)$$

$$CH_3 + H_2 \rightarrow CH_4 + H \quad (5)$$

$$C_2H_5 + H \rightarrow C_2H_6 \quad (6)$$

The stabilizing third body M is included in reaction (2) since these processes are known to be pressure-dependent at the temperatures and pressures of this study. Considering only the reactions occurring in the initial stages.

$$- R_{C_2H_4} = R_{C_2H_6} = \frac{k_3 k_2 [M]^x K_1^{1/2} [H_2]^{3/2} [C_2H_4]}{k_{-2}[M]^x + k_3[H_2]} \qquad (6\text{-}3)$$

where x, having values between 1 and 0, represents the dependence of the rates R_2 and R_{-2} on the concentration of the third body M.

The characteristics of the rate depend critically on the ratio of rates $k_{-2}[C_2H_5][M]^x$ and $k_3[C_2H_5][H_2]$.

Case 1: If $k_{-2}[M]^x >> k_3[H_2]$, an equilibrium concentration of ethyl radicals will rapidly be attained through reaction (2). The rate may then be expressed as

$$- R_{C_2H_4} = k_3 K_2 K_1^{1/2} [H_2]^{3/2} [C_2H_4] \qquad (6\text{-}4)$$

Case 2: If $k_{-2}[M]^x << k_3[H_2]$, the rate expression simplifies as follows

$$- R_{C_2H_4} = k_2 [M]^x K_1^{1/2} [H_2]^{1/2} [C_2H_4] \qquad (6\text{-}5)$$

Since $[M] = [H_2]$ the total order in each case will be 2.5 if x is close to 1, as is expected under the present conditions. From the dependence of the rate on the concentration

of each reactant therefore it is not possible to determine whether reaction (2) or reaction (3) is the rate-controlling step.

On the other hand, the activation energy of the rate is quite different for each case. The measured activation energy is 33 kcal/mol. Taking ΔH_2 = - 41 kcal/mol (see Table 24) and ΔH_1 = 104.2 kcal/mol, Equation (6-4) gives E_3 = 22 kcal/mol. Although this value appears high, it will be shown later that the measured activation energy for reaction (3) is close to this. From Equation (6-5), using a value of E_2 of about 6 kcal/mol [64], the activation energy of the rate will be about 58 kcal/mol, which is far greater than the measured value.

A calculation of the relative magnitude of $k_{-2}[M]^x$ and $k_3[H_2]$ shows that $k_{-2}[M]^x$ is about 25 times greater than $k_3[H_2]$ at 1111 K and total pressure of 182 Torr. The value of $k_{-2}[M]^x$ may be estimated from the data of Lin and Back,[83] whose measurements were made under similar conditions of pressure and temperature, although the bath gas was ethane rather than H_2. Their data indicate that at 913 K and 120 Torr, the ratio $k_{-2}[M]^x/k_{-2}^\infty$ is about 0.3. Using their value for k_{-2}^∞, ($\log k_{-2}^\infty\ (s^{-1})$ = 13.6 - 38000/2.3 RT), $\log k_{-2}^\infty\ (s^{-1})$ = 6.12 at 1111 K and at 182 Torr $k_{-2}[M]^x \approx 4.0 \times 10^5 s^{-1}$. In the presence of hydrogen as third body instead of ethane this value may be further reduced by about a factor of four to ~ $10^5 s^{-1}$. This factor

may be slightly smaller as indicated by the present results, which are discussed in Chapter 9. Taking the value of log k_3 = 6.16 at 1111 K from this work, $k_3[H_2]$ is about 3.8 x $10^3 s^{-1}$ at a hydrogen pressure of 182 Torr and the ratio $k_{-2}[M]^x/k_3[H_2]$ is about 25. This estimate is not conclusive because rather long extrapolations are required for the rate constant k_{-2} and its pressure-dependence must be obtained. Taken together, the order and the activation energy of the rate suggest that the mechanism is best described by the conditions imposed by Case 1 and that Equation (6-4) adequately expresses the rate of disappearance of ethylene in the system.

Both the order with respect to hydrogen and the activation energy of the rate strongly suggest that hydrogen atoms are maintained at an equilibrium concentration. It may be questioned, however, that the homogeneous rate of dissociation of hydrogen is sufficiently fast to allow the equilibrium concentration to be obtained during the time of these reactions. Taking the value of 3.4 x 10^9 $(L\ mol^{-1})^2 s^{-1}$ for the third order rate constant for combination of hydrogen atoms

$$H + H + H_2 \rightarrow H_2 + H_2$$

measured at room temperature[75] and the equilibrium constant for dissociation, $K_1 = 1.23 \times 10^{-17}$ mol L^{-1} at

1111 K, the rate of the homogeneous dissociation of H_2 at 182 Torr can be estimated as

$$-\frac{d[H_2]}{dt} = 1.45 \times 10^{-13} \text{ mol } L^{-1}s^{-1}$$

In general the third order rate constant decreases with increasing temperature because at higher temperature, the lifetime of the bimolecular complex will be shorter. Therefore, the rate of dissociation of H_2 calculated above will be an upper limit for the homogeneous rate of production of H atoms.

Sepehrad, Marshall and Purnell[76] measured the rate of combination of hydrogen atoms on a clean quartz surface. In their system, hydrogen atoms disappeared at the wall in a first-order process

$$H \rightarrow \frac{1}{2} H_2 \qquad (W)$$

and a value of k_W of 20 ± 15 s^{-1} was estimated in the range of 600-800 K. In this temperature region, no change in k_W was observed within the error of measurement. Furthermore, the value was similar to that reported at room temperature.[71] It is reasonable, therefore, to assume this value in our region of temperature.

The rate of dissociation of hydrogen on the surface may be obtained from the rate constant k_W for combination on the surface and the equilibrium constant K_1 as follows:

$$\frac{k_{-W}}{k_W} = K_W^{-1} = (K_1)^{1/2}$$

At 1111 K,

$$k_{-W} = k_W(K_1)^{1/2} = 20 \times (1.27 \times 10^{-17})^{1/2} \text{ (mol } L^{-1})^{1/2} s^{-1}$$

At 182 Torr, the rate of heterogeneous dissociation of H_2 will be

$$-\frac{1}{2}\frac{d[H_2]}{dt} = k_{-W}[H_2]^{1/2} = 3.6 \times 10^{-9} \text{ mol } L^{-1} s^{-1}$$

Comparison of these two rates shows that homogeneous dissociation is indeed too slow by at least a factor 10^4. It must be concluded that dissociation and recombination are catalyzed by the quartz surface in the present vessel. The fact that the rate was not affected by an increase in S/V ratio of the reaction vessel is in agreement with the attainment of an equilibrium concentration of hydrogen atoms in both unpacked and packed vessels.

Other reactions may affect the concentration of radicals in the system. The occurrence of reaction (6) could reduce the concentration of hydrogen atoms below equilibrium.

At 1111 K and a pressure of hydrogen of 182 Torr, the equilibrium concentration of hydrogen atoms is 1.79×10^{-10} mol L^{-1}. Under the same conditions, with 10 ppm C_2H_4, the equilibrium ratio of C_2H_5/H equals 10^{-3}. If combination at the wall occurs by reaction (W), the ratio of the rate of reaction (W) and (6) may be expressed as follows:

$$\frac{R_W}{R_6} = \frac{k_W[H]}{k_6[C_2H_5][H]} = \frac{k_W}{k_6K_2[H][C_2H_4]} \qquad (6\text{-}6)$$

and with the condition described above ($K_2 = 1.7 \times 10^4$ L mol^{-1} at 1111 K)

$$\frac{R_W}{R_6} = 2.6 \times 10^4 \qquad (6\text{-}7)$$

Therefore, termination by reaction (6) is probably not sufficiently important to reduce the concentration of hydrogen atoms significantly below equilibrium. Furthermore, this reaction probably requires collisional stabilization, making the rate of reaction (6) slower than estimated. Without stabilization, the ethane molecule will dissociate into two methyl radicals which will rapidly convert to methane, returning hydrogen atoms to the system.

Reactions other than (2) which lead to loss of ethylene may be considered. Ethylene may react directly with hydrogen to give an ethyl radical and a hydrogen atom

$$C_2H_4 + H_2 \rightarrow C_2H_5 + H \qquad (8)$$

The rate constant for reaction (8) may be estimated from values of ΔH and ΔS (Table 24) and the rate constant k_{-8}. The rate constant k_{-8} represents the disproportionation reaction of the overall combination process of a hydrogen atom and an ethyl radical. Taking the overall combination rate constant as $\log k_c = 10.81 - 200/2.3RT$[125] and $k_d/k_c = 0.05$,[71] therefore k_{-8} can be expressed as

$$\log k_{-8} = 9.51 - 200/2.3RT$$

The value of k_8 can be deduced as

$$\log k_8 \ (L\ mol^{-1}s^{-1}) = 10.07 - 67300/2.3RT$$

At 1111 K, $k_8 = 6.53 \times 10^{-4}\ L\ mol^{-1}s^{-1}$.

The rate of disappearance of ethylene by reaction (8) may be written as

$$-R_{C_2H_4} = k_8[C_2H_4][H_2] \qquad (6\text{-}8)$$

Taking the conditions of 182 Torr of hydrogen and 10 ppm C_2H_4 as an example, the rate of disappearance of ethylene may be estimated as 6×10^{-14} mol $L^{-1}s^{-1}$, while the observed rate is 3×10^{-10} mol $L^{-1}s^{-1}$ (Table 22). Reaction (8) therefore does not appear to be important under these conditions. A further possibility for consumption of ethylene is the unimolecular dissociation

$$C_2H_4 \rightarrow C_2H_3 + H \qquad (9)$$

This reaction has been observed and measured in the shock-tube pyrolysis of ethylene[77][78] as a second-order process. A reasonable value for the unimolecular dissociation constant is

$$\log k_9(s^{-1}) = 16 - 10400/2.3RT \qquad (6\text{-}9)$$

and at 1111 K, $k_9 = 3.5 \times 10^{-5}\ s^{-1}$. Taking the same conditions as above,

$$-R_{C_2H_4} = k_9[C_2H_4] = 8.8 \times 10^{-13} \text{ mol } L^{-1}s^{-1} \qquad (6\text{-}10)$$

This must be an upper limit since the dissociation will undoubtedly be partly pressure-dependent at the temperature of these experiments. Therefore reaction (9) is also not

sufficiently fast to account for the rate of disappearance of ethylene.

The rates of reactions (8) and (9) may also be compared to the rate of production of hydrogen atoms in the system. The rate constant k_{-W} for the dissociation of H_2 on the surface has been estimated as

$$k_{-W} = 7.1 \times 10^{-8} \text{ (mol L}^{-1}\text{)}^{1/2} \text{ s}^{-1} \text{ at 1111 K.}$$

The ratio of rates may be expressed as follows:

$$\frac{R_{-W}}{R_8} = \frac{k_{-W}[H_2]^{1/2}}{k_8[C_2H_4][H_2]} = 5.8 \times 10^4 \qquad (6\text{-}12)$$

$$\frac{R_{-W}}{R_9} = \frac{k_{-W}[H_2]^{1/2}}{k_9[C_2H_4]} = 4.2 \times 10^3 \qquad (6\text{-}13)$$

Even though this represents an upper limit to the rate of formation of hydrogen atoms from hydrogen, it is unlikely that reactions (8) or (9) are important in the present system.

(f) Rate of Formation of Methane

Methane is a secondary product, formed by decomposition of ethane by reaction (4). If all methyl radicals react with

hydrogen to give methane (reaction (5)), the rate of formation of methane is given as follows:

$$R_{CH_4} = 2k_4[C_2H_6] \qquad (6\text{-}14)$$

The maximum rate of formation of methane will be observed at the maximum concentration of ethane. Since the product ethane achieves its maximum concentration at a very short time of reaction, the maximum rate of formation of methane may be obtained by an extrapolation procedure similar to that used to obtain the initial rate of disappearance of ethylene. In other words, a maximum rate will be indistinguishable from an initial rate on the time scale of the present experiments. These rates of formation of methane are shown in Table 23. The maximum concentration of ethane is obtained when the rate of formation equals the rate of disappearance,

$$k_3[C_2H_5][H_2] = k_{-3}[C_2H_6][H] + k_4[C_2H_6]$$

and therefore

$$[C_2H_6]_{max} = \frac{k_3[C_2H_5][H_2]}{k_{-3}[H] + k_4} \qquad (6\text{-}15)$$

The maximum rate of formation of CH_4 is then

$$R_{CH_4} = 2k_4 \left[\frac{k_3[C_2H_5][H_2]}{k_{-3}[H] + k_4}\right] \qquad (6\text{-}15)$$

If the concentration of the ethyl radical is determined through the equilibrium of reaction (2) and the concentration of hydrogen atoms is controlled through reaction (1), the maximum rate of formation of methane is

$$R_{CH_4} = \frac{2k_4k_3K_2K_1^{1/2}[H_2]^{3/2}[C_2H_4]}{k_{-3}K_1^{1/2}[H_2]^{1/2} + k_4} \qquad (6\text{-}16)$$

Since $k_{-3} = k_3/K_3$ the rate constant k_3 may be expressed as

$$k_3 = \frac{R_{CH_4}k_4}{K_1^{1/2}[H_2]^{1/2}[2k_4K_2[H_2][C_2H_4] - R_{CH_4}/K_3]} \qquad (6\text{-}17)$$

The relative importance of the terms in the denominator of Equation (6-16) may be deduced from the measured activation energy of the rate of formation of methane. If $k_4 >> k_{-3}K_1^{1/2}[H_2]^{1/2}$ and ethane is removed primarily by dissociation, the rate of formation of methane becomes

$$R_{CH_4} = 2k_3K_2K_1^{1/2}[H_2]^{3/2}[C_2H_4] \qquad (6\text{-}18)$$

which is exactly twice the rate of disappearance of ethylene. In this case the activation energies for the rate of disappearance of ethylene and the rate of formation of methane should be the same. The value observed for the latter rate was 38 kcal/mol while for the former was 33 kcal/mol. It

may be concluded that the simplified expression Equation (6-18) closely describes the mechanism for the formation of methane.

For the case in which k_4 may be neglected in the denominator of Equation (6-16) the rate of formation of CH_4 is given as follows:

$$R_{CH_4} = 2k_4K_3K_2[H_2][C_2H_4]$$

The activation energy predicted from this equation is about 63 Kcal/mole. This case, therefore, does not describe the mechanism of the reaction. Nevertheless, the initial rate of formation of methane was not exactly twice the initial rate of disappearance of ethylene, indicating that some ethane may be lost by the reverse of the reaction (3). The complete Equation (6-17) was therefore used to calculate k_3.

(g) Calculation of the Rate Constant k_3

Using Equations (6-4) and (6-17) values of k_3 were calculated from the rate of disappearance of ethylene and from the rate of formation of methane. The results of the former calculation are included in Table 22 and the latter are given in Table 23. Values of K_1, K_2, K_3 and k_4 are included where applicable. The equilibrium constant K_3 was calculated using a value of 28 kcal/mol for the heat of formation of ethyl radical, as recently reported.[94]

Table 23

INITIAL RATE OF FORMATION OF METHANE AND VALUES FOR k_3

Total Pressure: 182 Torr. $X_{C_2H_4}$: 9.33 ppm

T/K	$\frac{d}{dt}[CH_4]$/ mol $L^{-1}s^{-1}x10^{-10}$	$K_3/10^{-3}$	k_4/s^{-1}	k_3/L mol $^{-1}s^{-1}x10^6$
1111	2.50	3.87	0.0676	1.10
1131	3.96	4.06	0.151	1.46
1151	4.92	4.21	0.282	1.76
1171	6.42	4.37	0.525	2.27
1192	8.62	4.54	1.00	2.29

Justification for the use of this value rather than the value of 26 kcal/mole given in most references[79][80] will be given later. The value of k_4 in the pressure-dependent region was estimated by extrapolation of the results of Lin and Back.[83] Other data used in the calculation are given in Table 24. A statistical analysis for the value of k_3 measured at 1111 K for the unpacked vessel gives $k_3 = (1.63 \pm 0.24) \times 10^6$ L mol^{-1} s^{-1}, corresponding to a standard deviation of 15% which comes mainly from the uncertainty of the estimate of the initial rate. An Arrhenius plot of k_3 gives an activation energy of 23±2 kcal mol^{-1}.

The activation energy for k_3 measured in the present experiment, 23 kcal/mole, is considerably higher than the average value obtained by including the results below 820 K. It might be argued that the high value obtained in the region of temperature of 1000 K indicates that the activation energy for this abstraction reaction increases substantially from about 800 K to 1000 K. Such non-Arrhenius behaviour has been observed and commented upon for other reactions involving small radicals.[59] This effect probably does not explain the high activation energy from the present results because the value of the rate constant is not substantially above the value expected on the basis of an Arrhenius behaviour. On the contrary, the rate constant lies close to an extrapolation of an Arrhenius expression of the low-temperature data.

Table 24

THERMODYNAMIC DATA*

	ΔH_f(298 K) kcal mol^{-1}	S^o(298 K) cal mol^{-1}deg^{-1}	C_p/cal mol^{-1}deg^{-1} 300	900	1000	1100	1200K
H	52.1	27.4	4.968	4.968	4.968	4.968	4.968
H_2	0	31.2	6.895	7.139	7.217	7.308	7.404
C_2H_5	28.0	59.0	11.1	24.3	25.7	26.8	27.9
C_2H_6	-20.2	54.9	12.648	27.69	29.33	30.77	32.02
C_2H_4	12.5	52.4	10.45	21.46	22.57	23.54	24.39

EQUILIBRIUM CONSTANTS

$$H + C_2H_4 \overset{K_2}{\rightleftharpoons} C_2H_5$$

T/K	ΔH_T/kcal mol^{-1}	ΔS_T/cal mol^{-1}deg^{-1}	$K/[(\text{mol L}^{-1})^{-1} \times 10^4]$
1000	-38.7	-24.5	10.7
1100	-39.0	-24.7	2.03
1200	-39.2	-24.9	0.50

$$C_2H_5 + H_2 \overset{K_3}{\rightleftharpoons} C_2H_6 + H$$

T/K	ΔH_T/kcal mol^{-1}	ΔS_T/cal mol^{-1}deg^{-1}	$K/10^{-3}$
298	3.90	- 7.90	0.0270
900	4.16	- 7.42	2.33
1000	4.28	- 7.24	3.03
1100	4.39	- 7.10	3.80
1200	4.45	- 6.98	4.61

* Standard State 1 atm, 298K.

Figure 32B. Arrhenius Plot for k_3 Measured in the Present Experiments

□ - 9.3 pmm C_2H_4

O - 10.8 ppm C_2H_4

Δ - calculated from the yield of CH_4

I - range of values at 1111 K for five concentrations of C_2H_4

Filled symbols: packed vessel

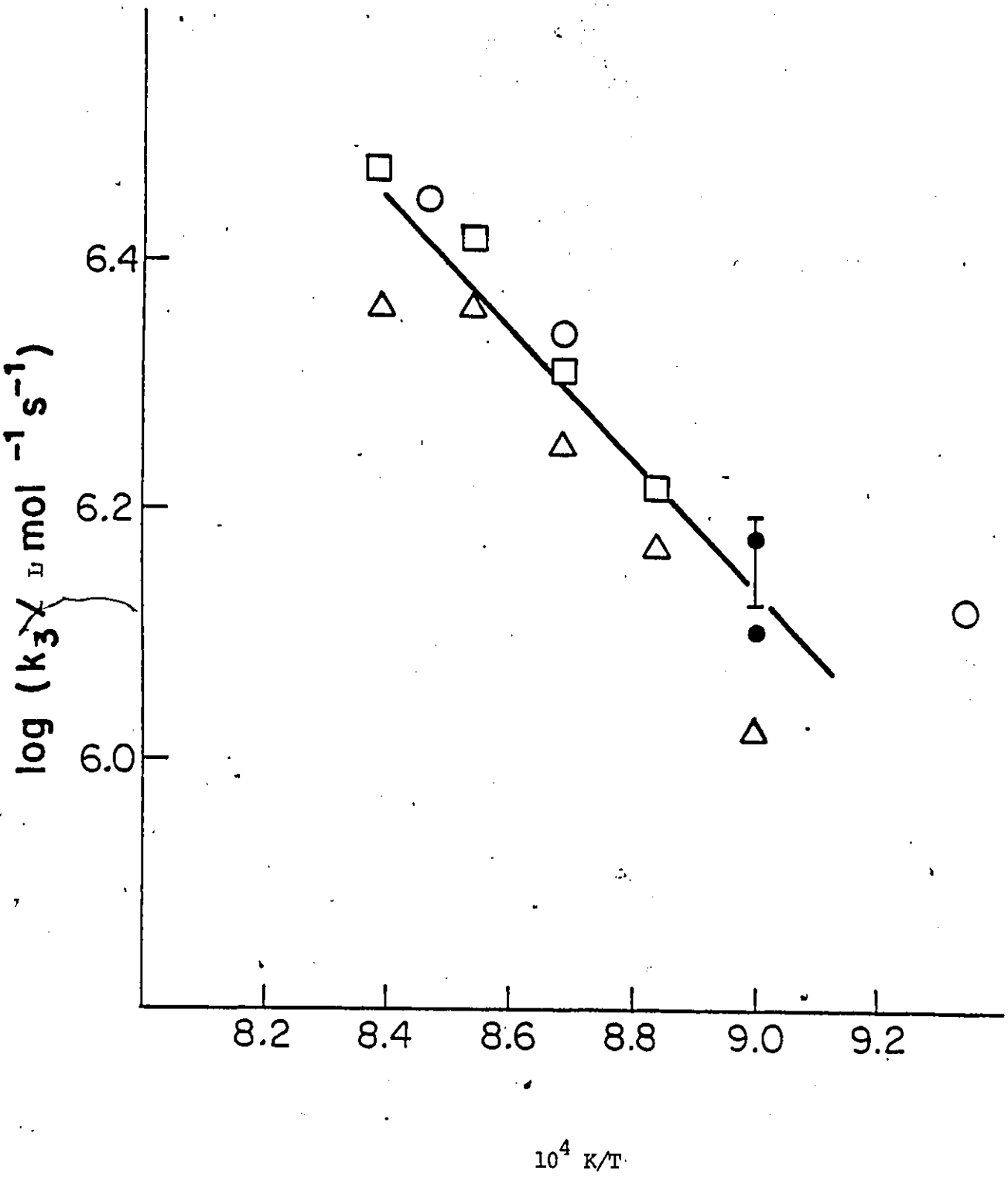
6.4
6.2
6.0
log ($k_3 \chi_n$ mol $^{-1}$ s^{-1})
8.2
8.4
8.6
8.8
9.0
9.2
10^4 K/T

In measurements of rate constants for radical reactions the activation energy obtained is not itself as significant as the value of the rate constant. More reliable activation energies are obtained by combining a series of perhaps less accurate results, which are obtained over a wide temperature range, than by relying on results from a narrow range of temperature. Only four direct measurements of the rate constant k_3 were reported in the literature, summarized in Table 25. These measurements were all made relative to the rate constant for the combination of ethyl radicals k_c, which in each case was taken as 2.2×10^{10} L mol^{-1}s^{-1}. More recent work [81][82] indicates that $k_c \sim 10^{10}$ L mol^{-1}s^{-1}, and these values should, therefore, be corrected by a factor $\sqrt{2.2}$.

The corrected values of these measurements of k_3 together with the present measurements are shown in Figure 33. The results are reasonably fitted by an Arrhenius equation, as follows:

$$\log k_3 \text{ (L mol}^{-1}\text{s}^{-1}\text{)} = 9.0 - 12600/2.3RT \qquad (6\text{-}19)$$

It appears therefore that, although the present measurement of E_3 suggests the activation energy may increase at high temperature, the values of the rate constant k_3 correlate with an Arrhenius expression covering the whole range of

Table 25

DIRECT MEASUREMENT OF k_3 $C_2H_5 + H_2 \overset{k_3}{\rightarrow} C_2H_6 + H$

Reference	T/K	E/kcal mol^{-1}	$\log(A/L\ mol^{-1}s^{-1})$	$\log(k/L\ mol^{-1}s^{-1})$	$\log(k^*/L\ mol^{-1}s^{-1})$
Boddy, P.J. Steacie, E.W.R. [60]	355-595	11.3	8.51	1.56-4.37	1.39-4.20
Reid, L.E. LeRoy, D.J. [61]	513-593	13.7	9.60	3.77-4.56	3.60-4.39
Halstead, M.P. Quinn, C.P. [62]	823			5.68	5.51
Baldwin, R.R. et al. [63]	713			5.33	5.16
This work	1111-1200	23.0	10.6	6.07-6.41	

Figure 33. Arrhenius Plot for k_3 open symbols Represent Direct measurements of k_3 Reported in Literature

● - this work
□ - reference 60
◇ - reference 61
Δ - reference 62
O - reference 63

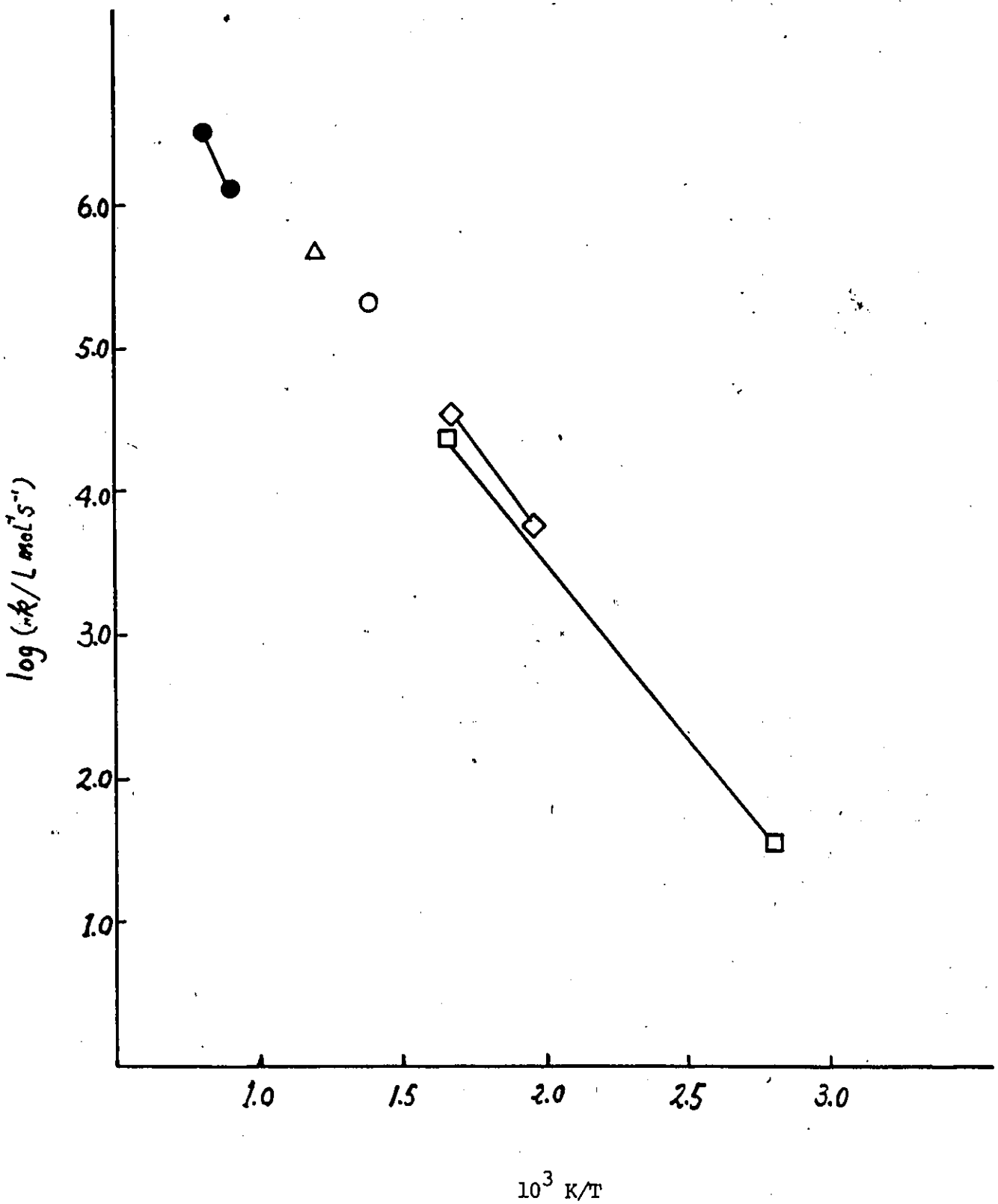
6.0
5.0
4.0
3.0
2.0
1.0
log (k/L mol⁻¹s⁻¹)
1.0
1.5
2.0
2.5
3.0
10³ K/T

temperature illustrated in Figure 33. The question of curvature in the Arrhenius plot of k_3 is therefore not answered by the present results. This question will be discussed in the next chapter with respect to k_{-3} and in the comparison of the independent measurements of k_3 and k_{-3}.

(h) Evaluation of the Method

A possible source of error in the present measurements which would lead to an underestimate of k_3 is an overestimate of either the hydrogen atom concentration or the ethyl radical concentration. It seems unlikely that the hydrogen atom concentration is much below equilibrium since the large increase in surface area had no effect on the rate. It is known that hydrogen atoms are strongly adsorbed on quartz surfaces, leading to heterogeneous reactions, but the absence of a perturbing effect of the surface is easily explained if atoms and molecules are in equilibrium. The concentration of ethyl radicals, on the other hand, may be reduced below the equilibrium value under conditions where $k_3[H_2]$ may become comparable in rate to the dissociation of the ethyl radical, reaction (-2). The overall activation energy of the rate indicated that an equilibrium concentration of ethyl radicals was achieved. Estimates of the relative magnitude of these two rates

suggests that neglect of reaction (-2) could cause an underestimate of k_3 at most by perhaps a factor 2.

CHAPTER 7

KINETICS OF THE REACTION H + C_2H_6 → H_2 + C_2H_5 IN THE TEMPERATURE REGION OF 1000 K

This chapter describes the results obtained from a study of the kinetics of the reaction of mixtures of H_2 with the reactant ethane and the values measured for the rate constant for the abstraction of hydrogen atoms from ethane

$$H + C_2H_6 \rightarrow H_2 + C_2H_5$$

(a) Products and Measurement of Initial Rate

At temperatures below about 975 K ethylene was the principal product. Figure 34A shows a set of yield-time curves for the formation of ethylene at various concentrations of ethane with a fixed total pressure. Methane was a minor product, which became undetectable below about 900 K. Yield-time curves showing methane formation at 996 K are given in Figure 34B. Higher molecular weight products were not observed even at long reaction time. Since the yield-time curves were linear initial rates could be determined directly from plots such as illustrated in Figure 34A. Rates were measured at 922 K at five pressures ranging from 365 to 175 Torr. At each pressure four

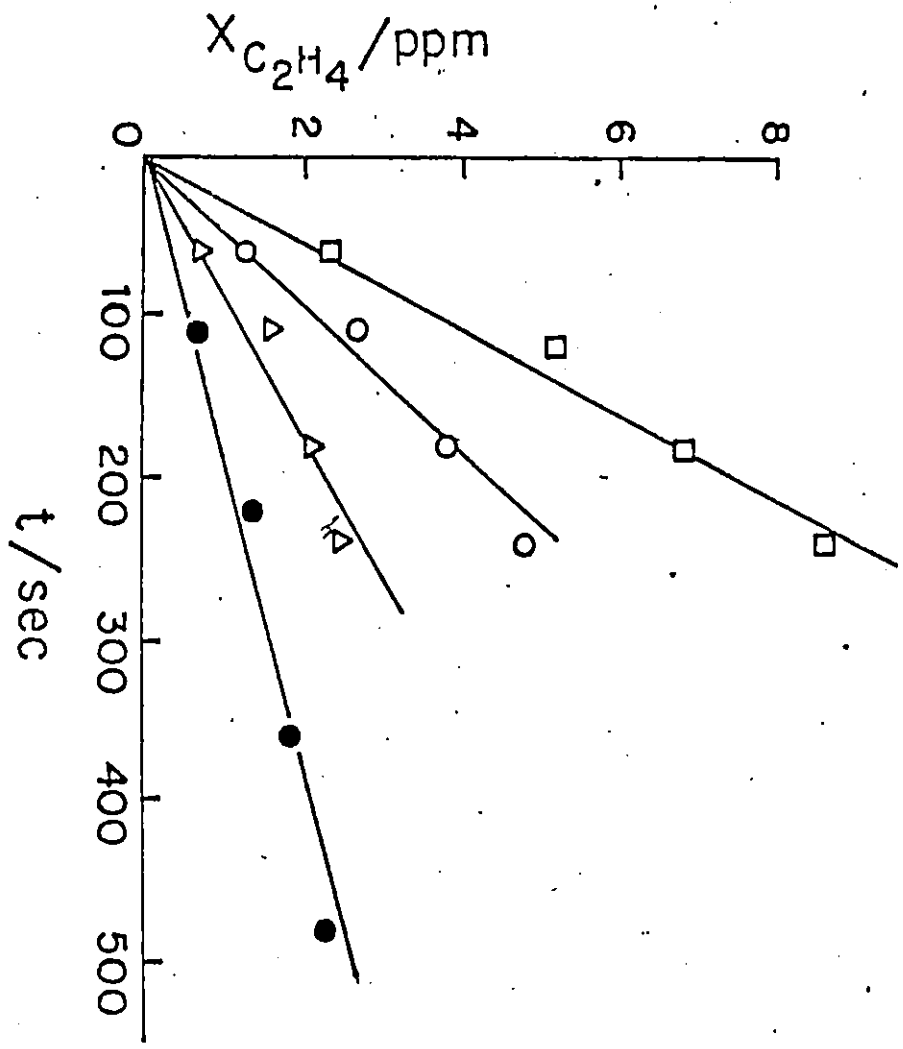

Figure 34A. Yield of Ethylene, Expressed as Mole Fraction, as a Function of Time at 922 K and Total Pressure of 113.5 Torr

$X_{C_2H_6}$ ppm

● - 16.4
Δ - 24.8
O - 37.8
□ - 56

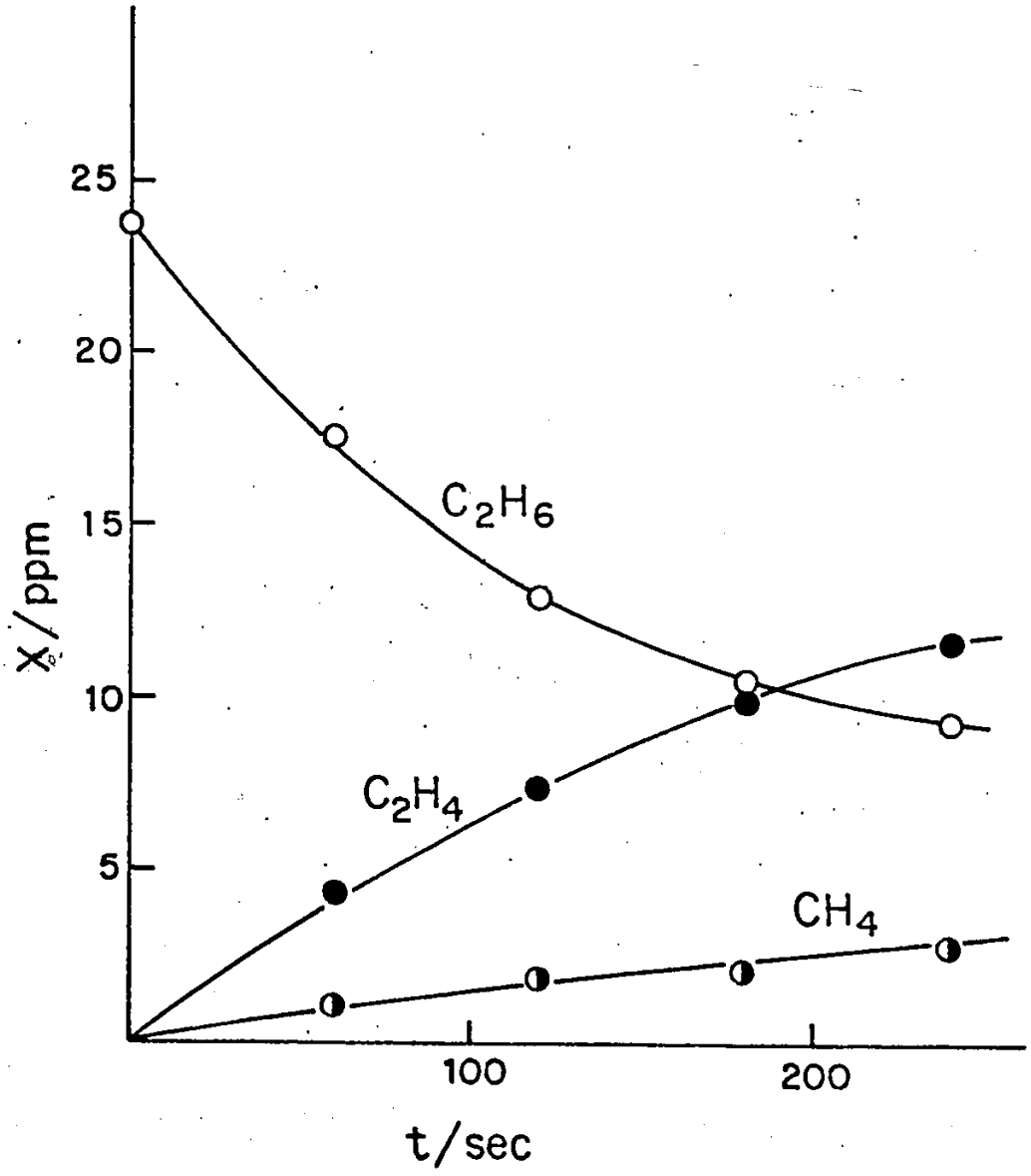

Figure 34B. Yield-Time Curves, Expressed as Mole Fraction at 996 K and Total Pressure of 37.5 Torr

compositions of the reacting mixture were studied ranging from 16.4 to 56 ppm ethane. Rates were also measured at 12 temperatures from 876 to 1016 K at various pressures. The data are summarized in Tables 26 and 29.

(b) Determination of the Order with Respect to Each Reactant

The rate of formation of ethylene may be expressed as follows:

$$R_{C_2H_4} = k[H_2]^m[C_2H_6]^n \qquad (7\text{-}1)$$

where k is an overall rate constant and m and n represent the order of the rate with respect to hydrogen and ethane respectively. The measurements of the rate for a constant composition of ethane and hydrogen at various total pressures allow the determination of the total order m + n. The results are plotted in Figure 35A, as log of the initial rate of formation of ethylene as a function of log of the total pressure. From the slope of these plots, $m + n = 1.70 \pm 0.05$. To determine n the rate was measured at constant total pressure for various mixtures of ethane in hydrogen (as illustrated in Figure 34A). A log-log plot of the initial rate of formation as a function of the concentration of ethane is shown in Figure 35B. From the slopes of these lines a value of n of 1.25 ± 0.05 is obtained.

Table 26

INITIAL RATE OF FORMATION OF C_2H_4

922 K, S/V = 1.0 cm^{-1}

Total Pressure/Torr	$X_{C_2H_6}$/ppm	$C_2H_6/10^{-7}$ mol L^{-1}	$R^{o}_{C_2H_4}/10^{-11}$ mol $L^{-1}s^{-1}$
175.0	56	1.71	15.4
	37.8	1.15	10.2
	24.8	0.755	4.87
	16.4	0.500	3.05
113.0	56	1.10	9.21
	37.8	0.744	4.15
	24.8	0.488	2.28
	16.4	0.328	1.08
82.5	56	0.804	4.48
	37.8	0.543	2.40
	24.8	0.356	1.38
	16.4	0.236	0.775
52.0	56	0.507	1.84
	37.8	0.342	0.869
	24.8	0.224	0.543
	16.4	0.148	0.296
36.5	56	0.356	0.830
	37.8	0.240	0.508
	24.8	0.158	0.270
	16.4	0.104	0.171

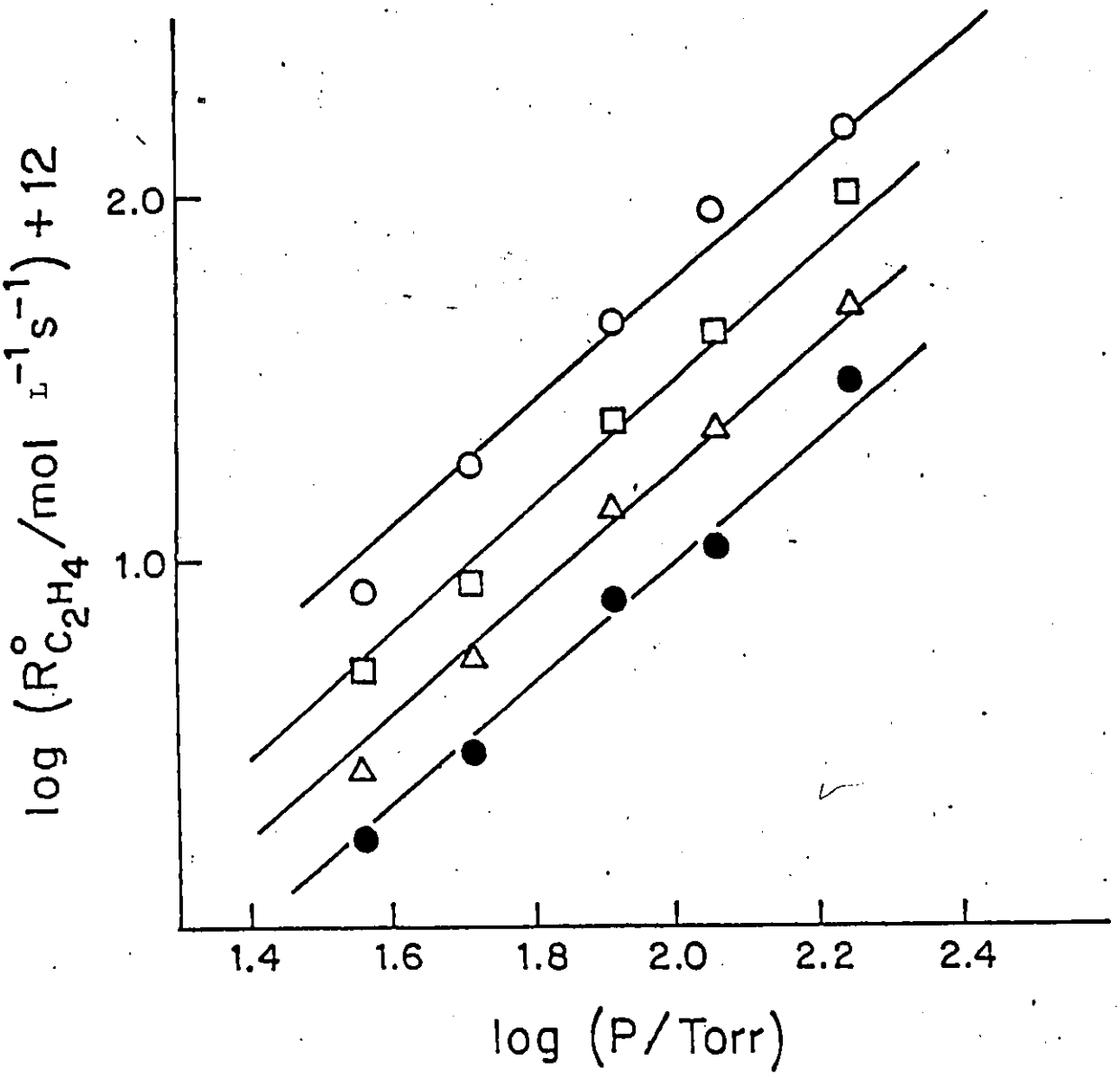

Figure 35A. Log-Log Plot of the Initial Rate of Formation of Ethylene as a Function of the Total Pressure at 922 K

$X_{C_2H_6}$ pmm

● - 16.4
△ - 24.8
□ - 37.8
○ - 56

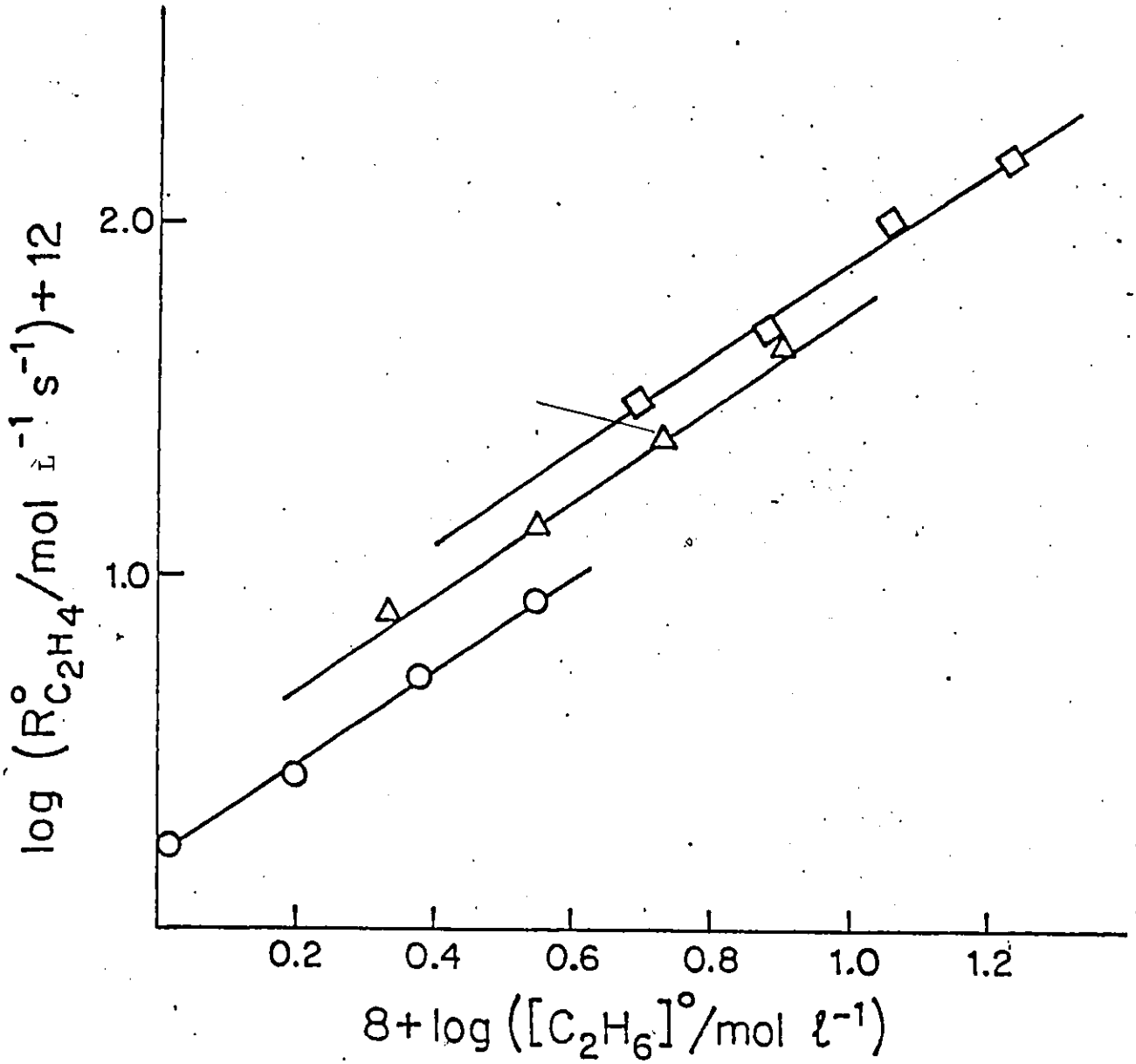

Figure 35B. Log-Log Plot of the Initial Rate of Formation of Ethylene as a Function of the Concentration of Ethane at 922 K

Total Pressure, Torr

○ - 36.5
△ - 82.5
◇ - 175

The value of m is therefore 0.45 ± 0.1. The order of the rate with respect to hydrogen may therefore be considered to be 0.5 while the order with respect ethane is somewhat greater than 1.

(c) Measurements in the Packed Vessel

The rate of the reaction was measured in the packed vessel at four temperatures and for a range of pressures and concentrations of ethane. The results are given in Table 27. At temperatures where the rate of formation of methane was measurable no change in its rate was observed in the packed vessel. The rate of formation of ethylene, however, was increased by a factor between two and three. Furthermore, the order of the rate of formation of ethylene with respect to the concentration of ethane was found to be 1.95 ± 0.15, a stronger dependence than observed in the unpacked vessel. In both vessels the order was essentially constant over the temperature range of the experiments. It seems reasonable to conclude that a contribution from a heterogeneous reaction in the unpacked vessel could lead to an erroneously high order for the rate of formation of ethylene. In order to assess the magnitude of this heterogeneous reaction and to make a correction for it, the following procedure was adopted. The observed order was plotted as a function of S/V ratio and

Table 27

INITIAL RATE OF FORMATION OF C_2H_4

$S/V = 7.0\ cm^{-1}$

T/K	P/Torr	$X_{C_2H_6}$/ppm	$C_2H_6/10^{-7}$ mol L^{-1}	$R^{o}_{C_2H_4}/10^{-11}$ mol $L^{-1}s^{-1}$
894	185	7.96	0.264	0.896
		17.5	0.581	6.64
		35.7	1.190	16.6
956	120	9.70	0.195	5.23
		20.7	0.416	24.1
		39.8	0.800	64.3

an extrapolation was made to S/V = 0. The order obtained at S/V = 0 was 1.1. It may be concluded, therefore, that the homogeneous reaction producing ethylene is first order with respect to the concentration of ethane and 0.5 order with respect to the concentration of hydrogen. The rate measured in the unpacked vessel has nevertheless a significant contribution from the heterogeneous reaction. In order to obtain a rate constant relating to the homogeneous reaction (-3), it would be desirable to apply a correction to the measured rates. The method of making the correction as well as possible reasons for the strong dependence of the rate on the concentration of ethane in the packed vessel will be discussed later.

(d) Mechanism of the Reaction

These results suggest that the following simple mechanism may describe the formation of ethylene in the present system:

$$H_2 \rightleftharpoons 2H \qquad (1)$$

$$H + C_2H_6 \rightarrow C_2H_5 + H_2 \qquad (-3)$$

$$C_2H_5 \rightarrow C_2H_4 + H \qquad (-2)$$

The hydrogen atom concentration is controlled by the equilibrium with hydrogen molecules and every ethyl radical

produced in reaction (-3) yields ethylene by reaction (-2). The reverse of reaction (-2) should not be important in the initial stage. Other reactions of the ethyl radicals which may be important are

$$H + C_2H_5 \rightarrow C_2H_6 \qquad (6)$$

$$C_2H_5 + H_2 \rightarrow C_2H_6 + H \qquad (3)$$

Taking into account reactions (1), (-3), (-2), (3) and (6), the steady-state concentration of ethyl radicals may be expressed as follows:

$$[C_2H_5] = \frac{k_{-3}(K_1[H_2])^{1/2}[C_2H_6]}{k_{-2} + k_3[H_2] + k_6(K_1[H_2])^{1/2}} \qquad (7\text{-}2)$$

and the rate of formation of ethylene is therefore

$$R_{C_2H_4} = k_{-2}\left[\frac{k_{-3}(K_1[H_2])^{1/2}[C_2H_6]}{k_{-2} + k_3[H_2] + k_6(K_1[H_2])^{1/2}}\right] \qquad (7\text{-}3)$$

The order of the rate with respect to hydrogen was 0.5. This result is a strong indication that neither reaction (3) nor (6) is important in the mechanism. The rate definitely increased as the pressure of hydrogen increased whereas if reaction (3) were important the rate should decrease as the pressure of hydrogen increased, or if

reaction (6) were important, should remain independent of the pressure of hydrogen. That this conclusion is reasonable may be seen from an estimation of the relative magnitudes of the terms in the denominator. The estimation of the ratio $k_{-2}/k_3[H_2]$ has been discussed in Chapter 6. At 956 K and 120 Torr, this ratio is estimated to be about 3 ~ 5. This estimation is only approximate, but shows that the conclusion concerning the ratio based on the order of the rate with respect to hydrogen is acceptable. Using a collision rate constant for k_6 of 5×10^{10} L mol^{-1}s^{-1} the product $k_6(K_1[H_2])^{1/2}$ is about 10^4 time less than k_{-2}. It may be concluded therefore that the last two terms in the denominator of Equation (7-3) do not make an appreciable contribution and the rate of formation of ethylene may be expressed by the simple equation:

$$R_{C_2H_4} = k_{-3}(K_1[H_2])^{1/2}[C_2H_6] \qquad (7\text{-}4)$$

The activation energy of the rate of formation of ethylene was found to be 70 kcal/mol (Figure 37A). The activation energy may be estimated from Equation (7-5) as follows:

$$E_{C_2H_4} = E_{-3} + \frac{1}{2}\Delta H_1 \qquad (7\text{-}5)$$

Using the value of 12.8 kcal/mol for E_{-3} (see later)

$$E_{C_2H_4} = 12.8 + 51 = 64 \text{ kcal/mol}$$

which is in reasonable agreement with the measured value. If reaction (3) is important in controlling the concentration of ethyl radicals then $E_{C_2H_6} = E_{-2} + \Delta H_{-3} + \frac{1}{2} \Delta H$, and $E_{C_2H_4}$ would have a value of about 92 kcal/mol. If reaction (6) is important, the value of $E_{C_2H_4}$ would be higher still. It appears, therefore, that the simple sequence of reaction (1), (-3) to (-2) can account for the formation of ethylene in the initial stages of the reaction.

(e) Calculation of k_{-3}

Values for k_{-3} were calculated using Equation (7-4) and the rates measured at low concentration of ethane, in the neighbourhood of 20 ppm, where the contribution from heterogeneous processes was a minimum. The rate constant k_{-3} was calculated in the same way for the measurements made in both the unpacked and the packed vessel. These values for k_{-3} were plotted as a function of S/V and an extrapolation was made to S/V = 0. The values obtained were about 15% lower than the values obtained in the unpacked vessel. Examples of these plots are shown in Figure 36 and the results are given in Table 28. The results obtained from measurements at various temperatures are given in Table 29, which includes both uncorrected and corrected

Table 28

$\log k_{-3}(L\ mol^{-1}s^{-1})$

T/K	Packed Vessel S/V = 7.0 cm^{-1}	Unpacked Vessel S/V = 1.0 cm^{-1}	S/V = 0
956.0	9.194	8.822	8.75
915.5	9.094	8.696	8.65
894.0	9.005	8.625	8.56

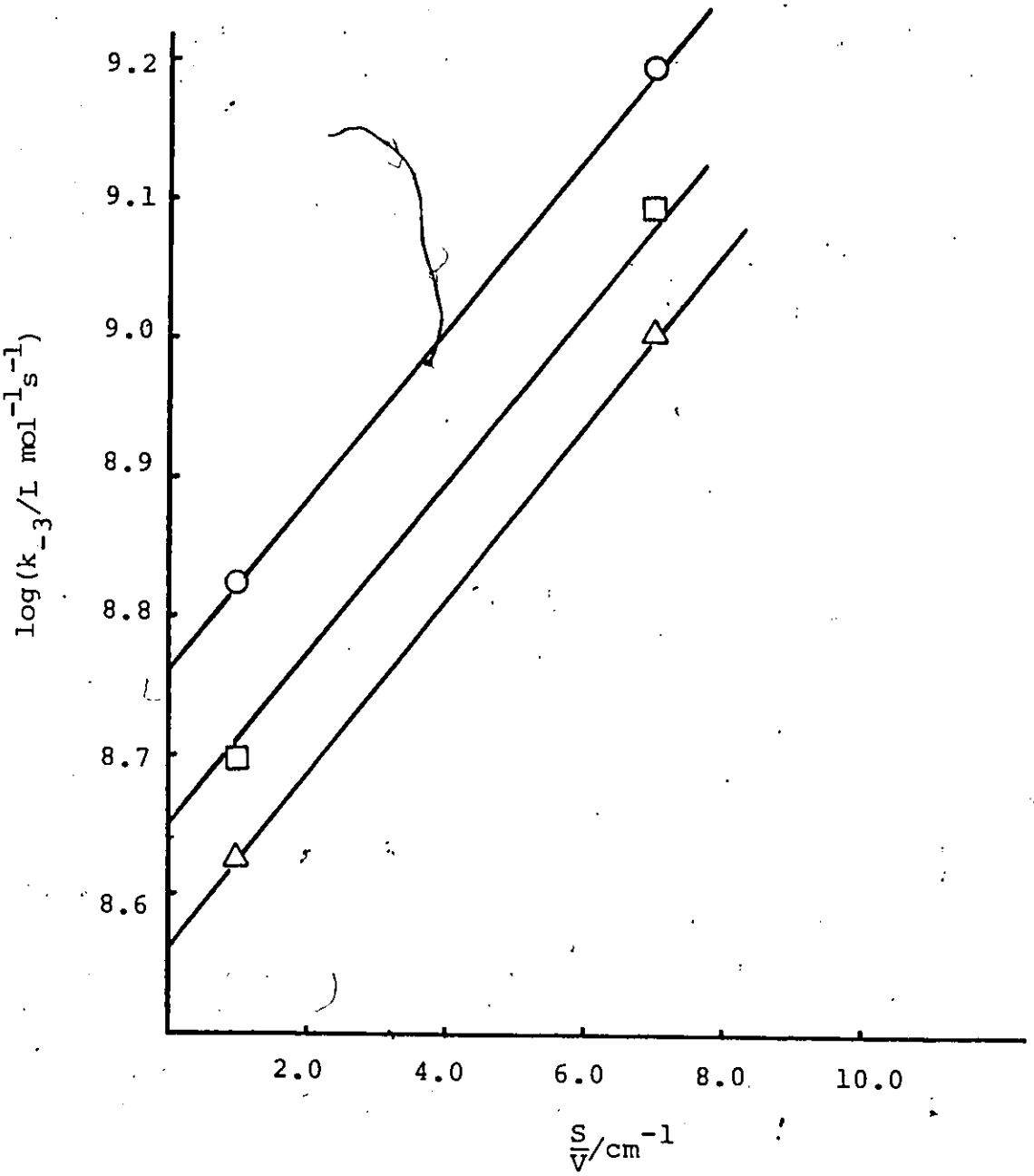

Figure 36. Apparent Rate Constant k_{-3} as Function of S/V

O - 956 K
□ - 915.5 K
△ - 894 K

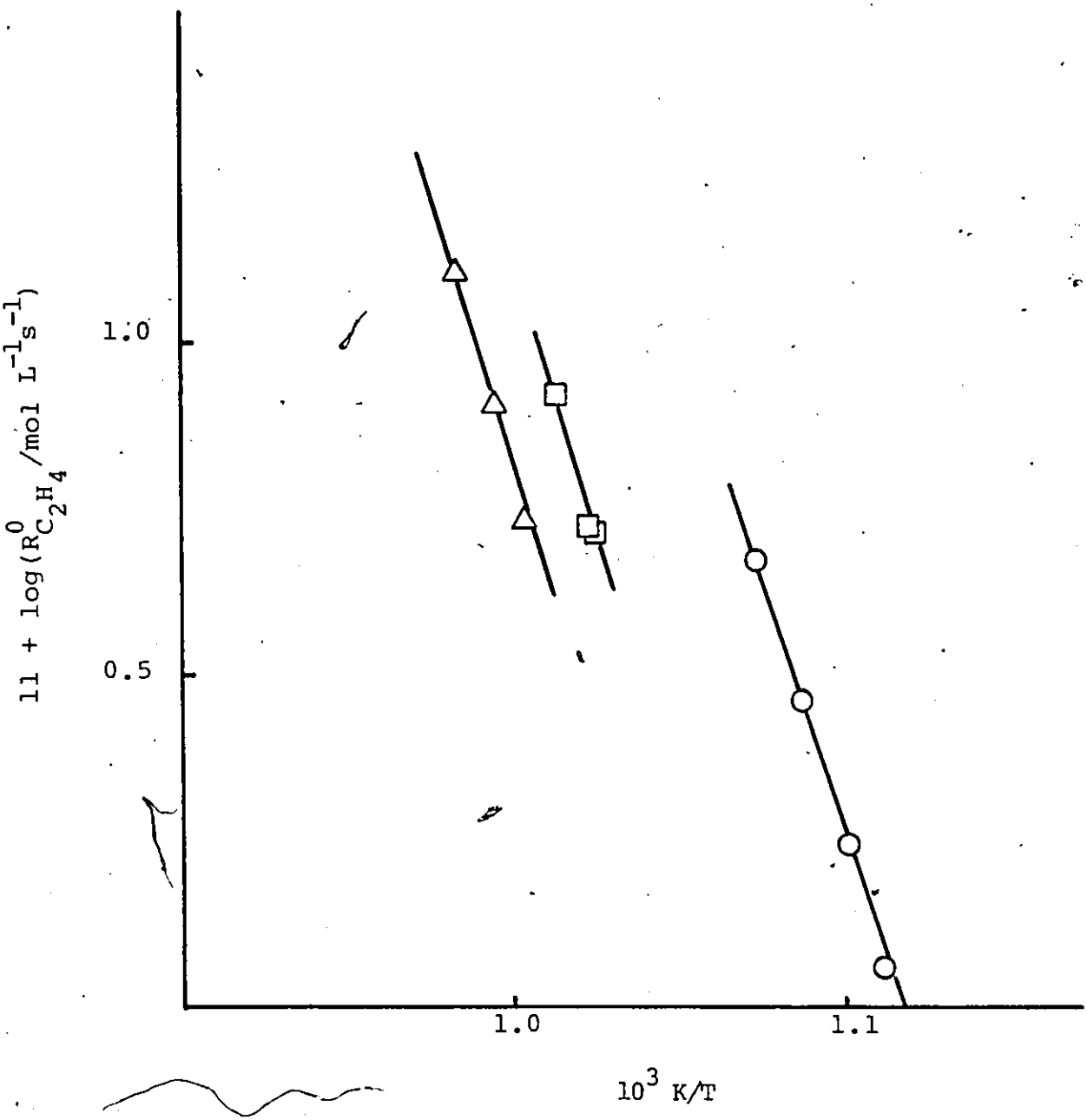

Figure 37A. Arrhenius Plot of Rate of Formation of C_2H_4

O - 23.7 ppm C_2H_6 - 113 Torr of Total Pressure
□ - 23.7 ppm C_2H_6 - 52.5 Torr of Total Pressure
Δ - 23.7 ppm C_2H_6 - 37.5 Torr of Total Pressure

Table 29

k_{-3} AS A FUNCTION OF TEMPERATURE

T/K	P_{H_2}/Torr	[H] 10^{-13} mol L^{-1}	$[C_2H_6]$ 10^{-8} mol L^{-1}	$R^{o}_{C_2H_4}$ 10^{-11} mol $L^{-1}s^{-1}$	log k_{-3} L $mol^{-1}s^{-1}$	log k^{*}_{-3} L $mol^{-1}s^{-1}$
908	113.0	7.84	4.73	1.74	8.672	8.620
920	113.0	11.45	4.67	2.89	8.733	8.681
921.5	113.5	11.45	7.44	4.15	8.688	8.636
931	113.0	15.25	4.62	4.68	8.822	8.770
899	112.5	5.99	4.76	1.14	8.602	8.550
975.5	52.5	35.1	2.05	5.11	8.851	8.799
986	52.5	45.9	2.03	8.29	8.950	8.898
1005.5	37.5	59.8	1.42	8.08	8.978	8.926
1016	37.5	82.3	1.40	12.7	9.042	8.990
876	112.5	2.89	11.1	1.15	8.554	8.502
996	37.5	49.5	1.43	5.38	8.881	8.829
977	52.5	36.8	2.08	5.22	8.842	8.790

* Corrected for heterogeneous reaction.

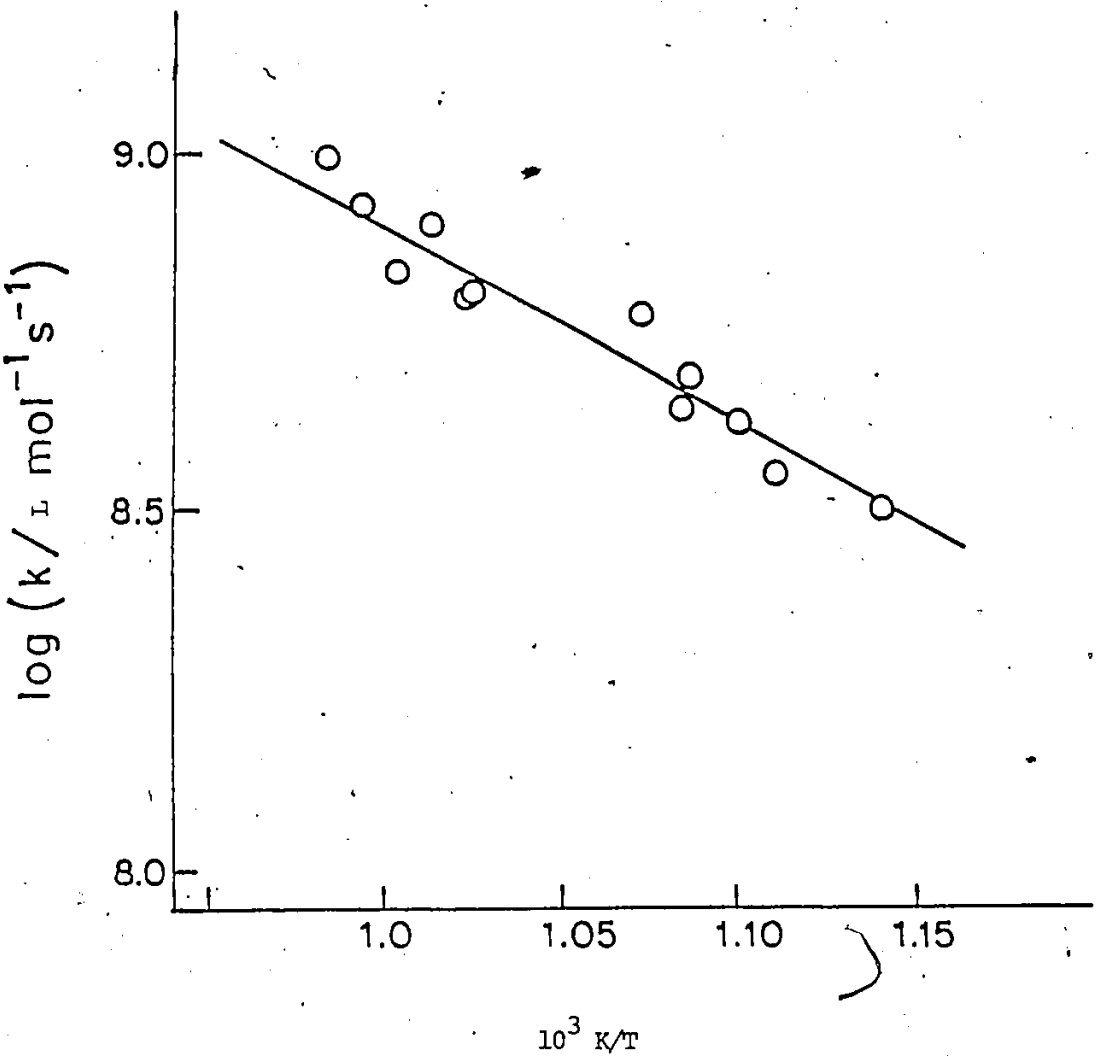

Figure 37B. Arrhenius Plot of the Corrected Values of k_{-3}

values for k_{-3}. The Arrhenius plot is shown in Figure 37B. The value of k_{-3} may be expressed as follows:

$$\log k_{-3}(\text{L mole}^{-1}\text{s}^{-1}) = 11.72 \pm 0.05 - \frac{12800 \pm 200}{2.303\ RT} \quad (7\text{-}6)$$

$$(R = 1.987 \text{ cal mol}^{-1}\text{deg}^{-1})$$

(f) Comparison with Literature Values of k_{-3}

The values of the rate constant k_{-3} obtained in the present study and their relation to other values measured with other techniques covering the range 300-1400 K are shown in Figure 38 and Table 30. Not included in the summary are values of k_{-3} which, although quoted in the recent compilation,[64] were not directly measured in the work described. These are values reported by Skinner and Ringrose,[84] Bradley[85] and Clark, Izod and Kistiakowsky.[86] Also omitted are the early measurements by Darwent and Roberts[73] because it has been shown that the photolysis of H_2S, which was used as a source of hydrogen atoms, produced 'hot' hydrogen atoms with consequent possibility for overestimation of the rate of reaction.[88]

Rate constants measured by addition of hydrocarbon to reacting mixtures of hydrogen and oxygen are determined relative to the branching reaction of hydrogen atoms with oxygen:

Table 30

RATE CONSTANTS FOR REACTION

$$H + C_2H_6 \rightarrow C_2H_5 + H_2$$

Reference	E/kcal mol^{-1}	$\log(k/L\ mol^{-1}s^{-1})$	T/K
Fenimore & Jones [69]	9.7	8.696 - 9.621	993 - 1433
Parsamvan et al. [90]	9.7	8.59* - 8.85*	853 - 953
Voevodsky & Kondratiev [87]	14.0	8.05* - 8.62*	773 - 898
Baldwin [93]		8.30	793
Camilleri et al. [71]	9.4	7.036 - 8.392	503 - 753
Gorban & Nalbandyan [92]	12.2	7.57* - 7.99*	673 - 753
Yang [72]	9.0	4.41 - 6.74	323 - 523
Azatyan & Fillippov [68]	9.1	4.03 - 6.98	290 - 509
Berlie & LeRoy [74]	6.8	5.32 - 6.12	353 - 436
This work	12.8	8.53 - 8.97	876 - 1016

* After normalization.

Figure 38. Arrhenius Plot of Measurements of k_{-3} Covering the Temperature Range 300-1400 K

◐ - reference 69
■ - reference 90
◇ - reference 87
▼ - reference 93
△ - reference 92
◓ - reference 71
◆ - reference 68
● - reference 74
▮ - reference 72
O - present work
... - reference 59

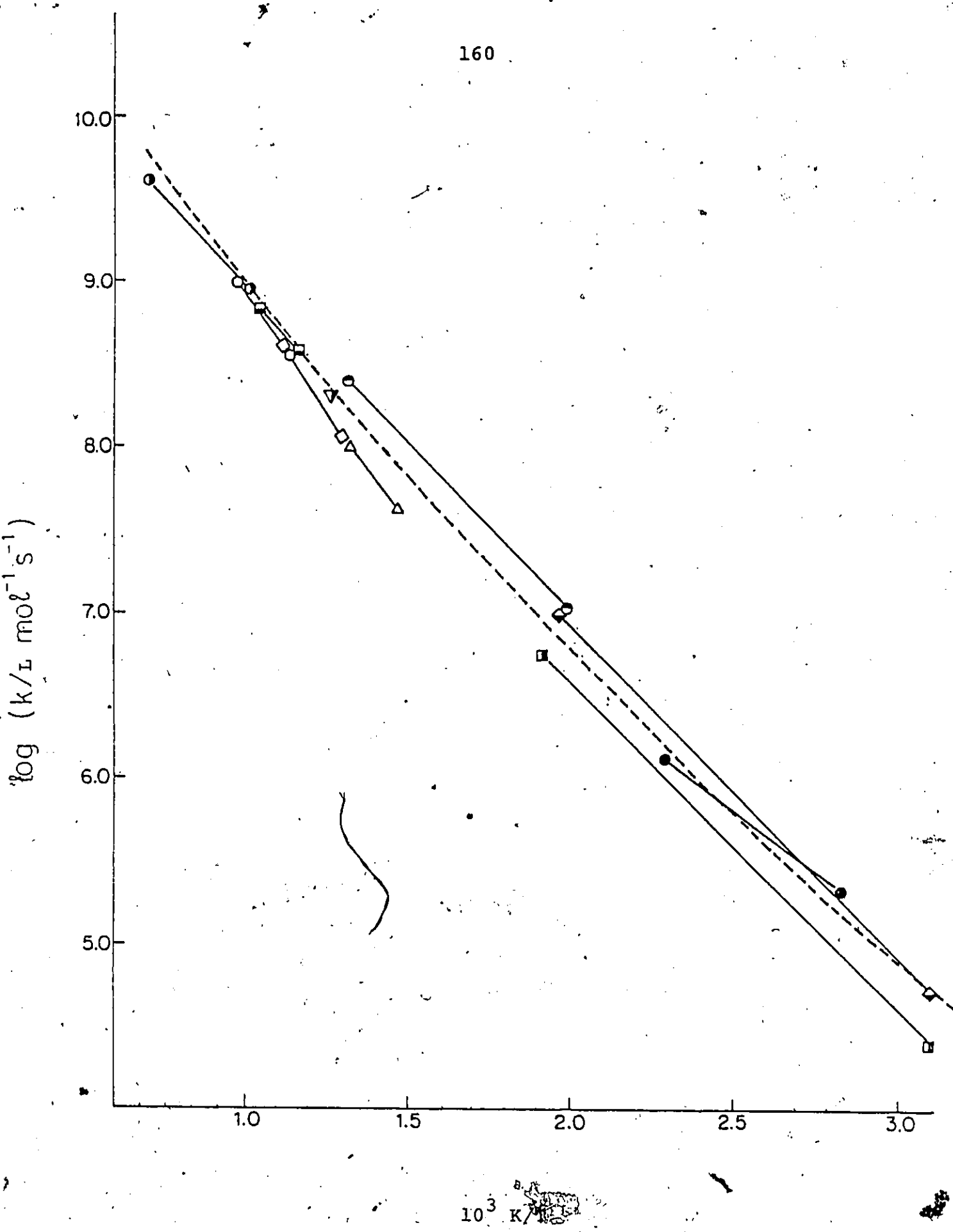
10.0
9.0
8.0
7.0
6.0
5.0
log (k/L mol^{-1} s^{-1})
1.0
1.5
2.0
2.5
3.0
10^3 K/T

$$H + O_2 \rightarrow OH + O \qquad (11)$$

Although there is essential agreement on the rate parameters for this reaction[64] the actual values used by different laboratories may lead to a difference in the rate constant by as much as a factor of three. The results of Tikhomirova and Voevodsky[89], Parsamyan, et al.[90] and Gorban and Nalbandyan[92] have therefore been normalized to the value of k_{11} used by Baldwin and Melvin.[91]

$$\log k_{11}(\text{L mol}^{-1}\text{s}^{-1}) = 11.33 - 16500/2.3\ RT \qquad (7\text{-}7)$$

This procedure gives better consistency among the values reported by this method.

The agreement between the results obtained in the present study and those obtained from the H_2/O_2 hydrocarbon system is very good. It should be noted that all measurements reported above 750 K were obtained by the latter technique. The one exception was the unpublished data of Dove and Wagner, quoted in Reference [59], which were not included in Figure 38. Agreement with results obtained by a completely different approach is useful confirmation. Below 770 K corrections based on a stoichiometric ratio have been made by Camilleri, et al.,[71] which bring the data of Berlie and LeRoy[74] and Azatyan, et al.[68] close to an average value. It also appears that the value reported by Yang[72]

measured relative to the addition of hydrogen atoms to propylene will be increased by using a more recent value for the reference reaction.[64].

The data shown in Figure 38 may be examined in order to address the question of whether the Arrhenius relation for reaction (-3) shows curvature over the temperature range 300-1400 K. This question of non-linearity in the Arrhenius relation has been much discussed for abstraction reactions of small radicals[59][58] and has undoubtedly been observed in some cases. The problem was discussed by Clark and Dove[59] who calculated values of k_{-3} by considering such non-Arrhenius effects as temperature variation of quantum effects on vibrations and quantum mechanical tunnelling. Their values for k_{-3} are included as a dotted line in Figure 38. This curve is a reasonable fit to most of the measurements and shows the apparent activation energy varies from 8 kcal mol^{-1} at 400 K to 14 kcal mol^{-1} at 1200 K. At about 1000 K, the apparent activation energy is about 12 kcal mol^{-1}, in good agreement with the result of the present study of 12.8 kcal mol^{-1}.

This agreement, however, is probably not a strong argument in favour of curvature for k_{-3} as calculated by Clark and Dove.[59] An activation energy measured over a relatively narrow temperature range is not as significant as the values obtained for the rate constant and their relation to other values measured in different temperature

regions with different techniques. From an examination of the data, Camilleri, et al.[71] suggested that the variation of k_{-3} with temperature can be described by an Arrhenius expression over the temperature range covered by the measurements. On this basis the following Arrhenius expression was derived from all measurements of k_{-3} after normalization and correction, as shown in Figure 38:

$$\log k_{-3}(\text{L mol}^{-1}\text{s}^{-1}) = 11.0 \pm 0.1 - \frac{9600 \pm 200}{2.3\ RT} \quad (7\text{-}8)$$

This is essentially the same as suggested by Camilleri, et al.[71] Again it must be concluded that the question of non-Arrhenius behaviour of k_{-3} over the range of temperature 300-1200 K is not solved by the present measurements. It appears that such curvature is probably less than suggested by Clark and Dove.

(g) Comparison of k_{-3}, k_3 and the Heat of Formation of the Ethyl Radical

It is of interest to compare the direct measurements of k_3 and k_{-3} with a value of the equilibrium constant K_3 obtained from thermodynamic data. The comparison is made of the direct measurements of k_3 and values of k_3 calculated from the measurements of k_{-3} together with the equilibrium constant K_3.

As mentioned earlier, some question exists concerning the value for the heat of formation of the ethyl radical. For the present comparison, two values were used, as indicated in Table 31. In Figure 39A, the equilibrium constant K_3 was calculated using $\Delta H_f(C_2H_5)$ = 28 kcal/mol, while in Figure 39B the value $\Delta H_f(C_2H_5)$ = 26 kcal/mol was used. Figure 39A shows good agreement between the direct measurements of k_3 and those calculated from k_{-3}, but in Figure 39B the direct measurements of k_3 appear higher than those calculated from k_{-3}, particularly in the low temperature region. The value of the heat of formation of the ethyl radical is given in most references [79][80] as 26 kcal mol^{-1}. A recent measurement of the heat of formation of the ethyl radical relative to that of the methyl radical using a radical buffer system in an isooctane solution[94] have given a value of 28 kcal/mol, using $\Delta H_f(CH_3)$ = 34.4 kcal/mol. The fact that the independent measurements of k_3 and k_{-3} are in better agreement using the value of $\Delta H_f(C_2H_5)$ = 28 kcal mol^{-1} rather than 26 kcal mol^{-1} suggests that the higher value may be preferable. A similar comparison between forward and reverse rate constants for the reaction of methyl radicals with hydrogen led to the acceptance of a higher value for the heat of formation of the methyl radical.[76][126][127]

Figure 39A shows good agreement between almost all the data for k_3 and k_{-3}, except the direct measurements of k_3 from the present work. This value is lower by a

Table 31

k_3 CALCULATED FROM k_{-3} THROUGH EQUILIBRIUM CONSTANT K_3

	$\Delta H_f(C_2H_5)$ = 26 kcal mol^{-1}		$\Delta H_f(C_2H_5)$ = 28 kcal mol^{-1}		
T/K	log K_3	log(k_3/L mol^{-1}s^{-1})	log K_3	log(k_3/L mol^{-1}s^{-1})	Reference
993-1433	-2.97 - -2.51	5.995 - 7.111	-2.54 - -2.19	6.43 - 7.43	[69]
853- 953	-3.20 - -3.03	5.39 - 5.82	-2.71 - -2.58	5.89 - 6.27	[90]
773- 898	-3.39 - -3.12	4.66 - 5.50	-2.83 - -2.67	5.22 - 5.95	[87]
793	-3.33	4.97	-2.79	5.51	[93]
503- 753	-4.34 - -3.48	2.70 - 4.96	-3.48 - -2.86	3.56 - 5.53	[71]
673- 753	-3.65 - -3.43	3.92 - 4.56	-3.00 - -2.86	4.57 - 5.13	[92]
323- 523	-5.73 - -4.23	-1.319 - 2.509	-4.39 - -3.41	0.021 - 3.33	[72]
290- 509	-6.14 - -4.30	-2.107 - 2.683	-4.65 - -3.47	-0.617 - 3.51	[68]
353- 436	-5.40 - -4.72	-0.08 - 1.402	-4.17 - -3.74	1.15 - 2.38	[74]
876-1016	-3.12 - -2.94	5.41 - 6.03	-2.63 - -2.51	5.90 - 6.46	This work

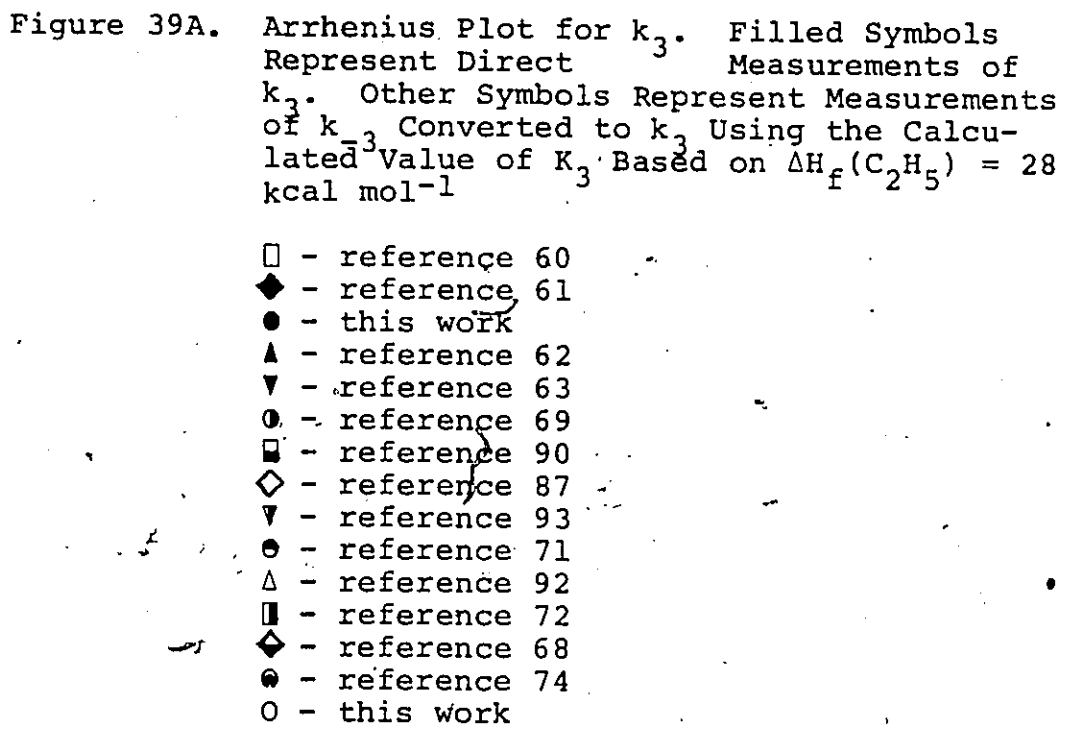

Figure 39A. Arrhenius Plot for k_3. Filled Symbols Represent Direct Measurements of k_3. Other Symbols Represent Measurements of k_{-3} Converted to k_3 Using the Calculated Value of K_3 Based on $\Delta H_f(C_2H_5)$ = 28 kcal mol^{-1}

□ - reference 60
◆ - reference 61
● - this work
▲ - reference 62
▼ - reference 63
◐ - reference 69
◘ - reference 90
◇ - reference 87
▼ - reference 93
◓ - reference 71
△ - reference 92
▮ - reference 72
◈ - reference 68
◍ - reference 74
O - this work

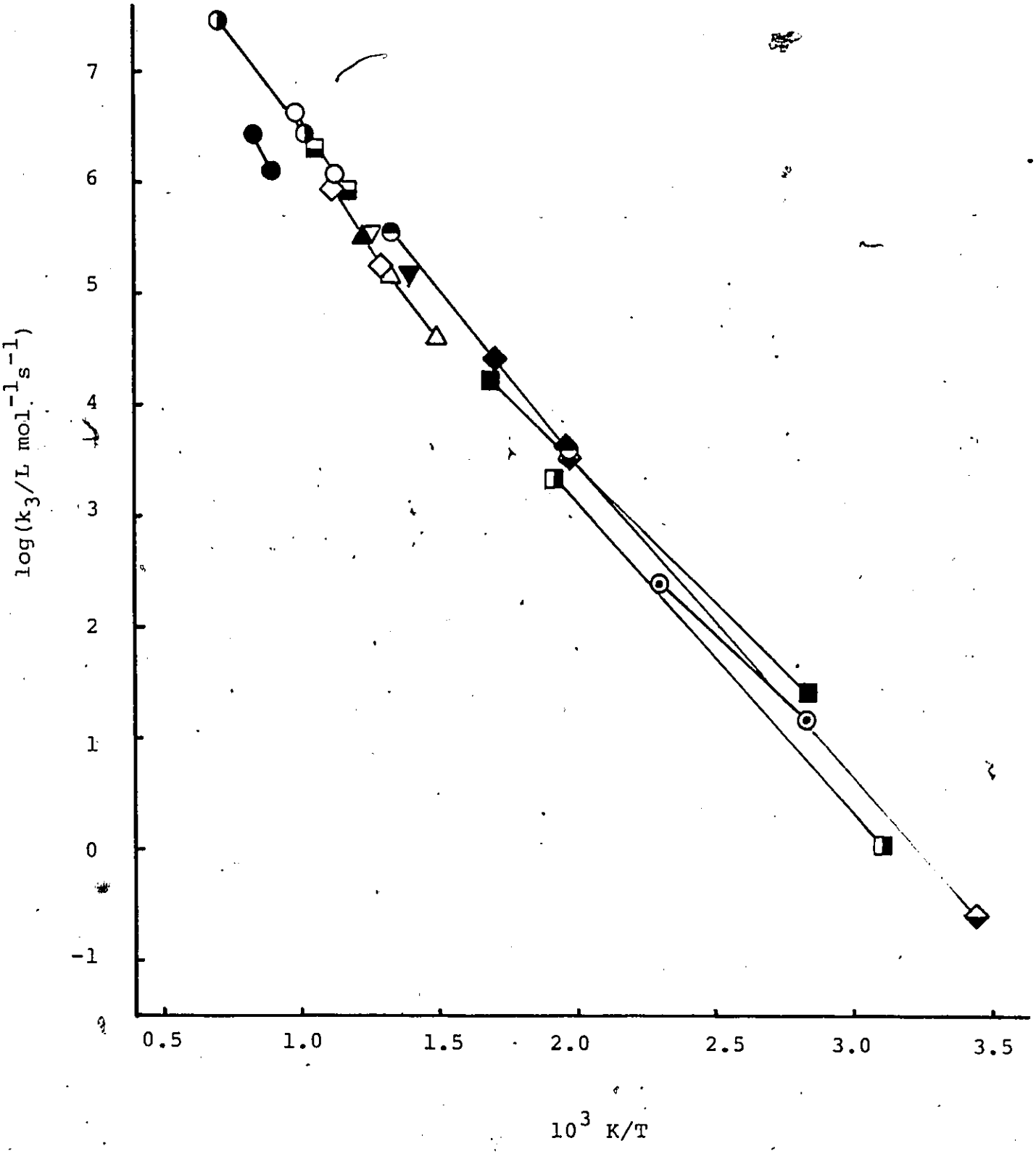
7
6
5
4
3
2
1
0
-1
0.5
1.0
1.5
2.0
2.5
3.0
3.5
log(k_3/L mol^{-1}s^{-1})
10^3 K/T

Figure 39B. Arrhenius Plot for k_3. Filled Symbols Represent Direct Measurements of k_3. Other Symbols Represent Measurements of k_{-3} Converted to k_3 Using the Calculated Values of K_3 Based on $\Delta H_f(C_2H_5)$ = 26 k cal/mol

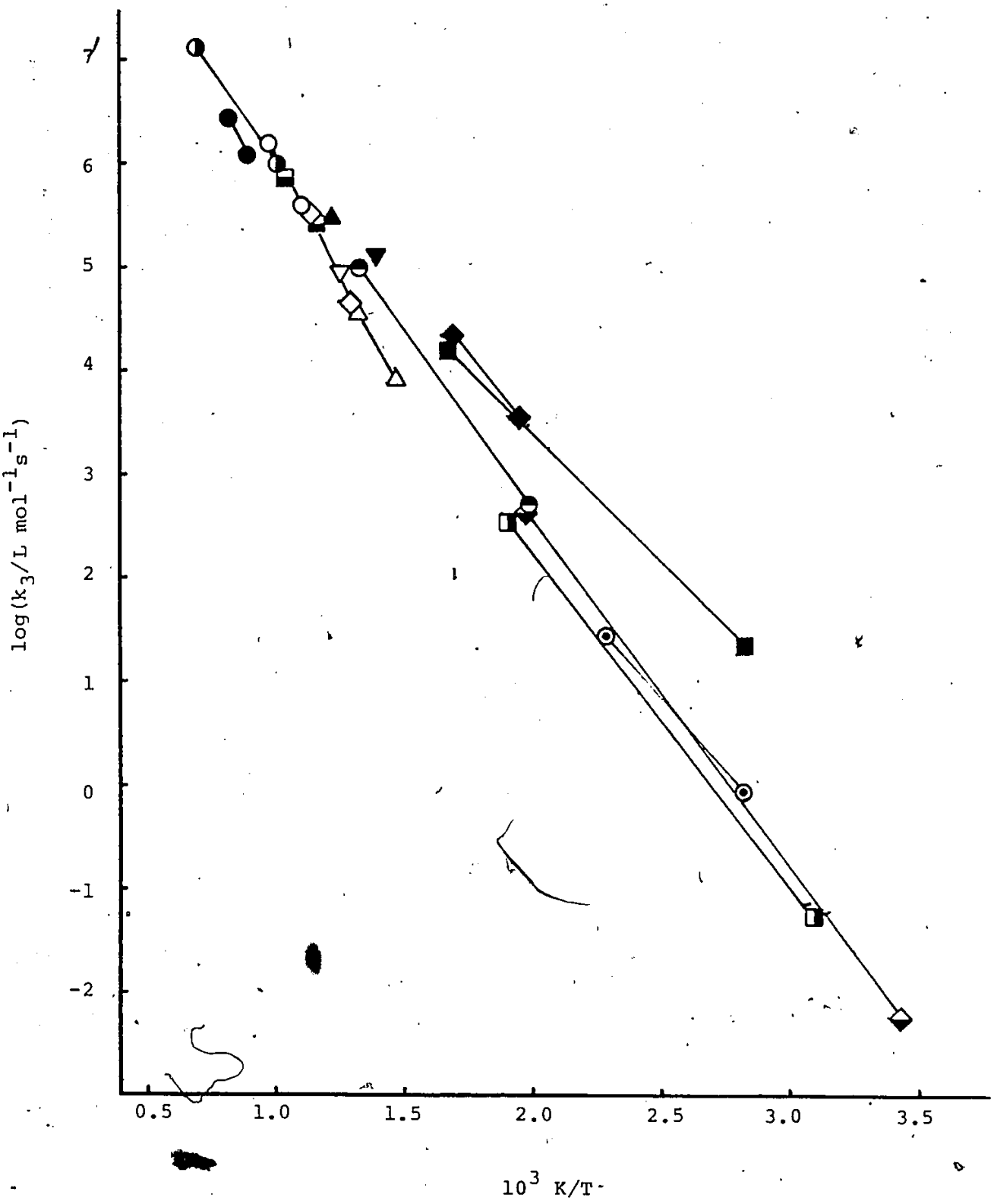
7
6
5
4
3
2
1
0
-1
-2
log(k_3/L mol^{-1}s^{-1})
0.5
1.0
1.5
2.0
2.5
3.0
3.5
10^3 K/T

Table 32A

THERMODYNAMIC DATA*

	ΔH_f(298 K) kcal mol^{-1}	S^0(298 K) cal mol^{-1}deg^{-1}	C_p/cal mol^{-1}deg^{-1} 300	900	1000	1100	1200 K
C_2H_6	-20.2	54.9	12.648	27.69	29.33	30.77	32.02
C_2H_5	28.0	59.0	11.1	24.3	25.7	26.8	27.9
H_2	0	31.2	6.895	7.139	7.217	7.308	7.404
H	52.1	27.4	4.968	4.968	4.968	4.968	4.968

* Standard State 1 atm, 298 K.

Table 32B

CALCULATED ΔH_T AND ΔS_T FOR REACTION

$$C_2H_5 + H_2 \rightarrow C_2H_6 + H$$

T/K	ΔH_T^*/kcal mol^{-1}	ΔS_T^{**}/cal mol^{-1}deg^{-1}
298	3.90	-7.90
900	4.16	-7.42
1000	4.28	-7.24
1100	4.39	-7.10
1200	4.45	-6.98

* $\Delta H_T = \Delta H^0 + \Delta \overline{C}_p (T-298)$

** $\Delta S_T = \Delta S^0 + 2.303\ \Delta \overline{C}_p \log T/298$

Table 32C

T/K	(E_3-E_{-3})/kcal mol^{-1}	ΔH_3^*/kcal mol^{-1}	ΔH_3^{**}/kcal mol^{-1}
298	3.0	3.9	5.9
1200	3.0	4.45	6.45

* Using $\Delta H_f(C_2H_5) = 28$ kcal mol^{-1}

** Using $\Delta H_f(C_2H_5) = 26$ kcal mol^{-1}

factor of 2 than the average value and it seems likely that k_3 has been underestimated, as discussed in Chapter 6.

A more exacting test of these measurements of k_3 and k_{-3} may be made by a comparison of the Arrhenius parameters of the rate constants with the corresponding thermodynamic quantities of the equilibrium constant

$$\Delta G^0 = - RT \ln K_3 = - RT \ln k_3/k_{-3}$$

Since $\ln k_3 = \ln A_3 - E_3/RT$ and $\ln k_{-3} = \ln A_{-3} - E_{-3}/RT$

$$\Delta G^0 = (E_3 - E_{-3}) - RT \ln (A_3/A_{-3})$$

and $E_3 - E_{-3} = \Delta H_3^0$ and $\Delta S^0 = R \ln A_3/A_{-3}$.

This treatment is also valid if k takes the more complex form $k = AT^n e^{-E/RT}$, provided that n is the same for both forward and backward reactions. Thermodynamic values are given in Table 32A and B. Standard entropies at 298 K for H, C_2H_6 and H_2 are accurately known,[80] but the value of S for C_2H_5 is less certain and probably accurate to ± 1.0 e.u. At 300 K, $\Delta S_3^0 = - 7.9$ e.u. decreasing to - 6.9 e.u. at 1200 K. From the Arrhenius expressions (7-8) and (6-19) for the k_3 and k_{-3}, ΔS^0 is estimated as

$$\Delta S^0 = 2.3 \ R \log (A_3/A_{-3}) = - 9.1 \text{ e.u.}$$

This is in reasonable agreement with the calculated entropy considering the errors involved in measurements of frequency factors.

Table 32C compares the values of ΔH^0 obtained from the Arrhenius expressions (6-19) and (7-8) with those calculated by using $\Delta H_f(C_2H_5)$ = 28 and 26 kcal mol^{-1} respectively. It should be noted that ΔH increases by only 0.7 kcal mol^{-1} from 300 K to 1400 K. The variation of both ΔS and ΔH with temperature indicates the possibility of a small curvature in the Arrhenius relation for the rate constants k_3 and k_{-3}. Nevertheless, the value of 28 kcal mol^{-1} for $\Delta H_f(C_2H_5)$ is preferable even with a small increase in activation energy with increasing temperature.

In summary, the results presented here and in Chapter 6 demonstrate the validity of the technique for the utilization of the equilibrium concentration of hydrogen atoms obtained through the thermal dissociation of hydrogen molecules for the measurement of rate constants for reactions of hydrogen atoms and other small radicals. It should be emphasized that the principal assumption in the measurements is maintenance of an equilibrium concentration of hydrogen atoms and that under these circumstances absolute rather than relative values of the rate constants are obtained.

A critical review of all measurements of k_3 and k_{-3} shows that these rate constants may be represented by the

following Arrhenius expressions

$$\log k_3(\text{L mol}^{-1}\text{s}^{-1}) = 9.0 - 12600/2.3\ RT$$

$$\log k_{-3}(\text{L mol}^{-1}\text{s}^{-1}) = 11.0 - 9600/2.3\ RT$$

The comparison between the two sets of independent measurements of k_3 and k_{-3} and the comparison of the measured values of ΔS, ΔH with those calculated from thermodynamic data suggest that the value of 28 kcal mol $^{-1}$ for the heat of formation of the ethyl radical is preferable to that of 26 kcal mol $^{-1}$.

CHAPTER 8

BASIC THEORY OF COLLISIONAL ENERGY TRANSFER IN UNIMOLECULAR REACTION SYSTEMS

The basic unimolecular reaction theory, including the earlier HRRK and Slater theories and the more recent RRKM theory, treats the collisional energization and de-energization as essentially single-step processes. This is called the strong-collision assumption. In thermal systems the average energy of the reacting molecules is usually not more than 10 kcal mol^{-1} above the critical energy. In most cases this is easily removed in a single collision and the strong-collision assumption is justified. In chemically activated systems, energized molecules may be formed with much higher excess energies, in the range of 40-50 kcal/mol, and one collision may not be sufficient to reduce the energy below the critical energy. This situation, where several collisions are needed to energize or de-energize a molecule, is called the weak collision case. Treatment of this case is complex and involves a detailed consideration of the unimolecular reaction from each energy level, together with all the collisional processes which transfer molecules from one energy level to another. Present theories will not be discussed in detail in this introduction but rather a qualitative consideration of the measurements of weak collisional efficiencies and their interpretation will be briefly discussed.

Theoretical treatments of energy transfer in thermal unimolecular systems have been developed and recently reviewed by Tardy and Rabinovitch.[95] Other discussions have been given by Troe, et al.[108]

8.1 The Strong Collision Assumption

The simplest formulation of unimolecular reactions, called the Lindemann-Hinshelwood mechanism, is the following set of equations:

$$A + M \overset{k_1}{\rightarrow} A^* + M \qquad (8\text{-}1)$$

$$A^* + M \overset{k_2}{\rightarrow} A + M \qquad (8\text{-}2)$$

$$A^* \overset{k_3}{\rightarrow} \text{Product} \qquad (8\text{-}3)$$

Step (8-1) is an activating collision which raises the energy of A above a critical value. The collision partner M, is called the bath molecule, which may be A itself. Step (8-2) is the collisional deactivation of A^* after collision with a bath molecule. Step (8-3) represents the dissociation of the energized molecule.

A more precise description of reaction (8-1), considering the eigenstates of A, M and A^* is

$$A_j + M_k \xrightarrow{k_1^{\ell m}{}_{jk}} A_\ell^* + M_m$$

where j, k etc. are quantum numbers that describe the internal states of A and M as well as their relative motion. Similarly, the deactivation step (8-2) may be represented by $k_{2\ell m}^{jk}$. These general reactions may be simplified by considering only the formation and loss of the various energy levels of A^*. The Lindemann scheme becomes

$$A + M \xrightarrow{k_{1.\ell}} A_\ell^* + M \qquad (8\text{-}1')$$

$$A_\ell^* + M \xrightarrow{k_{2.\ell}} A + M \qquad (8\text{-}2')$$

$$A_\ell^* \xrightarrow{k_{3.\ell}} \text{Product} \qquad (8\text{-}3')$$

where the states of M are omitted and $k_{3.\ell}$ is averaged over the allowed states of the products that arise from A_ℓ^*. The general expression for the specific reaction rate constant can then be written as follows:

$$k_{uni} = \sum_\ell k_{1.\ell} k_{3.\ell} C_m / (k_{2.\ell} C_m + k_{3.\ell}) \qquad (8\text{-}4)$$

where C_m is the concentration of bath gas. For $C_m \to 0$, the limiting expression is

$$k_0 = \sum_{\ell} k_{1.\ell} C_m \qquad (8\text{-}5)$$

while for sufficiently high pressures of bath gas,

$$k_\infty = \sum_{\ell} k_{1.\ell} k_{3.\ell} / k_{2.\ell} \qquad (8\text{-}6)$$

In the application of unimolecular theory to experimental studies, it was soon recognized that the Lindemann mechanism fails at low values of the threshold E_0, where E_ℓ approaches the level of the average energy of the relevant degrees of freedom. This failure lies in the assumption of strong collision, or the simple sequence of reactions (1) and (2). The conditions under which strong collisions give way to weak collisions are determined by the whole nature of the system and experimental measurements are an important part of defining these conditions.

8.2 The Definitions of Collisional Efficiency

In thermal systems, it is convenient to define relative collision efficiencies, which of necessity are average quantities. Collisional efficiencies define the transition probabilities per collision for a particular set of collision partners. In any system, the collision frequency (ω) is calculated from the pressure using the appropriate collision cross-section (S^2) and the reduced mass μ of the

colliding pair.

Collisional efficiencies are obtained by comparison of fall-off curves for various bath molecules. The comparison may be made from the change in collision frequency for a particular value of k or from the change in k for a value of the collision frequency. In addition, both a differential and an integral quantity may be obtained.

(a) Differential Quantity

This is useful in the second-order region or with small additions of M.

$$\beta_{\omega}(D) = \Delta\omega(SC)/\Delta\omega(WC), \text{ for } \Delta k_{(SC)} = \Delta k_{(WC)} \qquad (8\text{-}7)$$

and

$$\beta'_{\omega}(D) = \Delta k_{(WC)}/\Delta k_{(SC)}, \text{ for } \Delta\omega(WC) = \Delta\omega(SC) \qquad (8\text{-}8)$$

(b) Integral Quantity

This is appropriate at higher dilutions, especially in the fall-off region.

$$\overline{\beta}_{\omega}(D) = \omega_{(SC)}/\omega_{(WC)}, \text{ for } k_{(SC)} = k_{(WC)} \qquad (8\text{-}9)$$

and

$$\overline{\beta}'(D) = k_{(WC)}/k_{(SC)}, \text{ for } \omega(WC) = \omega(SC) \qquad (8\text{-}10)$$

where WC represents weak collision

SC represents strong collision

D represents dilution with bath molecules (weak collider)

In the second-order region β_ω becomes β_0 and since in this region the rate constant is a linear function of pressure, $\beta_0(D) = \beta_0'(D)$.

8.3 Calculation of Collisional Efficiencies

The process of collisional energy transfer can be completely understood only by considering the general equation referred to earlier which describes the changes from each energy state of the reactants to each energy state of the energized molecules. From this, a master equation is developed which describes the time evolution of each microscopic internal energy state. Solution requires a knowledge of transition probabilities, which are not usually available in such detail. Various approaches have been used to obtain solutions, and the relevant rate constants, for a variety of systems. Two parameters are used to define the transition probabilities, namely, average energy removed on collision, $\langle \Delta E \rangle$, and the form of the distribution of energy in the system. The models for energy transfer were chosen to represent limiting cases.

The stepladder (SL) model involves the transfer of a single unique amount of energy from the energized substrate to the bath molecule. In the exponential model (EXP), the probability for transfer decreases exponentially as the energy removed increases (i.e., a high probability for zero energy transfer). Other models using Gaussian and Poisson statistical distribution functions have been suggested.

Tardy and Rabinovitch have calculated weak collision effects for a number of systems.[103][104] As expected, the results showed that for a given collision frequency, ω, the steady-state populations of substrate activated by weak collisions were always less than those for strong collisions. The calculations were made for both the stepladder and the exponential models. Differences between the models although not large were greatest at energies near to the critical value and at low collisional frequencies.

The calculated rate constants, which are determined by the steady-state populations, are also affected by the proportion of bath molecules, the reaction order, ϕ, and the temperature. At low dilution, where most collisions occur between reactant molecules, the populations below the critical level are determined by a Boltzmann distribution. At high dilution, these populations are depleted from Boltzmann distribution, since most collisions are with weak collider bath molecules. As dilution increases, the

average energy transfered per collision decreases with dilution in a linear fashion.

At high dilution, $\overline{\beta}'_{\omega}(\infty)$ increases with pressure while $\overline{\beta}_{\omega}(\infty)$ decreases. The two quantities describe different aspects of the energy transfer process. $\overline{\beta}'_{\omega}$ relates to the efficiency of the reaction process and shows that collisions are less important towards the first-order region. The quantity $\overline{\beta}_{\omega}$ stresses the collision process and shows that the high-energy levels are depleted at high dilution with a weak collider.

The behaviour of $\overline{\beta}_{0}(\infty)$ for the two models, step-ladder and exponential, in the second-order region, was calculated for various reactants by T.R. They defined a dimensionless parameter $E' = \langle\Delta E\rangle/\langle E^{+}\rangle$, where $\langle E^{+}\rangle$ is the Boltzmann average energy of the reacting molecules. Their results showed that for a particular model distribution function[95] a universal curve was obtained for all reactants. A similar universal relation between $\overline{\beta}_{\omega}(\infty)$ or $\overline{\beta}'_{\omega}(\infty)$ and E' was also found for all regions of the fall-off.[95]

The importance of these universal curves is the direct connection between the observed collisional efficiencies β_{c} and the value of E', which lead to the average energy transferred per collision by the weak collider.

The dependence of both β_{ω} and $\langle\Delta E\rangle$ on temperature is important for applications of the theory to a wide range of temperature. In general, the collisional efficiency decreases

with increasing temperature. Since $\langle E^+ \rangle$ increases with temperature, it was suggested that this could account for the decrease in β_ω with increase in temperature.[105] The step size of the energy transfered $\langle \Delta E \rangle$ may also change with temperature and the contribution of $\langle \Delta E \rangle$ to the temperature dependence of β_ω is not clear. It is therefore important to learn how $\langle \Delta E \rangle$ varies with temperature.

Experiments at temperatures below 1200 K have not yet provided clear evidence. Chemical activation studies[106] suggest that as the temperature increases, $\bar{\beta}_\omega$ drops but the change in $\langle \Delta E \rangle$ was not well defined. Thermal isomerization of methyl isocyanide in the presence of He[99] over a temperature range of 115 K showed a small decrease of both β_ω (by 25%) and $\langle \Delta E \rangle$ (by 3%). In the photoisomerization of cycloheptatriene,[108] however, an increase in temperature gave a decrease of β, while the average $\langle \Delta E \rangle$ increased in the case of mono- and diatomic-bath gases and decreased for polyatomics. Thus, even the direction of the variation of $\langle \Delta E \rangle$ was uncertain. Undoubtedly, the experimental difficulties in obtaining this data make the conclusions uncertain.

Recently, Klein and Rabinovitch[102] have approached the problem with a technique called collisional competitive reaction spectroscopy. Their results showed that the variation of $\langle \Delta E \rangle$ with temperature was the leading contribution to the temperature dependence of β_ω.

The present studies describe a system in which the effect of the weak collider, H_2, in the thermal unimolecular dissociation of ethane has been measured at temperatures in the neighbourhood of 1000 K. The results show that both $\overline{\beta}_\omega$ and $\overline{\beta}'_\omega$ declined significantly over the relatively small range of temperature (940-1040 K) and that the decrease in $\langle \Delta E \rangle$ was the most important factor in the decrease in collisional efficiency.

CHAPTER 9

WEAK COLLISIONAL EFFICIENCIES IN THE THERMAL UNIMOLECULAR DISSOCIATION OF ETHANE

Mechanism of the Reaction

The unimolecular dissociation of ethane has been studied many times over a wide range of pressures. The rate constant for the dissociation under conditions of high pressure, k^{∞}, is well established and the fall-off curve has been measured at several temperatures with ethane itself as the bath gas. This reaction therefore is a useful one to study the effects on the pressure-dependence of a weak collider.

In the present experiments, the dissociation of ethane has been measured under conditions of infinite dilution with hydrogen and with mixtures of hydrogen and xenon. In this system the chain reaction which occurs in the decomposition of ethane itself is suppressed by reaction of the radicals with hydrogen. The following mechanism describes the reaction

$$C_2H_6 \rightarrow 2CH_3 \qquad (4)$$

$$CH_3 + H_2 \rightarrow CH_4 + H \qquad (5)$$

$$H_2 \rightleftharpoons 2H \qquad (1)$$

$$H + C_2H_6 \rightarrow H_2 + C_2H_5 \qquad (-3)$$

$$CH_3 + C_2H_6 \rightarrow C_2H_5 + CH_4 \qquad (13)$$

$$C_2H_5 \rightarrow C_2H_4 + H \qquad (-2)$$

$$2CH_3 \rightarrow C_2H_6 \qquad (-4)$$

The products of the decomposition of ethane in the presence of hydrogen were methane and ethylene. It can be shown that these two products are formed by independent reactions. In Chapter 7, it was shown that C_2H_4 was formed only through reactions (1), (-3) and (-2) and that reaction (13) was not important. It may be assumed that this conclusion is valid in the slightly higher temperature range of the present experiments with similar concentrations of ethane. It is necessary in this system however to show that reaction (-4) does not remove methyl radicals. The relative rates of reaction (5) and (-4) depend on the concentration of methyl radicals in the system. When the rates of these reactions are equal, then

$$[CH_3] = k_5[H_2]/k_{-4}$$

At 1000 K with 126 Torr of H_2 and 100 ppm C_2H_6, the rates of reactions (5) and (-4) will be equal when

$$[CH_3] = 2.6 \times 10^{-6} \text{ mol L}^{-1}$$

The steady-state concentration of methyl radicals in the system may be calculated for the two cases where disappearance of the radicals is (a) by reaction (5) and (b) by reaction (-4). For the conditions mentioned above case (a) gives $[CH_3] = 3 \times 10^{-15}$ mol L^{-1} and case (b) give $[CH_3] = 1 \times 10^{-10}$ mol L^{-1}. Reaction (-4) therefore is not an important loss process for methyl radicals in the present experiments. This conclusion is further substantiated by the results of experiments with varying initial concentrations of ethane and pressures of hydrogen presented later. The rate of formation of methane, therefore, provides a direct measurement of the rate of reaction (4).

Measurement of k_4

The yield of methane was measured as a function of time for concentrations of ethane ranging from 25-210 ppm at total pressures from 25-400 Torr. Examples are shown in Figure 40. Initial rates were obtained with an estimated accuracy of 10%. The first-order rate constant for reaction (4) was calculated from the following equation:

$$\frac{d[CH_4]}{dt} = 2\, k_4 [C_2H_6]$$

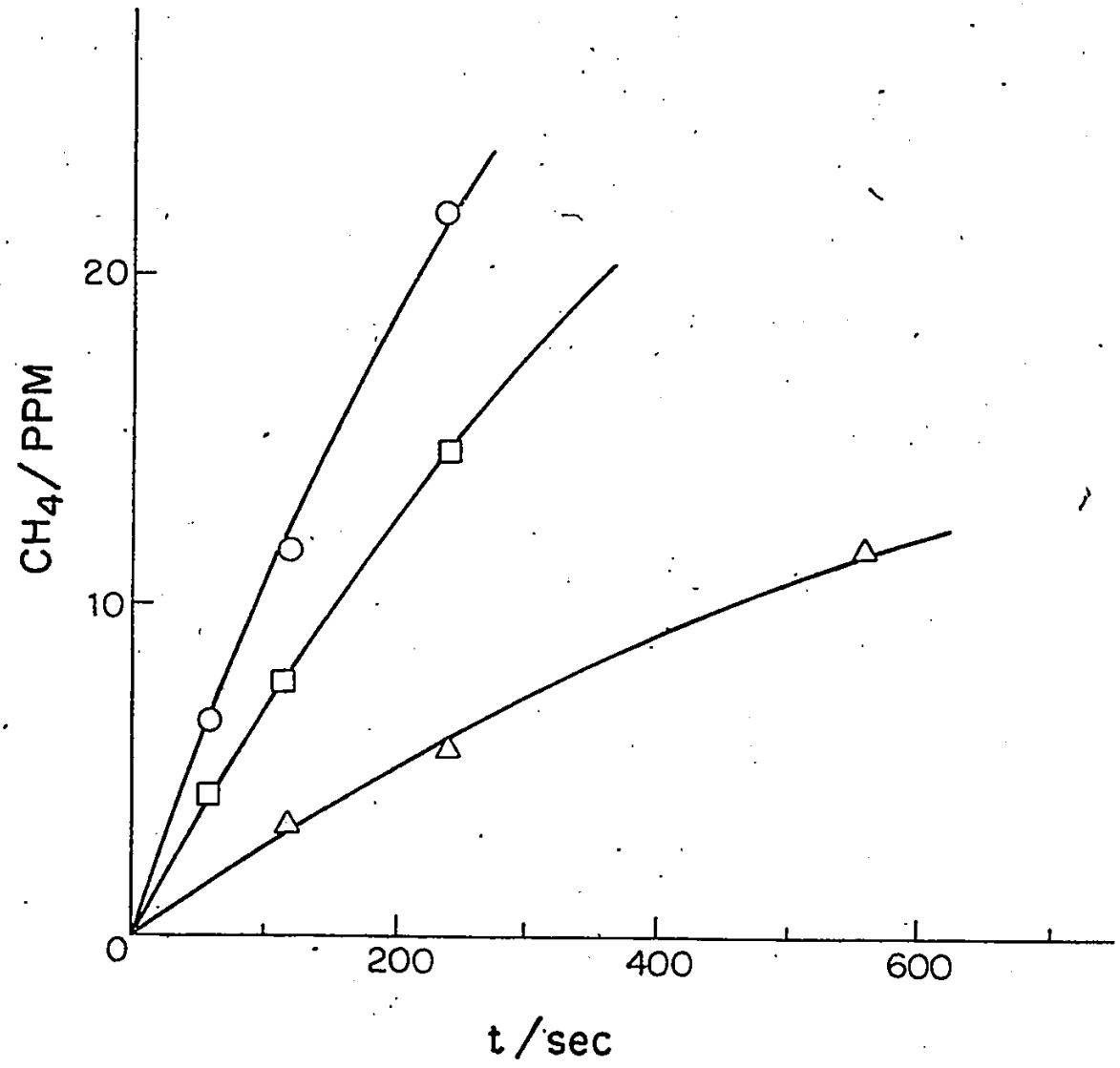

Figure 40. Yield of Methane as a Function of Time. $[C_2H_6]^\circ$ = 102 ppm

O - 998 K, 303 Torr
□ - 998 K, 177 Torr
Δ - 978 K, 83.5 Torr

Table 33

T/K	$X_{C_2H_6}$/ppm	P/Torr	$k_4/10^{-5}$ s^{-1}
938	210	52.0	3.40
	210	113.5	4.17
	210	175.0	4.55
	210	205.0	4.69
	210	329.0	5.21
		∞	8.77
958	210	52.0	7.38
	210	113.5	9.05
	52.9	113.5	9.45
	52.9	176.0	11.0
	210	207.0	10.5
	52.9	238.0	11.0
	52.9	299.0	12.3
	52.9	363.0	13.2
	210	424.0	12.9
		∞	24.4
978	102	52.0	12.6
	102	83.5	13.6
	102	114.0	16.2
	102	207.0	19.1
	102	332.0	25.3
		∞	62.5
997.5	102	53.0	25.6
	102	83.5	30.7
	102	115.0	33.1
	102	177.0	37.3
	102	208.0	42.2
	102	303.0	54.9
	49.8	115.0	37.0
	49.8	209.0	47.5
	49.8	335.0	55.5
		∞	167
1018	209	37.0	45.9
	209	53.5	52.6
	209	84.0	60.3
	209	115.5	67.4
	209	147.0	73.7
	209	178.0	90.9
	209	209.0	103.4
	209	335.0	153
	49.8	335.0	117

T/K	$X_{C_2H_6}$/ppm	P/Torr	$k_4/10^{-5}s^{-1}$
1018	49.8	209.0	81.7
	49.8	178.0	71.6
	49.8	115.5	71.6
	49.8	83.5	62.5
	49.8	52.0	53.9
		∞	298
1038	209	305.0	239
	209	209.0	197
	209	116.0	105
	209	116.0	112
	209	53.5	80.1
	209	179.0	172
	209	84.0	89.7
	209	37.5	69.4
	209	147.5	128
	24.9	336.0	160
	24.9	210.0	126
	24.9	115.0	105
	24.9	84.0	91.7
		∞	909

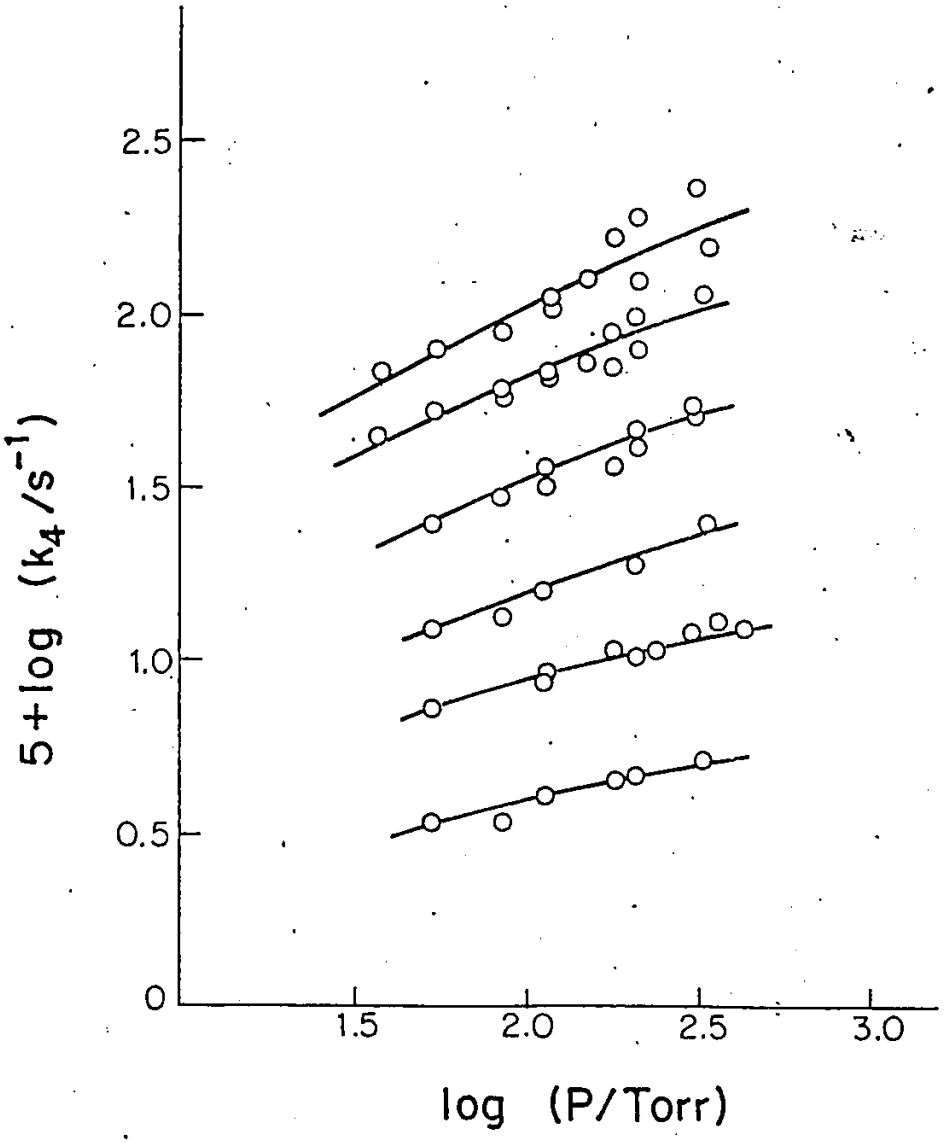

Figure 41. k_4 as a Function of Pressure at Six Temperatures: 938, 958, 972, 998, 1018 and 1038 K. Bath gas hydrogen

Figure 42. k_4^{-1} as a Function of $P^{-1/2}$ for Three Temperatures

O - $X^o_{C_2H_6}$ = 210 ppm

◑ - $X^o_{C_2H_6}$ = 102 ppm

● - $X^o_{C_2H_6}$ = 52 ppm

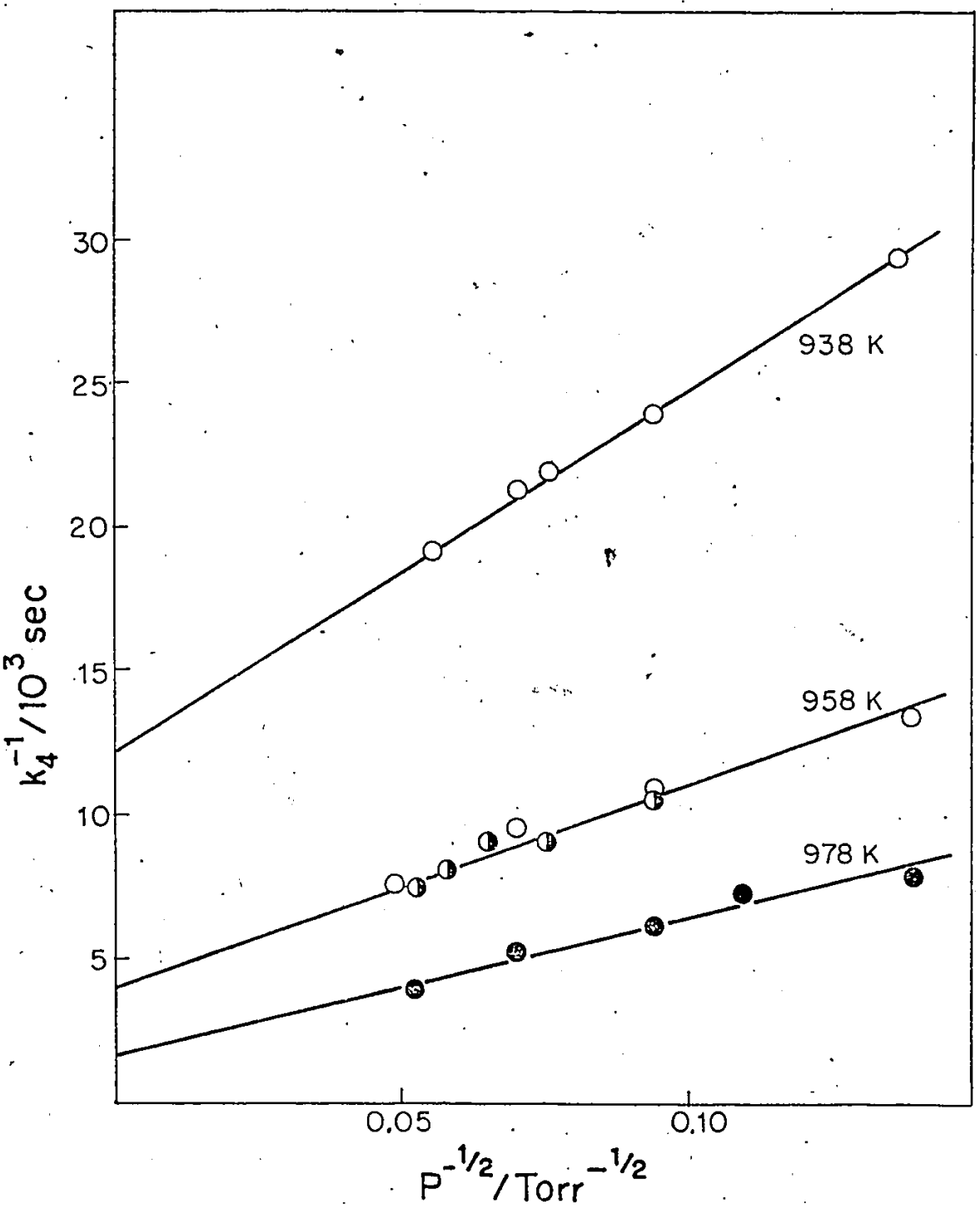
30
25
20
15
10
5
$k_4^{-1}/10^3$ sec
938 K
958 K
978 K
0.05
0.10
$P^{-1/2}/\text{Torr}^{-1/2}$

Values of k_4 were independent of the relative concentration of ethane and hydrogen, since all concentrations were infinitely dilute. The results are summerized in Table 33. The pressure-dependence of k_4 is shown in Figure 41. Values of k_4^∞ were obtained by extrapolation of plots of k^{-1} against $p^{-1/2}$[123] as shown in Figure 42. The values of k_4^∞ are included in Table 33 and were fitted by the following Arrhenius expression:

$$\log k_4^\infty \ (\text{sec}^{-1}) = 16.42 - \frac{87600}{2.3RT}$$

$R = 1.987$ cal deg^{-1} mol^{-1}

These results are in good agreement with a recent evaluation[124] of this rate constant which gave

$$\log k_4^\infty \ (\text{sec}^{-1}) = 16.38 \pm 0.5 - \frac{87400 \pm 700}{2.3RT}$$

The assumptions involved in the mechanism therefore appear reasonable under the conditions of the experiment.

Collisional Efficiency of Ethane and Hydrogen

The present measurements of k_4 in the pressure-dependent region allow an estimate of the relative collisional efficiency of ethane and hydrogen and of ethane and xenon in a

region of temperature not previously covered. The integral collisional efficiency, $\overline{\beta}_\omega$, is the quantity most appropriate for the present results. Both methods of measurement as defined in Chapter 8 have been used for the present results: (a) $\overline{\beta}_\omega$ the ratio of the collision rates in hydrogen and in ethane, $\omega_{C_2H_6}/\omega_{H_2}$ to produce the same rate constant for dissociation $k_4(H_2) = k_4(C_2H_6)$ and (b) $\overline{\beta}_\omega'$ the ratio of the rate constants for dissociation $k_4(H_2)/k_4(C_2H_4)$ for the same collision rate, $\omega_{H_2} = \omega_{C_2H_6}$. Both ratios are related to the dimensionless parameter $E' = \langle\Delta E\rangle/E^+$ and hence to the average energy transfered in a deactivation collision, $\langle\Delta E\rangle$. In the range $k/k^\infty \sim 0.4 \sim 0.8$, where the present measurements were made, the ratio $\overline{\beta}_\omega'$ changes more rapidly with extent of fall-off and provides a more sensitive estimate of E'. From the present results both ratios have been calculated as a function of k_4/k_4^∞ and of temperature.

(a) Estimation of $\overline{\beta}_\omega(\infty)$

At 958 and 998 K the rate constants measured in the present experiments may be compared directly with those measured in pure ethane by Lin and Back[82] over a range of pressures. The measurements are shown in Figure 43a and and Figure 43b. The extrapolation, shown as a solid line, was obtained from the plots of k^{-1} against $p^{-1/2}$. The collision frequency was calculated by the following relations:

$$\omega_A = P_A \frac{S_{AA}^2}{(\mu_{AA})^{1/2}} \quad \text{and} \quad \omega_M = P_M \frac{S_{AM}^2}{(\mu_{AM})^{1/2}}$$

where A refers to ethane and M to hydrogen. μ is the reduced mass and σ is an effective collision diameter,

$$S_{AM} = \sigma_{AM}^2 \, \Omega_{AM}^{(2.2)*}$$

calculated from the methods used by Tardy and Rabinovitch, using the integrals tabulated in Reference [116]. The values used in the calculations are summarized in Table 34.

Mixtures of Xe and hydrogen with mole fraction of hydrogen, $X_{H_2} = 0.55$, gave values of k_4 identical to those with hydrogen alone. The relative collisional efficiency for Xe, $\overline{\beta}_p$, was calculated assuming additivity as follows:

$$\overline{\beta}_p(H_2 + Xe) = \overline{\beta}_p(H_2) X_{H_2} + \overline{\beta}_p(Xe) X_{Xe}$$

$\overline{\beta}_\omega$ for Xe was then obtained as described in the preceeding paragraph

$$\overline{\beta}_\omega = \overline{\beta}_p \left(\frac{\mu_{AM}}{\mu_{AA}}\right)^{1/2} \left(\frac{S_{AA}}{S_{AM}}\right)^2.$$

Values of $\overline{\beta}_\omega(\infty)$ as a function of k_4/k_4^∞ are summarized in Table 35 and are shown as smoothed curves in Figure 44. In the present system it appears that $\overline{\beta}_\omega(\infty)$ declines as k_4/k_4^∞ approaches one and decreases as the temperature

Table 34

T = 1000 K

Pair	$\sigma/\mathring{A}$	$\Omega^{(2,2)*}$	$s^2/\mathring{A}^2$	μ/amu
C_2H_6 - C_2H_6	8.84	0.95	74.24	15.00
C_2H_6 - H_2	7.34	0.82	44.18	1.875
C_2H_6 - Xe	8.48	0.96	71.91	24.4

Figure 43. k_4 as a Function of ω.

(a) 958 K
(b) 998 K

O - pure ethane

■ - $C_2H_6 + H_2$ (infinite dilution)

--- - extrapolation from plots as in Figure 3

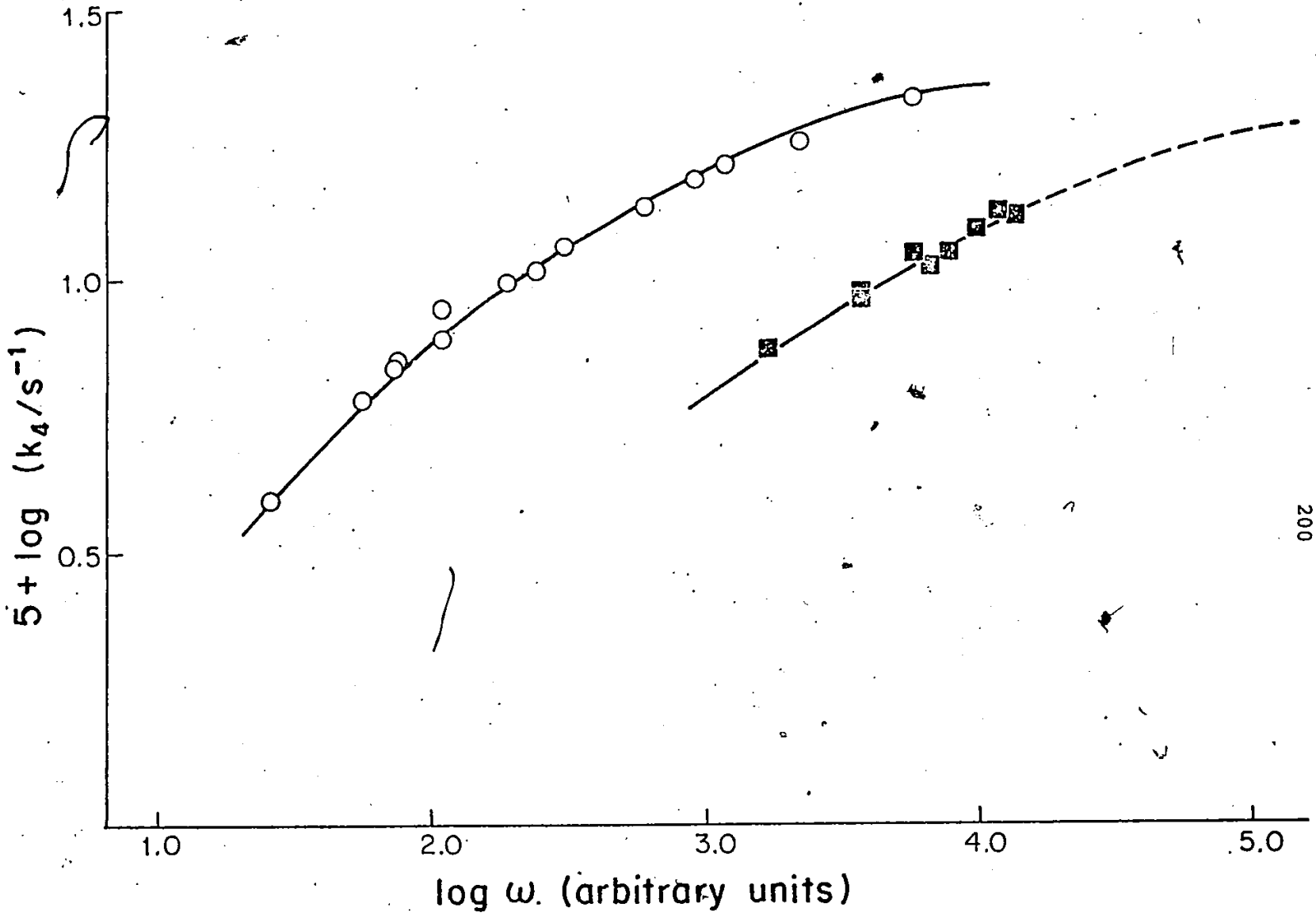

200

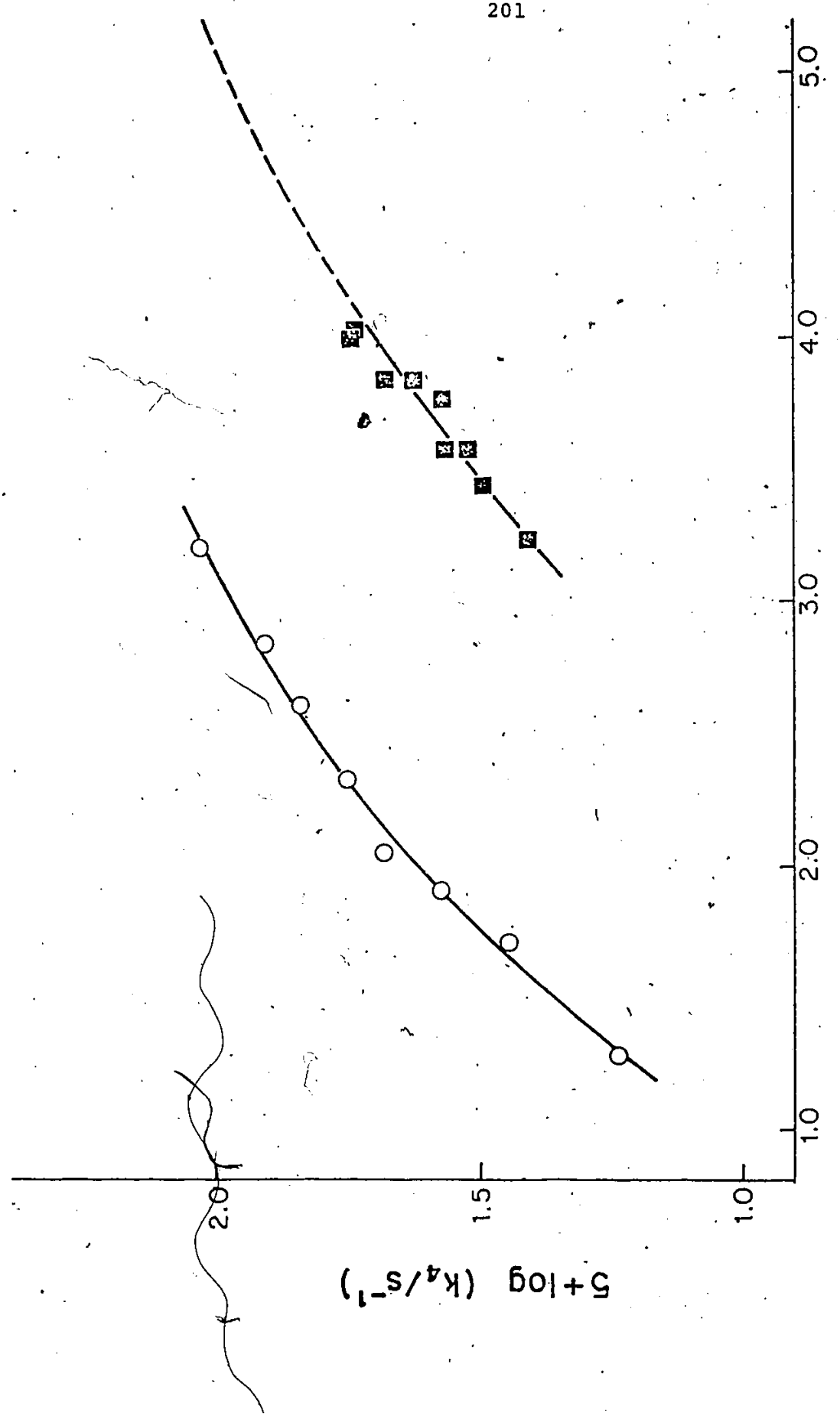
5+log (k4/s-1)
2.0
1.5
1.0
1.0
2.0
3.0
4.0
5.0
log ω. (arbitrary units)

Table 35

T/K	$1 + \log k/k^{\infty}$	$\bar{\beta}_{\omega}(Xe)$	$\bar{\beta}_{\omega}(H_2)$
998	0.2	-	0.0211
	0.3	-	0.0193
	0.4	0.0337	0.0174
	0.5	0.0309	0.0155
	0.6	0.0269	0.0135
	0.7	0.0245	0.0116
	0.8	0.0162	0.0099
958	0.4	0.123	0.0589
	0.5	0.110	0.0525
	0.6	0.098	0.0468
	0.7	0.089	0.0398
	0.8	0.071	0.0324
	0.9	0.055	0.0257

Figure 44. Log $\overline{\beta}_{\omega}(\infty)$ as a Function of log k_4/k_4^{∞}

solid lines - $\overline{\beta}_{\omega}(H_2)$

broken lines - $\overline{\beta}_{\omega}(Xe)$

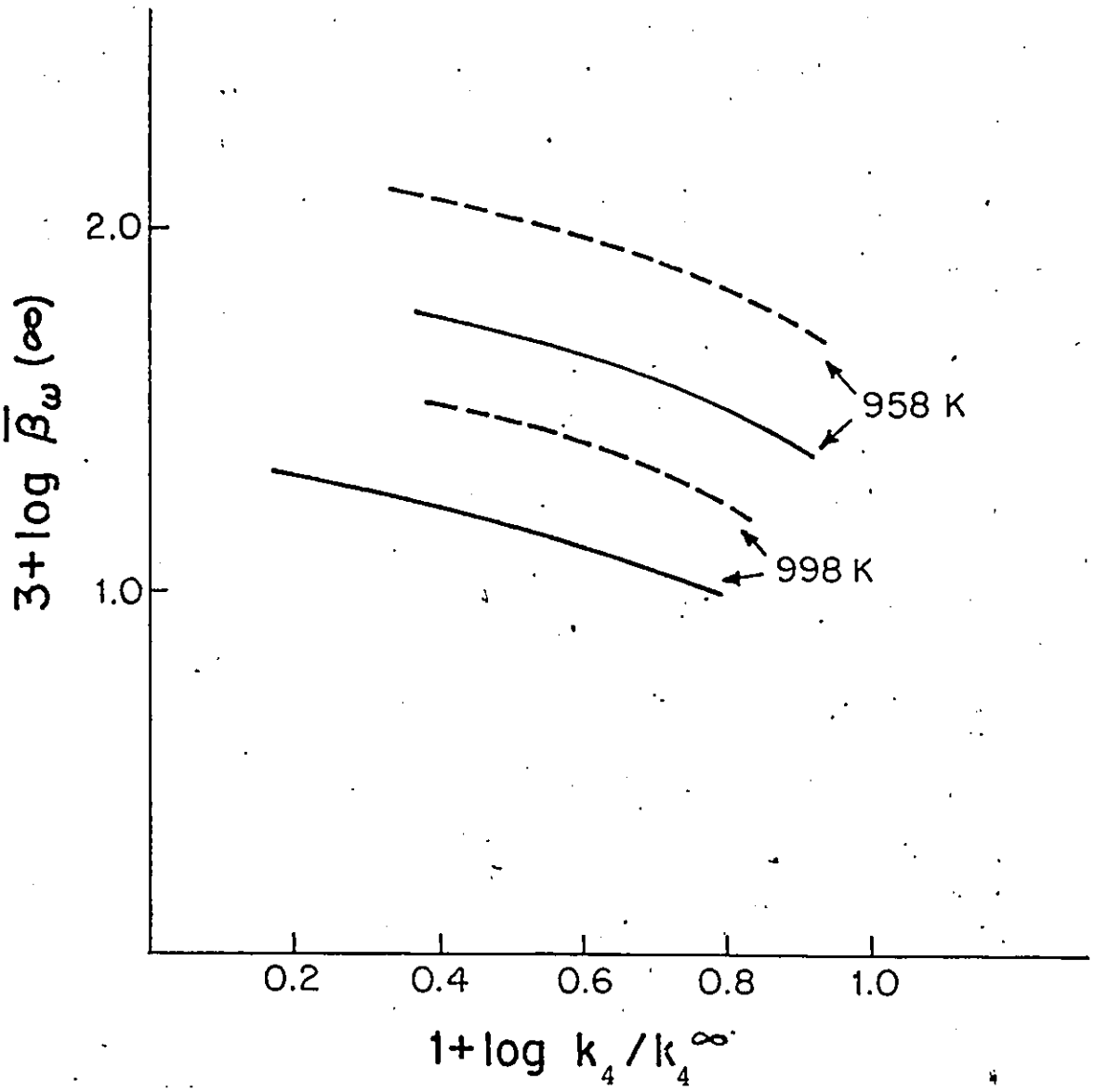
2.0
1.0
3+log $\bar{\beta}_\omega$ (∞)
958 K
998 K
0.2
0.4
0.6
0.8
1.0
1+log k_4/k_4^∞

increases. Extrapolation of the curves for hydrogen and xenon to $k_4/k_4^\infty = 0$ gives values for $\overline{\beta}_\omega$ in the second-order region, β_0. At 998 K $\beta_0(H_2) = 0.025$ and $\beta_0(Xe) = 0.046$. The values may be compared with collisional efficiencies for H_2 and Xe obtained from other systems. Values have been obtained for unimolecular dissociations, usually below about 600 K, and relative collisional efficiencies for H_2 of about 0.2 have been reported. A decline in β_0 with temperature is expected but the magnitude is uncertain. Kline and Rabinovitch[102] measured a decline in β_0 for helium in the unimolecular isomerization of 1,1-cyclopropane-d_2 from 0.078 at 773 K to 0.010 at 973 K. The present results suggest a similar decline for H_2.

Values of $\overline{\beta}_\omega$ have also been estimated from measurements of combination reactions in the third-order region combined with studies of the corresponding dissociation reaction in a shock tube.[101] For example, a value for β_0 for Ar at 1000 K was estimated as 0.12. If the collision efficiencies of Xe and Ar are similar the present results suggest a value for β_0 for Ar of about 0.05. In the methyl isocyanide isomerization[99] Xe was found to have about the same efficiency as hydrogen. This value placed Xe with the other rare gases, which showed no essential change in $\overline{\beta}_\omega$ with increasing boiling point. In the present system, β_ω for Xe was about twice the value of H_2. The larger relative

Figure 45. Log $P_{1/2}$ as a Function of 1/T

Present work - O - M = H_2

● - M = 0.55 H_2 + 0.45 Xe

Other data - M = C_2H_6

□ - reference 83

◨ - reference 120

■ - reference 118

Δ - reference 119

\+ - reference 121, 122

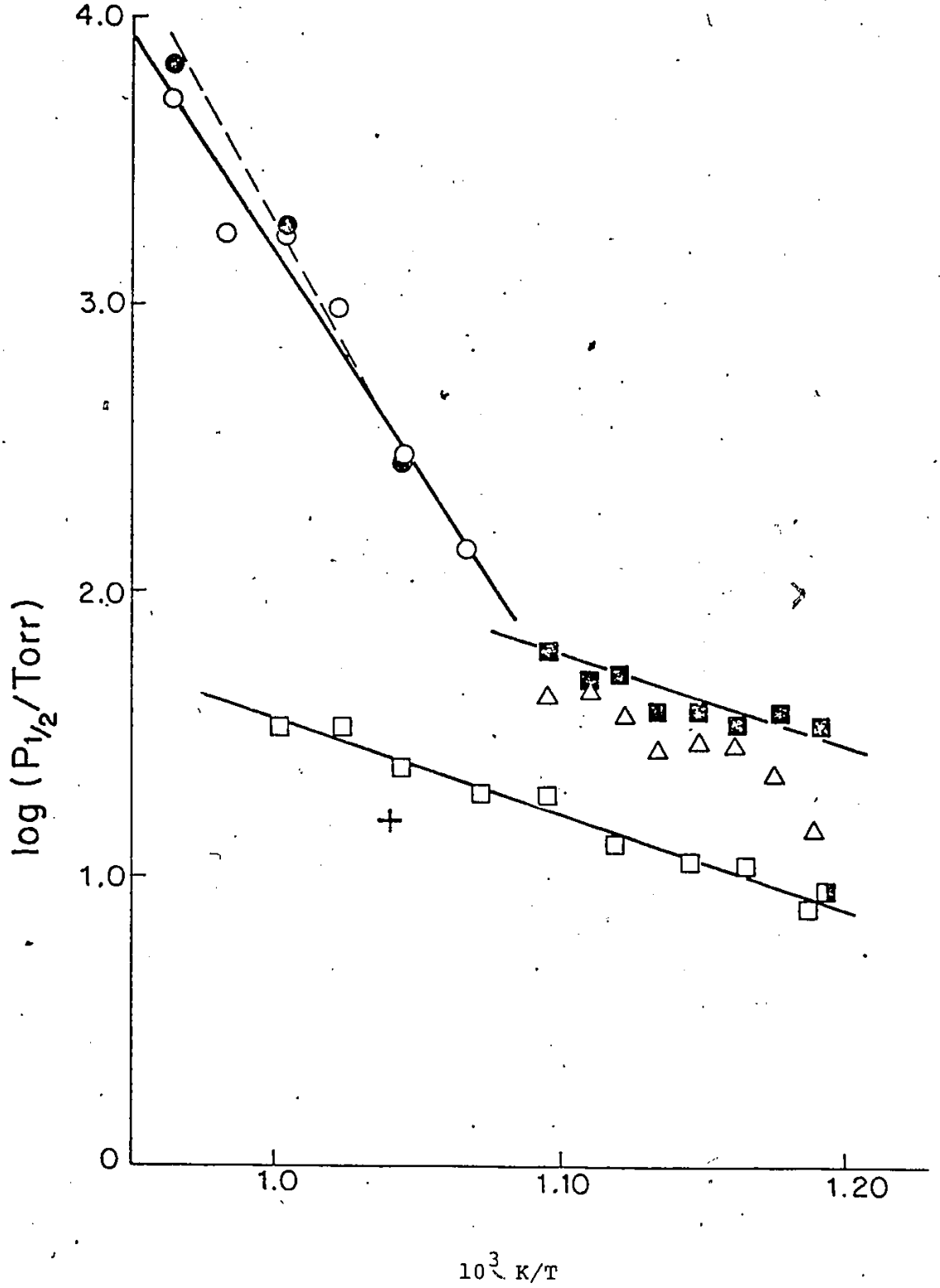
4.0
3.0
2.0
1.0
0
log ($P_{1/2}$/Torr)
1.0
1.10
1.20
10^3 K/T

efficiency found here would place Xe closer to the values found for diatomic and small linear molecules, where a small increase in $\overline{\beta}_\omega$ occurred with increase in boiling point.[99]

(a) Comparison of Values for $P_{1/2}$

Values of the pressure at which $k_4/k_4^\infty = 0.5$ have been reported in several studies of the dissociation of ethane. A great deal of variation in these values is observed, partly because $P_{1/2}$ is sensitive to the value of k_4^∞ obtained in the particular study. Figure 45 shows values of $P_{1/2}$ as an Arrhenius plot for dissociation in pure ethane and at infinite dilution in hydrogen and in mixtures of hydrogen and xenon. Since $\log \overline{\beta}_p$ equals $\log P_{1/2}(C_2H_6) - \log P_{1/2}(H_2)$, it is evident that, qualitatively, $\overline{\beta}_p$ for $k_4/k_4^\infty = 0.5$ decreases as the temperature increases. Estimates of $\langle\Delta E\rangle$ were not, however, made from this comparison but from the quantity $\overline{\beta}_\omega'$ which provides a more sensitive test of E' and hence of $\langle\Delta E\rangle$ and is described in the next section.

(b) Estimation of $\overline{\beta}_\omega'(\infty)$

A direct measurement of $\overline{\beta}_\omega'(\infty)$ was obtained by comparison of the rate constants at the two temperatures where

Table 36

T/K	log ω	$5+\log k^{wc}$	$5+\log k^{sc}$	$\bar{\beta}'_\omega$	ϕ
958	3.03	0.800	1.20	0.398	1.24
	3.25	0.875	1.25	0.422	1.21
	3.54	0.970	1.30	0.468	1.17
	3.94	1.077	1.35	0.533	1.09
998	3.20	1.495	2.060	0.272	1.26

measurements of k_4 in both pure ethane and mixtures of ethane and hydrogen were made (Figure 43a and Figure 43b). At 950 K measurements at four values of ω were made, while at 998 K, because of smaller overlap of the curves, only one value of ω could be used. The results are summarized in Table 36. $\overline{\beta}'_\omega(\infty)$ was estimated over a range of temperature by interpolation of the present and previous data.[87] An Arrhenius plot of k_4 was made for the measurements in pure ethane and at infinite dilution of ethane in hydrogen for three values of ω, as well as the value of k_4^∞. These data are plotted in Figure 46 showing the region of temperature where the two sets of measurements overlap. From the smoothed curves, $\overline{\beta}'_\omega(\infty)$ was obtained from the following equation

$$\log \overline{\beta}'_\omega(\infty) = \log k_4(H_2) - \log k_4(C_2H_6)$$

for seven temperatures, at each of the values of ω. The results are given in Table 37, which also include the order, ϕ, of the rate in pure ethane for each value of ω. A slight increase in $\overline{\beta}'_\omega$ is observed as the order decreases.

These measurements of $\overline{\beta}'_\omega$ may be related to the dimensionless quantity E' from the "universal" curves calculated by Tardy and Rabinovitch. The set of values of $\overline{\beta}'_\omega$ at the maximum value of $\phi(1.25)$, $\log \omega = 3.08$, were chosen for

Table 37

T/K	log ω	$5+\log k^{wc}$	$5+\log k^{sc}$	$\overline{\beta}'_\omega$	ϕ
943	3.083	0.570	0.905	0.462	1.23
	3.383	0.655	0.972	0.482	1.17
	3.683	0.740	1.040	0.501	1.12
952	3.083	0.705	1.085	0.417	1.24
	3.383	0.795	1.155	0.437	1.18
	3.683	0.885	1.225	0.457	1.13
962	3.083	0.840	1.264	0.377	1.25
	3.383	0.940	1.340	0.398	1.19
	3.683	1.030	1.410	0.417	1.14
971	3.083	0.970	1.440	0.339	1.255
	3.383	1.080	1.525	0.359	1.20
	3.683	1.170	1.600	0.372	1.15
980	3.083	1.100	1.620	0.302	1.26
	3.383	1.220	1.710	0.324	1.21
	3.683	1.315	1.790	0.335	1.16
990	3.083	1.235	1.800	0.272	1.27
	3.383	1.360	1.890	0.295	1.23
	3.683	1.460	1.970	0.309	1.18
1000	3.083	1.365	1.980	0.243	1.28
	3.383	1.505	2.070	0.272	1.24
	3.683	1.610	2.155	0.285	1.19

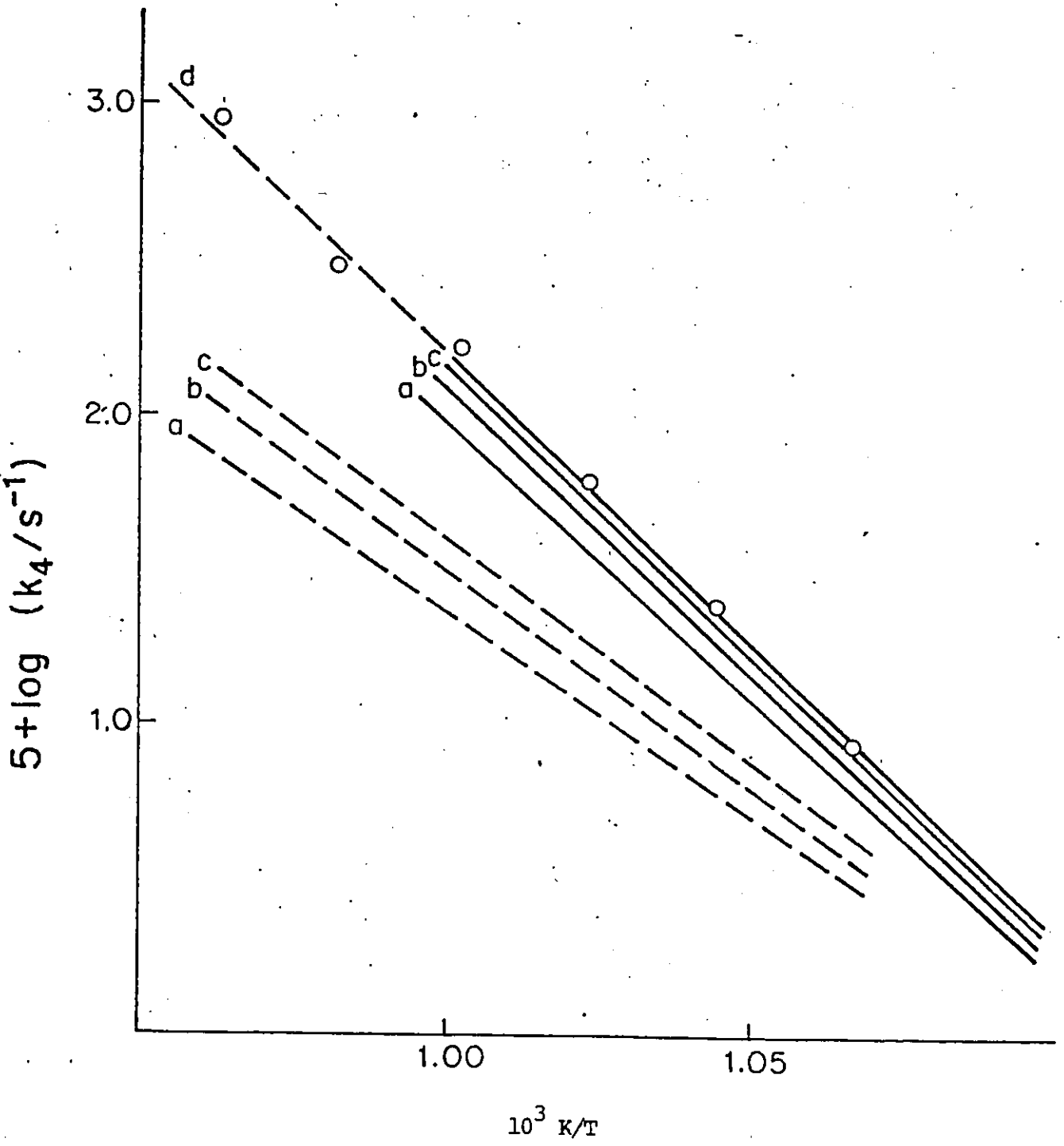

Figure 46. Log k_4 as a Function of 1/T for Various Values of ω

Solid lines - M = C_2H_6

Broken lines - M = H_2

a - log ω = 3.083
b - log ω = 3.383
c - log ω = 3.683
d - log ω = ∞
0 - present measurements of k_4^{∞}

each temperature to provide the most sensitive test of E'. The values obtained are given in Table 38. From these values of E' the energy transfered per collision, $\langle\Delta E\rangle$, is obtained from the relation $E' = \Delta E/E^+$. Values of E^+ were calculated from the approximate relation:

$$E^+ = RT\left[1.1 + \sqrt{\frac{sRT}{E^0}} + \left(\frac{sRT}{E^0}\right)^2\right]$$

taking $E^0 = 88$ kcal mole^{-1} and $s = 12$.[83] The results are included in Table 38. The variation of both functions, ln $\bar{\beta}'_\omega$ and ln $\langle\Delta E\rangle$, with temperature is shown in Figure 47. Over the temperature range of the present experiments these functions are linear, but because the range of temperature available for the present experiments was narrow, this functional dependence is not considered significant. It should be noted that ln $\bar{\beta}'_\omega$ is also a linear function of T^{-1}, as is ln $\bar{\beta}_\omega$ (Figure 45).

The quantity $\langle\Delta E\rangle$ is the energy transfered in a deactivating collision, as formulated by Tardy and Rabinovitch.[104] The quantity $\langle\Delta E_T\rangle$ is defined by Troe as the energy transfered per collision, both activating and deactivating. These quantities are related in the following way:[95]

$$\langle\Delta E_T\rangle = \frac{(\langle\Delta E\rangle)^2}{\langle\Delta E\rangle + RT}$$

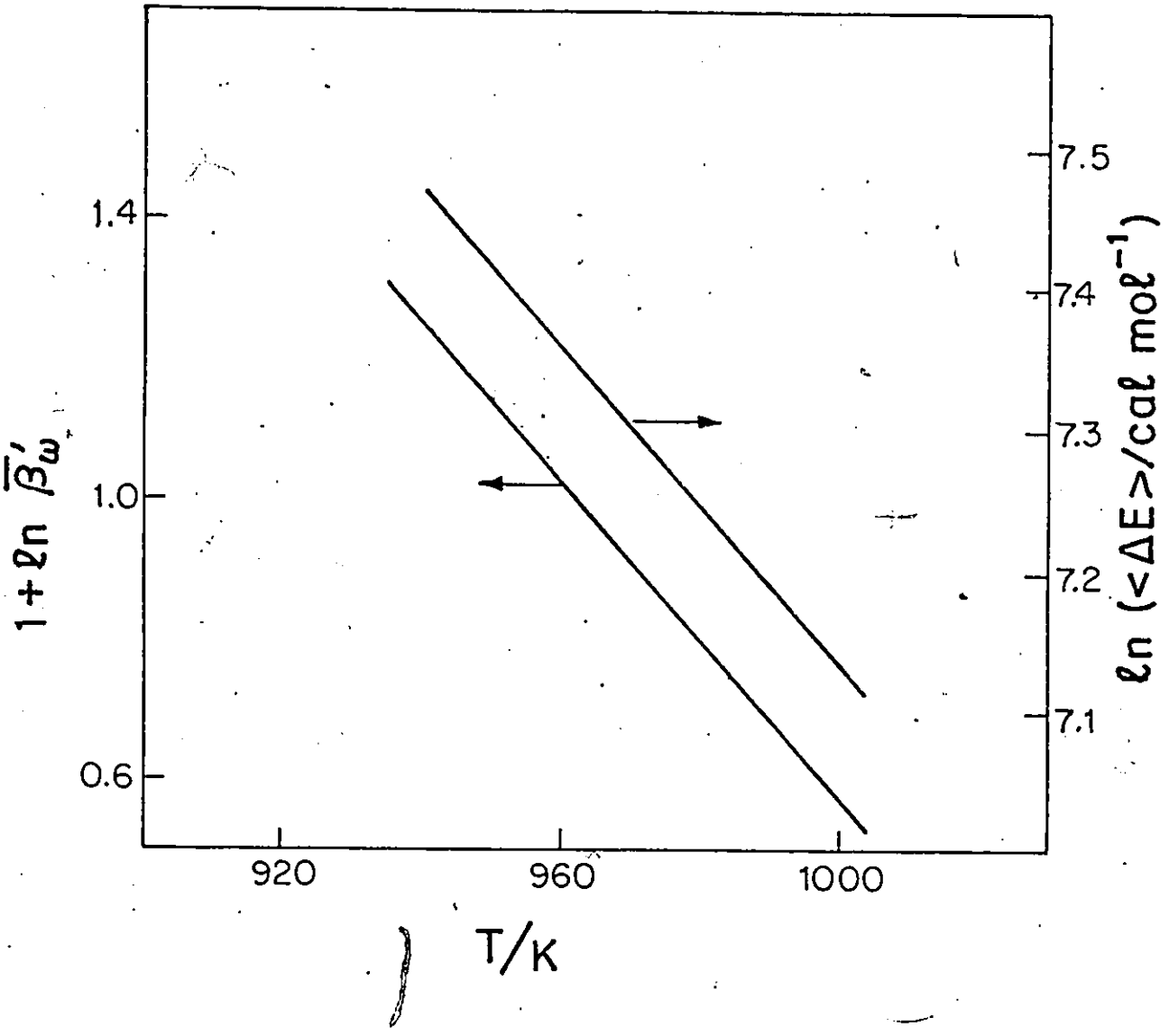

Figure 47. $\ell n\bar{\beta}_{\omega}'$ and $\ell n\langle\Delta E\rangle$ as a Function of Temperature

These energy increments will be similar for strong collisions, but not for weak collisions when $\langle \Delta E \rangle < RT$.

The quantity $\langle \Delta E_T \rangle$ may be obtained from the values of β_ω in the second-order region from the relation given by Troe[117]

$$\frac{\beta_\omega}{1 - \sqrt{\beta_\omega}} \approx \frac{- \langle \Delta E_T \rangle}{RT}$$

With the value of β_o of 0.025 for H_2 from the present results, $\langle \Delta E_T \rangle \sim 60$ cal mol^{-1}. From the results shown in Table 38, at 1000 K $\langle \Delta E \rangle = 1.25$ kcal mol^{-1} giving $\langle \Delta E_T \rangle = 50$ cal mol^{-1}. This is in reasonable agreement with the value of 60 cal $mole^{-1}$ obtained from β_0.

The variation of $\overline{\beta}'_\omega$ with temperature was examined with respect to the three principal factors, ϕ, E^+, and $\langle \Delta E \rangle$, as discussed by Tardy and Rabinovitch.[95] The function may be expressed as follows:

$$\frac{d \ln \overline{\beta}'_\omega}{dT} = \frac{\partial \ln \overline{\beta}'_\omega}{\partial \phi} \cdot \frac{d\phi}{dT} + \frac{\partial \ln \overline{\beta}'_\omega}{\partial \ln \langle \Delta E^+ \rangle} \cdot \frac{d \ln \langle E^+ \rangle}{dT}$$

$$+ \frac{\partial \ln \overline{\beta}'_\omega}{\partial \ln \langle \Delta E \rangle} \cdot \frac{d \ln \langle \Delta E \rangle}{dT}$$

or, briefly, using the formulation of Tardy and Rabinovitch [95]

$$\frac{d\ln \bar{\beta}'_\omega}{dT} = \Phi^* + EA + ED$$

Values for these three terms have been estimated in the following way. From the present measurements, $\frac{d\phi}{dT}$ and $\frac{d\ln\langle\Delta E\rangle}{dT}$ may be obtained directly using the results in Tables 37 and 38. $\frac{d\ln\langle E^+\rangle}{dT}$ is obtained from the calculated values of E^+ (Table 38). The values of

$$\frac{\partial \ln \bar{\beta}'_\omega}{\partial \phi} = 2.80 \text{ and } \frac{\partial \ln \bar{\beta}'_\omega}{\partial \ln\langle\Delta E\rangle} = -\frac{\partial \ln \bar{\beta}'_\omega}{\partial \ln\langle E^+\rangle} = 1.08$$

were estimated from the "universal" curves of Tardy and Rabinovitch[103] for $\phi = 1.25$ and $E' = 0.5$ using the data given in Reference [95]. The results are summarized in Table 39. In the present system it appears that the variation in the collisional efficiency with temperature is due largely to changes in $\langle\Delta E\rangle$. Over the temperature range 940-1000 K, $\langle\Delta E\rangle$ has decreased by about 30%. The change in the order with temperature, for constant ω, is also significant while the change in E^+ with temperature is the least important term.

Table 38

$\log \omega = 3.08$

T/K	E^+/kcal mole^{-1}	E'	ΔE/kcal mole^{-1} (cm^{-1})
943	2.66	0.647	1.72 (480)
952	2.70	0.613	1.65 (460)
962	2.73	0.576	1.57 (440)
971	2.76	0.542	1.50 (420)
980	2.80	0.508	1.42 (400)
990	2.83	0.470	1.33 (370)
1000	2.87	0.434	1.25 (350)

Table 39

$(\frac{d\ln \bar{\beta}'_\omega}{dT})/K^{-1}$	Φ/K^{-1}	EA/K^{-1}	ED/K^{-1}	$(\Phi+EA+ED)/K^{-1}$
-1.13×10^{-2}	-2.47×10^{-3}	-1.39×10^{-3}	-7.35×10^{-3}	-1.22×10^{-2}

CLAIMS TO ORIGINAL RESEARCH

1. The hydrogenation of carbon by hydrogen over the temperature range 870-1150 K has been shown to be a process involving both heterogeneous and homogeneous reactions whose relative importance depends on the temperature. A mechanism for each of these reactions has been proposed.

2. The consecutive steps in the hydrogenation from ethylene to ethane to methane have been clearly demonstrated. It has also been concluded that a process causing inhibition occurs on the carbon surface, probably involving the formation of higher molecular weight products which remain strongly adsorbed.

3. The observed activation energy of 51 kcal mol^{-1} and the order of 0.5 ~ 0.6 with respect to H_2 for the rate of formation of CH_4 at temperatures above about 1000 K were interpreted to show that thermal dissociation of hydrogen provides an important source of radicals. This source of hydrogen atoms had not previously been recognized.

4. The effect of the surface oxide complex on the rate of hydrogenation of carbon was observed. It was shown that the presence of the surface complex had a positive effect on the reactivity of the carbon.

5. A new system for the measurement of rate constants for radical reactions at temperatures above 1000 K has been explored. The method is based on the maintenance of an equilibrium concentration of hydrogen atoms from the thermal dissociation of H_2.

6. Application of this technique has been made in studies of two systems: the homogeneous hydrogenation of C_2H_4 and the conversion of C_2H_6 to C_2H_4 in the presence of a large excess of H_2. From these studies measurements of absolute rate constants have been made for the elementary reactions:

$$C_2H_5 + H_2 \xrightarrow{k_3} C_2H_6 + H$$

$$C_2H_6 + H \xrightarrow{k_{-3}} C_2H_5 + H_2$$

7. From a critical review of the literature data, including a comparison of two sets of independent measurements of k_3 and k_{-3} it was suggested that a

value of 28 kcal mol^{-1} for the heat of formation of the ethyl radical is more consistent with the data than the value of 26 kcal mol^{-1} which has been accepted for many years.

8. The collisional efficiencies of hydrogen and xenon in the unimolecular dissociation of ethane, and the corresponding value of $\langle \Delta E \rangle$, were measured at temperatures in the neighbourhood of 1000 K and showed that both gases are weak colliders. Both $\bar{\beta}_\omega$ and $\bar{\beta}'_\omega$ declined significantly over the relatively small range of temperature of the present experiments. The decrease in average increment of energy transfered per de-activating collision, $\langle \Delta E \rangle$, was the most important factor in the decrease in collisional efficiency.

REFERENCES

[1] R.M. Barrer, E.K. Rideal. Proc. Roy. Soc., 149A, 231 1935.

[2] R.M. Barrer. Trans. Faraday Soc., 32, 481 (1936).

[3] R.M. Barrer. J. Chem. Soc. (London), 2, 1256 (1936).

[4] W.G. Burns. "The Reaction of Carbon and Hydrogen." AERE-C/M-248 (1955).

[5] P.L. Walker, F. Rusinko and L.G. Austin. Adv. Catalysis, 11, 138 (1959).

[6] J.B. Lewis. Modern Aspect of Graphite Technology, p. 129 (ed. L.C.F. Blackman), Academic Press (1970).

[7] R.A. Krakowski and D.R. Olander. U.S. At. Energy Comm. UCRL 19149 (1970).

[8] J.L. Johnson. Adv. in Chem. Ser. 131, 145 (1974).

[9] A. Tomita, O.P. Mahajan and P.L. Walker. Fuel 56, 137 (1977).

[10] J. Weber and M. Bastick, 14th Biennial Carbon Conf., p. 147. Penn. State University, University Park, Penn. (1979).

[11] J.G. McCarty and H. Wise. J. Catal. 57, 406 (1979).

[12] C.W. Zielke and E. Gorin. Ind. and Eng. Chem. 47, 820 (1955).

[13] F. Moseley and D. Patterson. J. Inst. Fuel 38, 13 (1965).

[14] J.D. Blackwood. Aust. J. Chem. 15, 397 (1962).

[15] H. Imai, S. Nomura and Y. Sasuki. Carbon 13, 333 (1978).

[16] A. de Koranyi, N.D. Parkyns and S.J. Peacock. Fifth Int. Conf. on Carbon and Graphite, London, p. 139 (1978).

[17] J.D. Blackwood. Aust. J. Chem. 15, 3, 397 (1962).

[18] J.D. Blackwood and F.K. McTaggart. Aust. J. Chem. 12, 4, 533 (1959).

[19] M. Boudart. J. Amer. Chem. Soc. 74, 3556 (1952).

[20] R.M. Barrer. Proc. Roy. Soc. (London) 149A, 253 (1935).

[21] D.P. MacMilland. Nucleonics 19, 85 (1961).

[22] E.A. Bulbransen, et al. (a) J. Electrochem. Soc. 112, 49 (1965). (b) Electrochem. Technol. 5, 217 (1967).

[23] J.T. Clarke and B.R. Fox. J. Chem. Phys. 46, 827 (1967).

[24] J.W.H. Chi and C.E. Laudahl. Nucl. Appl. 4, 159 (1968).

[25] R. Lowrie. U.S.A. E.C. Rept. NP-11311 (1961).

[26] P.G. Salgade. Ph.D. Dissertation, West Virginia University (1958).

[27] K. Hedden. Z. Electrochem. 66, 652 (1962).

[28] N.S. Corney and R.B. Thomas. AERE-C/K-2502 (1958).

[29] P. Breisacher and C.P. Marx. J. Am. Chem. Soc. 85, 3518 (1965).

[30] J.D. Rogers and A. Sesonski. U.S. At. Energy Comm. Report LADC-5433 (1962).

[31] J.T. Shaw. National Coal Board Gasification Note No. 29 (1977).

[32] S.J. Steck, G.A. Pressley, S.S. Lin and F.F. Stafford. J. Chem. Phys. 50, 8, 3196 (1969).

[33] C.J. Chen and M.H. Back. Carbon 17, 698 (1979).

[34] S.B. Tong, P. Pareja and M.H. Back. Carbon 20, 191 (1982).

[35] C.R. Baker and R.S. Paul. Chem. Eng. Prog. 59, 61 (1963).

[36] A.B. King and H. Wise. J. Phys. Chem. 67, 1169 (1961).

[37] A. Snelson. Advances in Chemistry Series 131, 54 (1974).

[38] M. Balooch and D.R. Olander. J. Chem. Phys. 63, 4772 (1975).

[39] N.R. Laine, F.J. Vastola and P.L. Walker. J. Phys. Chem. 67, 2030 (1963).

[40] A.K. Galwey. Adv. Cat. 26, 267 (1977).

[41] H. Marsh. Chem. Soc. Spec. Pub. No. 32, p. 133, London (1978).

[42] H. Marsh and A.D. Foord. Carbon 11, 421 (1973).

[43] A.B. Trenwith. J. Chem. Soc. Far. Trans. I 75, 614 (1979).

[44] C.-J. Chen, M.H. Back and R.A. Back. Can. J. Chem. 53, 3580 (1975).

[45] S.W. Benson. The Foundations of Chemical Kinetics. McGraw-Hill Book Co., Toronto (1960).

[46] B.R. Puri. Chem. Phys. Carbon 6, 191 (1970).

[47] H.P. Boehm and G. Bewer. Fourth Int. Conf. on Carbon and Graphite, p. 344. London (1974).

[48] N.R. Laine, F.J. Vastola and P.L. Walker. J. Phys. Chem. 67, 2030 (1963).

[49] J.R. Fryer. Third Conf. on Ind. Carbon and Graphite, p. 246. London (1970).

[50] R.C. Seymour and J.C. Wood. Third Conf. on Ind. Carbon and Graphite, p. 264. London (1970).

[51] H. Marsh and A.D. Foord. Carbon 11, 421 (1973).

[52] B.G. Tucker and M.F.R. Mulcahy. Trans. Far. Soc. 65, 274 (1969).

[53] R.C. Bansal, F.J. Vastola and P.L. Walker. Carbon 8, 443 (1970).

[54] J. Dollimore, C.N. Freedman and B.H. Harrison. Third Conf. on Ind. Carbon and Graphite. London (1970).

[55] N.R. Laine, F.J. Vastola and P.L. Walker. Proc. 5th Carbon Conf., p. 211. Pergamon Press, Oxford (1963).

[56] R.O. Lussow, F.J. Vastola and P.L. Walker. Carbon 5, 591 (1967).

[57] D.R. Olander, W. Siekhaus, R. Jones and J.A. Schwarz. J. Chem. Phys. 57, 408 (1972).

[58] W.C. Gardiner. Acc. Chem. Res. 10, 326 (1977).

[59] T.C. Clark and J.E. Dove. Can. J. Chem. 51, 2147 (1973).

[60] P.J. Boddy and E.W.R. Steacie. Can. J. Chem. 39, 13 (1961).

[61] L.E. Reid and D.J. LeRoy. Can. J. Chem. 46, 3275 (1968).

[62] M.P. Halstead and C.P. Quinn. Trans. Far. Soc. 64, 1560 (1968).

[63] R.R. Baldwin, et al. Thirteenth Int. Symp. Comb. Combustion Institute, Pittsburgh, 1971, p. 251.

[64] Handbook of Bimolecular and Termolecular Gas Reactions, ed. J.A. Kerr and S.J. Moss, CRC Press, Boca Raton, Florida, U.S.A. (1981).

[65] P. Roth and T.H. Just. NBS Special Publication No. 561, p. 1339 (1979).

[66] P. Roth, U. Barner and R. Löhr. Ber. Bun. Phys. Chem. 83, 929 (1979).

[67] J.V. Michael, D.T. Osborne and G.N. Suess. J. Chem. Phys. 58, 2800 (1973).

[68] V.V. Azatyan, S.B. Filippov, A.B. Nalbandyan and L.B. Ramanovich. Arm. Khim. Zh. 22, 193 (1969).

[69] C.P. Fenimore and G.W. Jones. Ninth Int. Symp. Combustion (Academic Press, New York and London, 1963), p. 604.

[70] Baldwin and Simmons. Trans. Faraday Soc. (1957), 53, 964.

[71] P. Camilleri, R.M. Marshall and J.H. Purnell. J. Chem. Soc. Far. Trans. 1, 70, 1434 (1974).

[72] K. Yang. J. Phys. Chem. 67, 562 (1963).

[73] Darwent, B. de B. and Roberts. R. Discussions Faraday Soc. 14, 55 (1953).

[74] M.R. Berlie and D.J. LeRoy. Disc. Faraday Soc., 14, 50 (1953).

[75] J.E. Bennett and D.R. Blackmore. Thirteenth Int. Symp. Comb., Combustion Institute, Pittsburgh, 1971, p. 51.

[76] A. Sepehrad, R.M. Marshall and J.H. Purnell. J. Chem. Soc. Far. Trans. 1, 75, 835 (1979).

[77] T.H. Just, P. Roth and R. Damm. Sixteenth Int. Symp. Comb., Combustion Institute, Pittsburgh, 1977, p. 961.

[78] T. Tanzawa and W.C. Gardiner. Comb. Flame, 39, 241 (1980).

[79] H.E. O'Neal and S.W. Benson. "Thermochemistry of Free Radicals" in "Free Radicals", Vol. 2, ed. J.K. Kochi, Wiley, New York (1973), p. 275.

[80] S.W. Benson. Thermochemical Kinetics, 2nd edition, John Wiley, New York (1976).

[81] D.M. Golden, K.Y. Choo, M.J. Perona and L.W. Piszkiewicz. Int. J. Chem. Kin. 8, 381 (1976).

[82] H. Adachs, N. Basco and D.G.L. James. Int. J. Chem. Kin. 11, 995 (1979).

[83] M.C. Lin and M.H. Back. Can. J. Chem. 44, 505, 2357 (1966).
M.C. Lin. Ph.D. Thesis. University of Ottawa, Ottawa, Canada (1966).

[84] G.B. Skinner and G.H. Ringrose. J. Chem. Phys. 43, 4129 (1965).

[85] J.N. Bradley. Proc. Royal Soc. London A337, 199 (1974).

[86] T.C. Clark, T.P.J. Izod and G.B. Kistiakowsky. J. Chem. Phys. 54, 1295 (1971).

[87] V.V. Voevodsky and V.N. Kondratiev. Progress in Reaction Kinetics. Pergamon Press, Oxford 1, 41 (1961).

[88] B. de B. Darwent and M.J. Allard. J. Phys. Chem. 71, 2346 (1967).

[89] N.N. Tikhomirova and V.V. Voevodsky. Chain Oxidation of Hydrocarbons in the Gas Phase (Russ.), Moscow, 1955.

[90] N.I. Parsamyan, E.A. Arakelyan, V.V. Azatyan and A.P. Nalbandyan. Izv. Akad. Nauk. SSSR. Ser. Khim. 496 (1968).

[91] R.R. Baldwin and A. Melvin. J. Chem. Soc. 1785 (1964).

[92] N.I. Gorban and A.B. Nalbandyan. Russ. J. Phys. Chem. 36, 946 (1962).

[93] R.R. Baldwin, D.E. Hopkins and R.W. Walker. Trans. Far. Soc. 66, 189 (1970).

[94] A.L. Castelhano, P.R. Marriott and D. Griller. J. Am. Chem. Soc. 103, 4262 (1981).

[95] D.C. Tardy and B.S. Rabinovitch. Chem. Rev. 77, 369 (1977).

[96] H.O. Pritchard. Reaction Kinetics Vol. 1, Spec. Per. Rep. Chem. Soc. London (1975), Accts. Chem. Res. 9, 99 (1976).

[97] A.P. Penner, R.C. Bhattacharjee and W. Forst, Int. J. Chem. Kin. 9, 371 (1977).

[98] M. Quack and J. Troe. Gas Kinetics and Energy Transfer, Vol. 2, 175, Chem. Soc. London (1977).

[99] S.C. Chan, B.S. Rabinovitch, J.T. Bryant, L.D. Spicer, T. Fujimoto, Y.N. Lin and S.P. Parlou. J. Phys. Chem. 74, 3160 (1970).

[100] H. Endo, K. Glänzer and J. Troe. J. Phys. Chem. 83, 2083 (1979).

[101] K. Luther and J. Troe, Int. Symp. Comb. 17, 535 (1979).

[102] I.E. Klein and B.S. Rabinovitch. Chem. Phys. 35, 439 (1978).

[103] D.C. Tardy and B.S. Rabinovitch. J. Chem. Phys. 45, 3720 (1966).

[104] D.C. Tardy and B.S. Rabinovitch. J. Chem. Phys. 48, 1282 (1968).

[105] Y.N. Lin and B.S. Rabinovitch. J. Phys. Chem. 74 (1970), 3151.

[106] G.H. Kohlmaier and B.S. Rabinovitch. J. Chem. Phys. 38 (1963), 1692, 1709.

[107] J.W. Simons, B.S. Rabinovitch and D.W. Setser. J. Chem. Phys. 41 (1964) 800. J. Chem. Phys. 40 (1964) 1751

[108] S.H. Lun and J. Troe. Ber. Bunsengers.Physik. Chem. 78 (1974) 766.

[109] J.F. Bott. J. Chem. Phys. 54 (1971) 181.

[110] H. Miyama and T. Takeyama. Bull. Chem. Soc. Japan. 38 (1965) 2189.

[111] E.A. Dorko, D.B. McGhee, C.E. Painter, A.J. Caponeechi and R.W. Crossley. J. Phys. Chem. 75 (1971) 2526.

[112] E.A. Dorko, R.W. Crossley, U.W. Grimm, G.W. Mueller and K. Scheller. J. Phys. Chem. 77 (1973) 143.

[113] J.N. Bradley and M.A. Freud. Trans. Faraday Soc. 67 (1971) 72.

[114] P. Jeffers, D. Lewis and M. Sarr. J. Phys. Chem. 77 (1973) 3037.

[115] J.A.Barnard, A.T. Cocks and R.K.Y. Lee. J. Chem. Soc. Faraday Trans. I, 70 (1974) 1782.

[116] J.O. Hirschfelder, C.F. Curtiss and R.B. Bird. "Molecular Theory of Gases and Liquids", Wiley, New York (1954), p. 1110.

[117] J. Troe. J. Chem. Phys. 66, 4745 (1977).

[118] A.B. Trenwith. J. Chem. Soc. Far. Trans. I, 75, 614 (1979).

[119] K. Kanan, J.H. Purnell and A. Sepherad. Int. J. Chem. Kin. in press.

[120] J.A. Clark and C.P. Quinn. J. Chem. Soc. Far. Trans. I, 72, 706 (1976).

[121] W.L. Hase. J. Chem. Phys. 57, 730 (1972).

[122] F.B. Growcock, W.L. Hase and J.W. Simons. Int. J. Chem. Kin. 5, 77 (1973).

[123] I. Oref and B.S. Rabinovitch. J. Phys. Chem. 72, 4488 (1968).

[124] D.L. Baulch and J. Duxbury. Comb. Flame 37, 313 (1980).

[125] G. Prutt and I. Veltman. J. Chem. Soc. Faraday Trans. I, 72, 1733 (1976).

[126] D.L. Allara and R. Shaw. J. Phys. Chem. Ref. Data 9, 523 (1980).

[127] R.W. Walker. J. Chem. Soc. A. 2391 (1968).